8-10-2015

Evaluation of Biodegradability and Cell Functionality of Injectable Glycol Chitosan Hydrogel

Aiswaria Padmanabhan
University of Connecticut - Storrs, aiswaria.padmanabhan@uconn.edu

Evaluation of Biodegradability and Cell Functionality of Injectable Glycol Chitosan Hydrogel

Aiswaria Padmanabhan

M.Sc., University of Kerala, 2009

B.Sc., University of Kerala, 2007

A Thesis

Submitted in Partial Fulfillment of the

Requirements for the Degree of

Master of Science

At the

University of Connecticut

2015

APPROVAL PAGE

Master of Science Thesis

Evaluation of Biodegradability and Cell Functionality of Injectable Glycol Chitosan Hydrogel

Presented by
Aiswaria Padmanabhan., M.Sc.

Major Advisor_____
Dr. Lakshmi S. Nair

Associate Advisor_____
Dr. Yusuf Khan

Associate Advisor_____
Dr. Kourosh Parham

University of Connecticut
2015

Dedicated to my husband, parents and family members for their loving support

ACKNOWLEDGEMENT

I would like to convey my gratitude to my advisor, Prof. Lakshmi S. Nair for giving me the opportunity to carry out this project in her research group. I was able to learn a great deal from her knowledge and experience and her mentorship was invaluable in the completion of my thesis. I would also like to thank Prof. Yusuf Khan and Prof. Kourosh Parham for agreeing to assess and guide my work as part of my advisory committee. Many thanks are in order to Dr. Shalini Gohil and Eva Homan Kan for all their tireless help with my experiments and data analysis. I would also like to mention the contribution of my friends who made working on this project an enjoyable experience – Deborah Dorcemus, Junqiu Cheng, Aja Aravamudhan, Eric James, Jessica Deschamps, Paulos Mengsteab, Mary Shimkus, Jeremy Heard, Christina Klecker, Toni Vella, Matthew Harmon, Fayekah Assanah and many others.

Finally, I would like to thank the Materials Science and Engineering Department at the University of Connecticut and the Institute for Regenerative Engineering at the University of Connecticut Health Center whose people and facilities made this pivotal endeavor in my life possible.

TABLE OF CONTENTS

LIST OF TABLES

LIST OF FIGURES

ABSTRACT

Chitosan hydrogels are increasingly being used as vehicles for the controlled delivery of drugs, cells and proteins for various biomedical applications. The most important advantages offered by chitosan include biocompatibility, biodegradability, antimicrobial activity and non-toxicity. Glycol chitosan (GC) is a derivative of chitosan that is gaining interest lately because of its water solubility. Previous studies in the lab demonstrated the feasibility of developing injectable enzymatically crosslinked hydrogels from GC. One of the disadvantages of GC hydrogel is its lack of biodegradation *in vitro* and *in vivo*. This work is the first attempt at studying acetylated derivatives of GC as a biodegradable hydrogel platform for different therapeutic applications. Enzymatic crosslinking was used to prepare biodegradable injectable hydrogels from acetylated GC as vehicles for protein delivery. Results indicated that the degradation-dependent protein release from the hydrogels increased with increasing degree of acetylation, which presents a unique mechanism to tailor macromolecule release properties. The cytocompatibility of the acetylated hydrogels was confirmed by following the viability of encapsulated osteoblast cells. Dependence of *in vivo* degradation of the hydrogels on the degree of acetylation was confirmed by subcutaneous implantation of the hydrogels in mouse model. Another disadvantage of GC hydrogel is its inability to support cell spreading upon cell encapsulation. Composite hydrogels prepared by incorporating gelatin in GC showed significant improvement in cell spreading as a function of gelatin concentration. However, the lack of uniform cell spreading in the composite hydrogels warrants the need to develop alternative approaches to incorporate cell-adhesive moieties in GC to improve cell adhesion and cell spreading in the hydrogel.

CHAPTER 1- INJECTABLE CHITOSAN HYDROGELS FOR BIOMEDICAL APPLICATIONS

1. Introduction

1.1. Hydrogels

Hydrogels are three dimensional networks of hydrophilic polymers that have the ability to imbibe aqueous fluids and swell while remaining mechanically stable (1-3). Hydrogels are attractive candidates for biomedical applications mainly due to their biocompatibility, biodegradability, ability to mimic natural tissue and support cell viability and functions (3, 4). Due to the excellent permeability of hydrogels, they are used as cell and drug delivery vehicles. Hydrogels used for regenerative engineering applications can be either preformed or injectable. Preformed hydrogels are fabricated *in vitro* followed by transplantation *in vivo* (5). Preformed hydrogels can be prepared in different forms – membranes, coatings, pressed powder matrices, molded solids, encapsulated solids, and micro-particles – depending on the intended application (1-3, 6). On the other hand, injectable hydrogels are formed by injecting polymer solutions into the body that can then form gels *in situ* (5). Injectable hydrogels have shown potential for minimally invasive delivery of cells as well as biomolecules because their physical properties can be easily tailored. Hydrogels are also useful for targeted, controlled and sustained release of drugs and bioactive molecules. Drug releasing mechanisms in hydrogels are mainly classified as diffusion-controlled, swelling-controlled or degradation-controlled (1). Studies have shown the feasibility of developing stimuli-responsive hydrogels, wherein the gel properties can be modulated by changing the external environmental conditions such as pH, temperature and ionic strength. These smart hydrogel systems are useful as cell or drug delivery systems (2). Hydrogels used in biomedical applications can also be classified in terms of whether they are derived from

natural or synthetic polymers. Table 1.1 provides a list of some of the natural and synthetic polymers used for hydrogel preparation. Hydrogels made from natural polymers have the advantages of bioactivity, biocompatibility and biodegradability but suffer from low mechanical strength, poor reproducibility, and the potential presence of pathogens that may lead to immune responses. On the other hand, hydrogels derived from synthetic polymers can be effectively and consistently tailored to provide desired mechanical properties and degradability, but lack inherent bioactivity (1).

Table 1.1: Natural and synthetic polymers used in hydrogel fabrication (7, 8)

Natural polymers	**Synthetic polymers**
Agarose	Poly(ethylene glycol) (PEG) and its derivatives
Chitosan	Pluronics
Cellulose	Poly Acrylamide (PAAm)
Hyaluronic acid	Polyvinylpyrrolidone (PVP)
Elastin	Poly Acrylic acid (PAA)
Collagen	Poly N-isopropylacrylamide (PNIPAM)
Gelatin	Poly (vinyl alcohol) (PVA)
Chondroitin sulfate	Poly (hydroxyethyl methacrylate) (PHEMA)

1.2. Injectable hydrogels

Injectable hydrogels can be easily delivered to even the deepest tissue inside the body in a minimally invasive manner and therefore have many advantages when compared to preformed hydrogels. Since the injectable systems exit as free-flowing liquid solutions that are easy to handle, they can form gels according to the size and shape of the wound/defect area (9), can provide

homogenous distribution of cells in gels (6), and can fill the defect area completely by successfully providing neovascularization to the area from healthy tissue. In contrast, conventional, preformed hydrogels are not easy to handle, require multiple surgeries, cannot reach the complete depth of the tissue, lead to incomplete defect filling, and are less adaptive to the defective area (10). The most commonly used injectable hydrogels are thermoresposive/thermogelling, pH-responsive, photocrosslinkable and enzymatically crosslinkable hydrogels. Thermogelling injectable hydrogels are formed when they are exposed to body temperature. This happens due to a change in solubility and phase transition due to the change in temperature. pH-responsive hydrogels, as the name suggests, are formed due to change in pH. Photocrosslinkable hydrogels are formed when the polymer solution is exposed to electromagnetic radiations such as ultraviolet (UV) and visible light. When the light interacts with the photoinitiators that are incorporated along with the polymer solution, free radicals are generated and crosslinking is initiated, thereby leading to hydrogel formation. Enzymatic crosslinking is extensively used for preparing injectable hydrogels because the process uses enzymes for crosslinking and therefore happens at the physiological temperature inside the body. The crosslinking process is generally mild and non-toxic resulting in biocompatible gels (10).

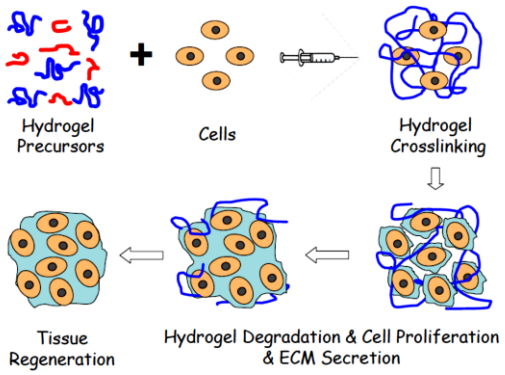

Figure 1.1: Schematic representation of injectable hydrogel for tissue engineering application (6)

1.3. Chitosan

Chitosan is derived from chitin, which is a naturally occurring linear polysaccharide. Chitin is comprised of repeating units of N-acetyl-D-glucosamine, as shown in Figure 1.2.

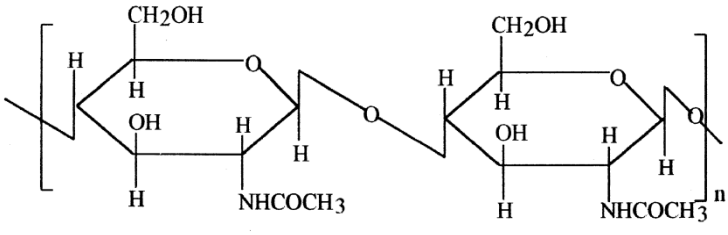

Figure 1.2: Structure of chitin (11)

Crab and shrimp shells currently serve as the common source of chitin. Despite its favorable structural and biological properties, the insolubility of chitin in water and common organic solvents prevents its extensive use for biomedical applications (11, 12). Hence, several approaches have been investigated to increase the aqueous solubility of chitin, including deacetylation (12), carboxymethylation (13) and sulfation (14). Among these, deacetylation of chitin by alkaline treatment is the most commonly used approach. The derivative of chitin with degree of deacetylation of approximately 50% is known as "chitosan", which is soluble in aqueous acidic solutions (12). Chitosan is a copolymer comprising of N-acetyl-D-glucosamine and deacetylated D-glucosamine units (11, 12, 14-17). The structure of chitosan obtained by the complete deacetylation of chitin is shown in Figure 1.3.

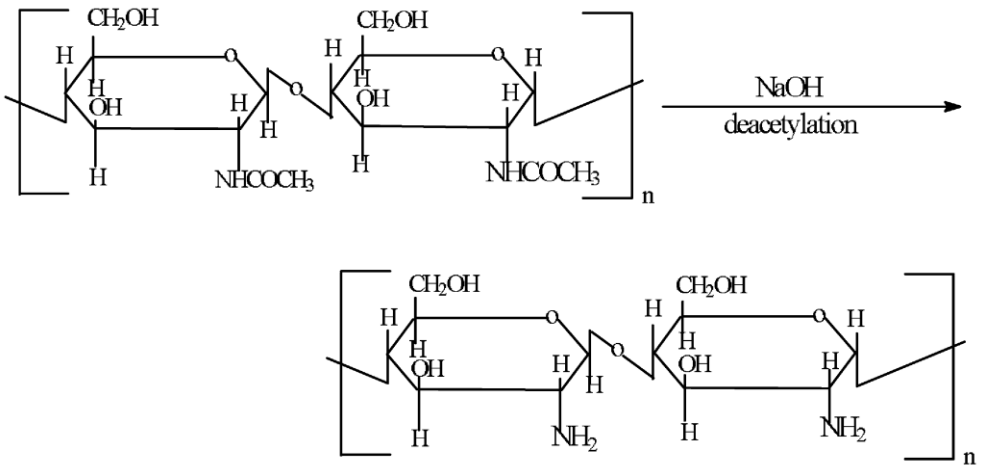

Figure 1.3: Preparation of chitosan by the complete deacetylation of chitin (11)

The most commonly used methods to determine the degree of deacetylation are ^{1}H (liquid state), ^{13}C (solid state) and ^{15}N (solid state) nuclear magnetic resonance (NMR) spectroscopy. Among these, ^{1}H is extensively used to determine acetyl groups in soluble samples. Other methods include infra-red (IR) and UV spectrometry, elemental analysis, potentiometric titration, and enzymatic reaction (12). Degree of deacetylation can significantly affect the biological as well as physiochemical properties of chitosan (18). Chitosan in solid state is reported to be a semi-crystalline polymer (12). Cartier *et al* determined the crystallinity of chitosan using X-ray and electron diffraction methods that allow calculation of the unit cell parameters. Electron diffraction of fully deacetylated chitosan single crystal indicated an orthorhombic unit cell with lattice parameters a = 0.807 nm, b = 0.844 nm, c =1.034 nm (19). Molecular weight is another important parameter that determines the physiochemical and biological properties of chitosan. It varies with the chitin source from which chitosan is obtained (18). Several methods can be used to determine the molecular weight of chitosan. The selection of an appropriate solvent system that does not lead to significant aggregation of chitosan is necessary while determining the molecular weight. A solution of 0.3 M acetic acid/0.2 M sodium acetate (pH = 4.5) has been reported to be a suitable

solvent system (20). The Mark-Houwink equation given below [1] is commonly used to determine the viscosity average molecular weight of chitosan

$$[\eta] = KM^{a} \quad -----[1]$$

Where η is intrinsic viscosity, M is molecular weight, and K and a are experimentally determined parameters for a given solvent system. If K and a are known, molecular weight can then be obtained by intrinsic viscosity measurements (21).

As mentioned earlier, the main motivation behind modifying chitin to obtain chitosan is to take advantage of the improved solubility. In solutions of pH less than ~6.0, the amine groups in chitosan become protonated, thereby allowing chitosan to be soluble in aqueous acidic solutions. The protonation does not occur in basic solutions, leading to a solubility-insolubility transition at pH value ~6.5 (15). The exact pH above which chitosan becomes insoluble, however, depends on the degree of deacetylation, the distribution of the acetyl groups on the linear chain, and the molecular weight. Another advantage of chitosan is that it can be chemically modified using the reactive amine group at the C-2 position or hydroxyl groups at the C-3 and C-6 positions to alter its functionality. Particularly, this allows the functionalization of chitosan for different biological applications (12). Table 1.2 lists some of the chemically modified chitosan derivatives that are water soluble along with some of their biomedical applications.

Table 1.2: Functionalized derivatives of chitosan (12, 22)

Derivatives of chitosan	Solubility	Example of applications	Reference
Carboxymethylchitosan	Water soluble	Drug delivery, Tissue engineering	(23, 24)
Glycol chitosan	Water soluble	Drug delivery	(25, 26)
PEG-grafted chitosan	Water soluble	Drug delivery, Tissue engineering	(27)
Sulfated chitosan	Water soluble	Tissue engineering, Anticoagulant	(28, 29)
N-methylene phosphonic chitosan	Water soluble	Gene delivery	(30, 31)
Cyclodextrin grafted chitosan	Water soluble	Drug delivery	(32)

1.4. Chitosan hydrogels

Chitosan has been widely investigated for a variety of applications in the biomedical industry. The beneficial properties of chitosan are its biocompatibility, biodegradability (33), antimicrobial activity (34), mucoadhesivity (35), wound healing and hemostatic properties (36), and low toxicity (33). Biodegradability of chitosan is dependent on different factors such as the degree of deacetylation, distribution of amine groups, presence of acetyl groups, and molecular weight of the polymer (17). Chitosan can be degraded using enzymes such as lysozyme, which is a glycosidic hydrolase present in the human body. Lysozyme is reported to hydrolyze the β (1-4) linkages between N-acetylglucosamine and glucosamine (37). Therefore, the degree of acetylation of chitosan plays an important role in its enzyme-mediated degradation. Chitosan with a higher degree of deacetylation undergoes limited degradation whereas increasing acetylation results in higher degradation (38). Antimicrobial property of chitosan stems from its interaction with the

negatively charged cell surfaces, which affects cellular permeability, or by its interaction with DNA, which inhibits microbial RNA synthesis (39). Mucoadhesive property of chitosan arises from its positively charged amine groups that can interact with the negatively charged groups in the mucin molecule (35). Hemostatic property is due to the presence of positively charged groups in chitosan that interact with the negatively charged surfaces of blood cells (17); chitosan-based hemostatic bandage called Hemcon® has been FDA-approved (40). Due to these unique biological properties, extensive research has gone in to develop chitosan-based hydrogels for biomedical applications. Both physical and chemical crosslinking methods can be used to develop chitosan hydrogels. Physically crosslinked hydrogels are formed by physical interactions such as electrostatic, hydrophobic or hydrogen bonding between the polymer chains. Hydrogel formation can be induced by mixing the constituents under suitable conditions to initiate the gelation. Physical crosslinking is usually triggered by stimuli such as pH and temperature. Controlling the concentration of chitosan with respect to that of the other components and thereby controlling the polymer interactions has been shown to significantly control gel properties (17, 41). Chemically crosslinked hydrogels are formed as a result of covalent bonding (17). Chemical crosslinking of chitosan can be achieved by using different crosslinkers or by modifying the $-NH_2$ or -OH groups present in the polymer (41).

1.5. Injectable chitosan hydrogels

1.5.1. Preparation of thermogelling injectable chitosan hydrogels

Thermogelling chitosan hydrogels undergo gelation in response to changes in temperature (42). Thermogelling chitosan hydrogels have been investigated as injectable carriers for biomedical applications (43). One of the most extensively studied thermogelling chitosan formulations is the chitosan-β-glycerophosphate (β-GP) system that can undergo sol-gel transition

at or near physiological temperature. Chitosan/β-GP system has been investigated mainly for cell, drug, or growth factor delivery due to the mild gelation process and the minimally invasive manner of delivery (44). For bone regeneration, Niranjan *et al* synthesized a novel thermosensitive carrier comprising of chitosan/β-GP doped with zinc. Metals such as zinc have been shown to provide thermal resistance and antibacterial property. Briefly, chitosan was dissolved in 0.1 M acetic acid. Zinc sulfate solution was added under stirring at a 1:1 (v/v) ratio followed by the addition of β-GP at a 1:9 (v/v) ratio. Addition of β-GP to the chitosan solution changed the solution pH from 3 to 7. Gelation time of zinc-doped chitosan/β-GP solution was ~5 min. Gelation resulted in a porous hydrogel with a pore size of around 200 µm (45). Liu *et al* used chitosan-4-thio-butylamidine (CS-TBA), (β-GP) and nano-hydroxyapatite (nano-HA) to develop a thermoresponsive composite hydrogel that can gel *in situ*. Thiolated chitosan can dissolve in neutral pH unlike unmodified chitosan. The hydrogel was prepared by adding nano-HA powder to CS-TBA solution under continuous stirring followed by dropwise addition of β-GP solution. The final solution was kept at 37 ^{o}C for 10 min for gel formation (46). The physical crosslinking has been attributed to the increased hydrogen bonding and hydrophobic attraction between chitosan chains at higher pH (47, 48). Additionally, thiol groups of CS-TBA also contributed to the gel formation through intra-/inter-molecular disulfide bond formation; the process was found to be time-dependent and temperature-independent (49). The gelation process was found to be dependent on factors such as concentration of the gel constituents and degree of deacetylation of the chitosan (46). For instance, an increase in deacetylation of chitosan has been shown to significantly decrease gelation time (50). Scanning electron microscopy (SEM) analysis showed that the hydrogel had a pore size of 40-80 µm. The presence of thiol group led to higher storage modulus (G') and loss modulus (G") for CS-TBA/β-GP/HA hydrogels in comparison to the unmodified CS/β-GP/HA hydrogels,

presumably due to the additional disulfide linkages (46). In addition to β-GP, inorganic phosphate salts have also been shown to impart thermogelling property to chitosan. Nair *et al* prepared an injectable thermogelling chitosan-inorganic phosphate hydrogel. Briefly, chitosan was dissolved in 0.5% acetic acid solution with pH ~5.6. Addition of ammonium hydrogen phosphate (AHP) to chilled chitosan solution increased the pH to 7-7.2 and the resultant solution showed effective sol-gel transition at or near physiological temperature. Depending on the amount of AHP, the gelling time was variable from 5 min to 30 h. Gelling time decreased with an increase in the concentration of AHP and chitosan. The mechanism of thermogelation is presumed to be a combination of electrostatic as well as hydrophobic attractions, similar to that of chitosan/β-GP solution (51). N-isoproplyacrylamide (NIPAM) is another material with inherent thermoresponsive properties. Chen *et al* developed a thermoresponsive chitosan hydrogel in which chitosan acted as the backbone on which poly (N-isopropylacrylamide) (PNIPAM) with a carboxylic acid end group was grafted. PNIPAM is reported to remain soluble under its lower critical solution temperature (LCST) but forms a gel when the temperature is increased above LCST. This mechanism can be explained as follows: increasing temperature above LCST causes the release of water molecules attached to the isopropyl moieties of the polymer, leading to a compact form with an increase in intra-/inter-molecular hydrophobic attraction between the isopropyl groups (22, 52, 53). Due to this property, PNIPAM grafting to natural polymers is widely used to impart thermogelling properties to these polymers. The grafting of PNIPAM to chitosan was done using 1-ethyl-3- (3-dimethylaminopropyl) carbodiimide hydrochloride (EDC)/N-hydroxysulfosuccinimide (NHS) chemistry, wherein the carboxylic acid group of PNIPAM-COOH was linked to the amine group of the chitosan. The reaction was carried out at 25 ^{o}C for 12 h followed by purification using thermoprecipitation and dialysis. A porous hydrogel was then prepared by re-dissolving the

polymer and incubating at 37 ºC. Gel formation was observed to be faster with an increase in the concentration of PNIPAM grafted on the chitosan. SEM analysis of the hydrogels showed a pore size of 10-40 μm. The study also revealed that phase-transition of the hydrogel was completely reversible, implying that the conjugated PNIPAM retained its property in the gel (54).

1.5.1.1. Biomedical applications

Dessi *et al* developed a thermosensitive β-tricalcium phosphate-chitosan hydrogel in the presence of β-GP and glyoxal to impart physical and chemical gelation. The presence of β-tricalcium phosphate in the *in situ*-gelling hydrogel resulted in a significant increase in cell attachment and proliferation (55). *In-situ*-gelling thermosensitive hydrogels made from chitosan/β-GP are used as carriers for lentiviral vector that expresses neurotropin-3. Use of this lentiviral system may have the potential for repairing injuries to the central nervous system by providing sustained release of the coded protein for longer durations (56). *In situ*-forming thermosensitive chitosan/β-GP hydrogel was investigated as a carrier for liposomes containing ofloxacin drug. The carrier provided extended transcorneal penetration of the drug, resulting in decreased side effects caused by the drug and reducing the frequency at which the drug was administered to the patient (57). Zhang *et al* used the insulating effect of chitosan-based thermosensitive hydrogels for microwave-assisted ablation of liver tissue. *In vivo* experiments performed in rabbits showed that the hydrogel formed *in situ* had the ability to protect the nearby stomach wall during microwave ablation of liver tissue (58). Cheng *et al* used an injectable thermosensitive chitosan/gelatin/glycerol phosphate (C/G/GP) hydrogel for the controlled delivery of ferulic acid (FA). FA is an antioxidant and can relieve H_2O_2-induced oxidative stress on the nucleus pulposus (NP) cells. Controlled delivery of FA from the hydrogel decreased the oxidative stress on NP cells and showed a decrease in cellular apoptosis (59). The potential of injectable thermosensitive

chitosan-pluronic hydrogel as a chondrocyte delivery system was demonstrated by encapsulating bovine chondrocytes. The encapsulated cells in chitosan gel showed enhanced cell proliferation and glycosaminoglycan production for 28 days when compared to cells encapsulated in alginate hydrogel (60). Another study investigated the potential of thermosensitive chitosan hydrogel for three dimensional culture of neuronal cells. The neuronal cells cultured in a poly-D-lysine (PDL)-immobilized chitosan/GP hydrogel showed good viability with larger cell bodies (61). Injectable thermosensitive poly (organophosphazene) hydrogel loaded with galactosylated chitosan-g-PEI/DNA complexes showed excellent transfection *in vitro* in HepG2 and *in vivo* in BALB/c mice. Results indicated that the galactosylated hydrogel complex was less toxic and was able to accumulate in the liver over time, indicating better hepatocyte targeting (62). Chitosan hydrogels have also been investigated to repair the cornea using stem cells. Chein *et al* used an injectable, thermogelling, amphipathic carboxymethyl-hexanoyl chitosan hydrogel as a delivery vehicle for human keratinocyte reprogrammed to induce pluripotent stem cells (iPSCs). Thermogelation occurred by the addition of β-GP. The study demonstrated the efficacy of the hydrogels for cell-based healing of corneal wounds (63). Miguel *et al* evaluated a thermoresponsive chitosan-agarose hydrogel for wound dressing application. Thermoresponsive nature was imparted to the system by agarose. *In vitro* and in *vivo* studies indicated that the hydrogel had the ability to provide wound-healing environment by preventing water loss and also had bactericidal properties that are essential for an 'ideal' wound dressing material (9). Figure 1.4 shows histological section of tissue samples isolated from the saline control group and chitosan-agarose hydrogel. The presence of hydrogel led to the complete re-epithelialization of the wound without signs of acute inflammation.

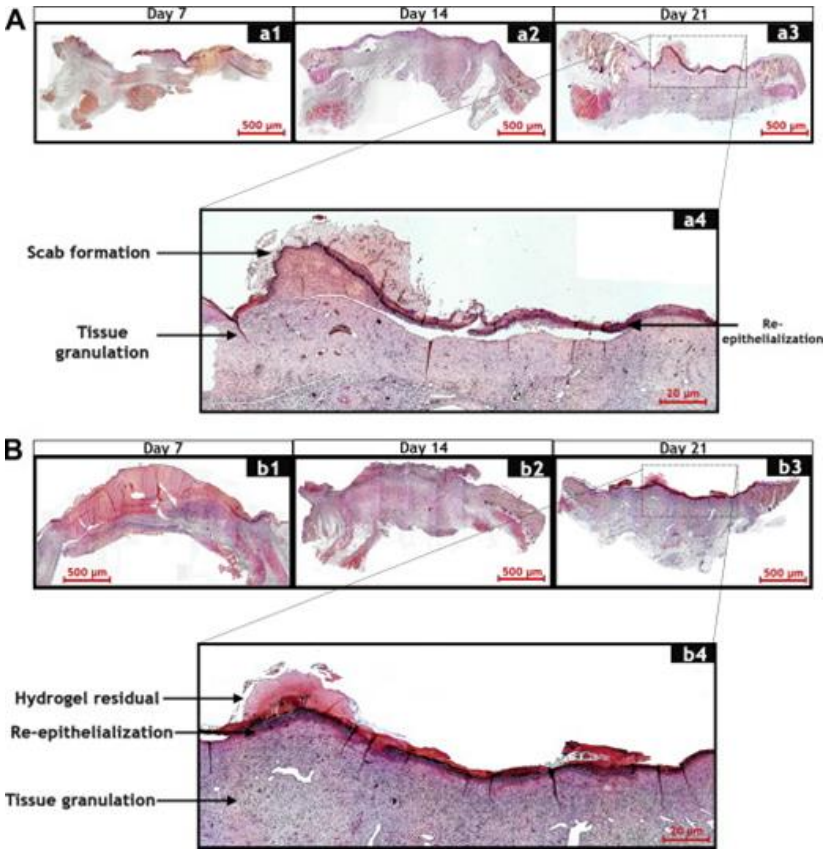

Figure 1.4: Hematoxylin and eosin-stained sections of tissue samples after 7, 14 and 21 days. (A) treated with saline solution (B) treated with CAH (3% ag–1.5% Ch) (9).

1.5.2. Preparation of pH-responsive injectable chitosan hydrogels

In addition to temperature, pH of the solution can also trigger polymer gelation. Many of these systems are pH-responsive and can undergo changes in shape, swelling and release properties depending on the pH of the environment. pH-responsive hydrogels are mostly used in drug delivery and biosensor applications (64). Chitosan is known to exhibit pH-sensitive behavior because of the amine groups, which, when protonated, become soluble in acidic media. On the other hand, this makes chitosan insoluble in basic and neutral pH (65). Studies have shown that injectable *in situ*-forming hydrogels can be developed using the pH-responsive properties of chitosan derivatives. Chiu *et al* designed an injectable hydrogel from N-palmitoyl chitosan (NPCS)

that exhibits pH-responsive changes in properties within a pH range of 6.5 to 7. The polymer solution at pH 6.5 exhibits sol-gel transition when injected using a needle as droplets into a saline solution at pH 7.4. The immediate gelation has been attributed to the physical crosslinking of the outer layer of the palmitoyl group at pH 7.4 while the inner core still remained at pH 6.5. With time, the physical crosslinking proceeded throughout the gel, thereby making the transparent gel opaque. The entire bead was shown to be crosslinked within 30 min. *In vivo* study confirmed that when sterile N-palmitoyl chitosan solution was injected subcutaneously in winstar rat, hydrogel formation was observed in the injected area, demonstrating its utility as an injectable delivery system. Figure 1.5 shows the synthesis of NPCS and its gelation *in vivo*. The mechanism behind the gelation is that, at lower pH, charge repulsion between the protonated amine groups is more prominent. As pH increases, the hydrophobic interaction of the palmitoyl groups becomes dominant, which causes the polymer to condense, thereby increasing the intermolecular physical crosslinking (66).

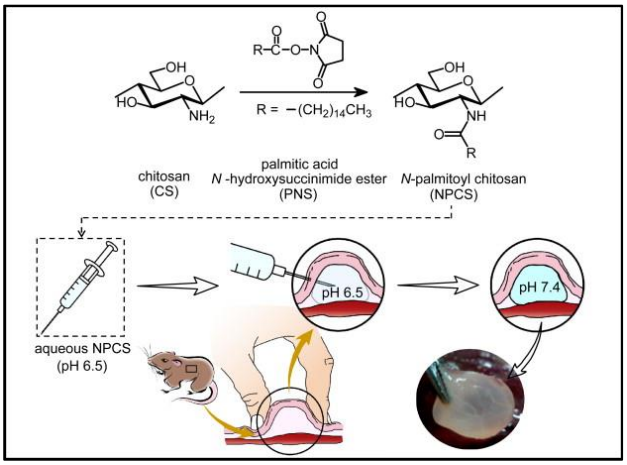

Figure 1.5: Schematic showing the synthesis of *N*-palmitoyl chitosan (NPCS) and the pH-triggered hydrogelation of aqueous NPCS injected into the subcutaneous space of rat model (66)

1.5.2.1. Biomedical applications

Li *et al* prepared an injectable hydrogel from phenylboronic-modified chitosan and oxidized dextran. They were able to incorporate anticancer drugs by *in situ*-crosslinking; the hydrogel showed controlled release of the drug upon change of pH as well as change of glucose concentration. In addition, they were able to culture cells in the hydrogel that remained viable and showed proliferation (67). Ding *et al* synthesized an injectable hydrogel using glycol chitosan (GC) and benzaldehyde capped with poly (ethylene glycol)-block-poly (propylene glycol)-block-poly (ethylene glycol) (PEO-PPO-PEO). The hydrogel was responsive to pH and temperature change and showed the potential for controlled release of hydrophobic as well as hydrophilic drugs. The hydrogel was also shown to be biocompatible during implantation in rat model (68).

1.5.3. Preparation of photocrosslinked injectable chitosan hydrogels

Photocrosslinkable hydrogels have been extensively investigated as scaffolds for tissue engineering (69), drug delivery (70), bioadhesivity (71) and endoscopic treatments (72). Photocrosslinkable hydrogels can be prepared *in situ* and are therefore potential candidates to develop minimally invasive delivery systems (73). Tsuda *et al* prepared a photocrosslinked chitosan hydrogel (Az-CS-LA) using chitosan (CS) incorporated with azide (Az) and lactose (LA) functional groups. The lactose group made the Az-CS-LA polymer water soluble. Briefly, the hydrogels were prepared by exposing a 20 mg/mL solution of Az-CS-LA to UV light for 30 s (74). Gelation time was dependent on the intensity of UV radiation; the higher the intensity, the lower was the gelation time. The mechanism behind gelation is that during UV irradiation, the azide group ($-N_3$) releases N_2 and gets converted to nitrene, which is a very reactive group. These nitrene groups either interact with other nitrene groups or with the amine groups of chitosan, resulting in the formation of azo groups ($-N=N-$) causing gelation (75). The hydrogels showed higher sealing

strength when compared to fibrin glue. Apart from this, light-mediated free radical polymerization has also been extensively investigated to develop chitosan hydrogels. Zhou *et al* used a water soluble (methacryloyloxy) ethyl carboxymethyl chitosan (MAOECECS) for the preparation of photocrosslinkable hydrogels for tissue engineering applications. MAOECECS was synthesized using Michael addition reaction between -NH_2 group of chitosan with C=C of acrylate group. Briefly, a solution of MAOECECS in water was prepared and mixed with the photoinitiator D-2959. The solution was exposed to UV light of wavelength 320-480 nm for 15 min to obtain the hydrogel. D-2959 was used as a photoinitiator due to its low cytotoxicity. SEM analysis showed a spongy macroporous structure. Crosslinking density played a key role in determining the pore structure of the hydrogel. Similarly, the swelling behavior of the hydrogel was dependent on the concentration of MAOECECS. Degradation of the hydrogel in the presence of lysozyme can also be modulated by varying the crosslinking density. Higher crosslinking density caused lower degradation whereas lower crosslinking density showed higher degradation; lower crosslinking makes the hydrogel more accessible for enzymatic attack as well as for enzyme penetration (73). Arakawa *et al* prepared a photocrosslinkable hydrogel using methacrylated glycol chitosan (MeGC) and collagen (Col). For the fabrication of the hydrogel, MeGC solution was prepared in phosphate buffered saline (PBS). Col was added to the solution to form a semi-interpenetrating network. Riboflavin was used as the photoinitiator for crosslinking. The hydrogel was formed when the composite solution was exposed to visible blue light of wavelength 400-500 nm in the presence of the photoinitiator. Use of visible light is more beneficial as it is less harmful, less mutagenic, does not generate heat, and transmits deeper into the tissue. Gelation time decreased with increase in riboflavin content. MeGC-Col hydrogel had a compressive strength of ~1.8 kPa,

which is higher than that of MeGC gel. Higher compressive strength of the MeGC-Col hydrogel has been attributed to the formation of a semi-interpenetrating network (76).

1.5.3.1. Biomedical applications

Using a photocrosslinkable chitosan hydrogel (Az-CS-LA), Tsuda *et al* demonstrated the effective prevention of ectopic bone formation for up to 8 weeks in rat model with calvarium and fibula defects. The hydrogels suppressed bone formation by forming granulated tissue in the defect area (74). Fujitha *et al* synthesized a photocrosslinked chitosan (Az-CS-LA) hydrogel for delivering fibroblast growth factor-2 (FGF-2) for treating chronic myocardial infarction in rabbit model. Significant improvement in systolic pressure at the left ventricle was observed along with increased angiogenesis and formation of viable myocaridium (77). Arakawa *et al* developed an injectable photocrosslinked hydrogel from MeGC and Col as a delivery system for bone marrow stromal cells (BMSCs) to support bone regeneration. The study showed that BMSCs showed greater cellular attachment, proliferation and osteogenic differentiation in MeGC-Col hydrogel when compared to MeGC hydrogel alone. Increased alkaline phosphate activity along with mineralization in BMSCs indicated that MeGC-Col hydrogel had the ability to promote bone regeneration (76). Horio *et al* prepared a blend of photocrosslinkable chitosan hydrogel mixed with photocrosslinked chitosan sponges (PCSM-S) and used it for treating liver injury in rat model. *In vivo* analysis in heparinized rats with penetrating wound confirmed that PCSM-S showed increased hemostatic effect and had no adverse effects (78). Kim *et al* developed a photocrosslinked hydrogel made of chitosan-lactide-fibrinogen (CLF) as a delivery system for bone morphogenetic protein (BMP)-2 (79). Chitosan and lactide in the hydrogel controlled the physiochemical properties of the hydrogel (80). Fibrinogen, which contains heparin-binding domains, was added to this system to improve BMP-2 binding. The incorporation of growth factor-

binding ligands to the hydrogel was shown to maintain protein bioactivity and provide sustained release of BMP-2 over a period of time. Efficiency of the hydrogel delivery system was evaluated *in vitro* as well as *in vivo* in rat defect model. The results indicated increased cell viability, neo-osteogenesis and bone healing; the responses were dependent on the dose of the growth factor (79). To increase the bioactivity of chitosan-based hydrogels, Choi *et al* developed a photocrosslinked MeGC hydrogel containing extracellular matrix (ECM) constituents such as collagen II and chondroitin sulphate for cartilage repair. The hydrogel demonstrated the ability to promote chondrogenesis and increase cell-matrix interactions (81). Rickett *et al* used a photocrosslinked chitosan hydrogel conjugated with 4-azidobenzoic acid as an adhesive for treating peripheral nerve anastomosis. Cell culture study revealed the hydrogel to be non-toxic with excellent mechanical properties, qualities that are essential for an efficient bioadhesive (82). Photocrosslinked collagen-chitosan hydrogels were used to design contractile cardiac tissue *in vitro*. Microgrooves 10 µm, 20 µm and 100 µm in size were formed on the hydrogel using polydimethylsiloxane (PDMS) molds. The cardiomyocytes showed oriented growth with respect to the microgrooves *in vitro*. Electrical stimulations caused further alignment of the cardiomyocytes. The study showed that cardiomyocytes seeded in three dimensional hydrogels with smaller grooves (~10 µm) produced beating heart tissue *in vitro*, indicating the efficacy of the smaller features in promoting cell-cell communication. Additionally, electrical stimulation improved cell density and helped in attaining tissue morphology that could mimic the native tissue upon implantation. Finally, biodegradability of the hydrogel could contribute towards translating this engineered technique to clinical applications (83).

1.5.4. Preparation of enzymatically crosslinked injectable chitosan hydrogels

Crosslinking of polymers to form hydrogels can be performed in the presence of enzymes. This type of crosslinking is beneficial for *in situ* hydrogel formation because of the mild activity of the enzymes (84). *In situ* hydrogel systems can be easily developed using enzyme-mediated reaction as physiological pH and temperature are optimum for many enzymatic reactions. Enzymes commonly used for crosslinking chitosan to form hydrogels are peroxidase (85), transglutaminase (86) and tyrosinase (87).

Transglutaminase enzyme catalyzes the formation of isopeptide bond between glutamine's γ-amine group and the amine group of lysine. Transglutaminase is found in microbes and other living organisms. Da Silva *et al* used microbial transglutaminase (mTGase) to crosslink chitosan and gelatin for preparing hydrogel. The enzyme was used to form the bond between chitosan's glucosamine and gelatin's glutamine. Chitosan was dissolved in acetic acid and gelatin was added to prepare the chitosan-gelatin solution. Solution pH was kept at 5, where mTGase shows optimal activity. Chemical crosslinking of chitosan and gelatin was performed at 37 ^{o}C by adding mTGase in the concentration range of 10-40 enzymatic units depending on the amount of gelatin used. Thermal deactivation of mTGase was then performed at 70 ^{o}C. Gelation time was found to be dependent on mTGase concentration; the higher the enzyme concentration, the lower was the gelation time. Mechanical property of the hydrogel was found to be dependent on the concentration of chitosan and mTGase. Increase in chitosan concentration led to gels with higher moduli. Instead of chemical crosslinking alone, physical-*co*-chemical gelation of the solution led to the formation of homogenous gels with higher modulus and gel transparency (86).

Tyrosinase is an enzyme derived from both plants and animals (84). It is known to catalyze the oxidation of phenol compounds containing tyrosine and other residues into o-quinones. Kang

et al used tyrosinase enzyme for crosslinking chitosan and silk fibroin. Chitosan solution was prepared by dissolving chitosan granules in water and adjusting the pH to 2 using hydrochloric acid. Prior to crosslinking, pH of the chitosan solution was adjusted to 5-5.5, which is required for tyrosinase activity. Silk fibroin solution was dissolved in a solution comprising of calcium chloride, ethanol and water, followed by dialysis and filtration. Chitosan and silk fibroin solutions were mixed together in different ratios and tyrosinase was added to the solution to initiate gelation. Chemical crosslinking was confirmed using UV spectroscopy. The mechanism behind crosslinking is that tyrosinase enzyme converts tyrosyl residues in silk fibroin to reactive o-quinones. The amine group in the chitosan then reacts with the o-quinones in silk fibroin through Michael addition reaction (87).

Horse radish peroxidase (HRP) enzyme is the most commonly used peroxidase enzyme for enzymatic crosslinking. Peroxidase enzyme oxidizes phenols and generates free radicals that mediate the crosslinking reaction. Sakai *et al* designed chitosan hydrogels using chitosan conjugated with 3-(4-hydroxyphenyl) propionic acid (HPP) prepared via standard EDC coupling reaction. The conjugated polymer showed limited solubility, so it was first dissolved in MES buffer with a pH of 3.5. The pH was then adjusted to pH 7 by using 1 M sodium hydroxide. The hydrogels were prepared by mixing the conjugated chitosan with HRP followed by chilled H_2O_2 solution. Gelation time of the hydrogel was found to be dependent on many factors such as concentration of HRP, H_2O_2, phenol groups present in the polymer, and temperature (85). Jin *et al* developed a biodegradable injectable hydrogel prepared from chitosan-*graft*-glycolic acid (GA) and phloretic acid (PA) using enzymatic crosslinking in the presence of HRP and H_2O_2 as scaffold for cartilage regeneration. Briefly, the hydrogel was prepared by adding HRP and H_2O_2 to the CS-GA/PA solution. CS-GA/PA concentration was shown to significantly affect the gelation time; increase in

the polymer concentration from 1 to 3 wt% decreased the gelation time from 4 min to 10 s. Similarly, water uptake by the hydrogel decreased with an increase in polymer concentration, which has been attributed to the increase in crosslinking density at higher polymer concentrations. The hydrogel also exhibited pH-dependent swelling behavior. Storage modulus of the hydrogel was between 1.3 and 5.5 kPa for 1 and 2 wt% polymer solution. Thus, the study indicated that the physiochemical and mechanical properties of the hydrogel could be tailored by varying the initial polymer concentration (88). Gohil *et al* recently reported the feasibility of developing enzymatically crosslinked injectable hydrogel using water soluble GC. GC modified with HPP using EDC/NHS chemistry was treated with HRP and H_2O_2 to initiate oxidative coupling of the phenol moieties. Similar to the previous study, the GC gel also showed an increase in storage modulus with increasing polymer concentration. SEM analysis showed that the hydrogel had a porous microstructure (89).

1.5.4.1. Biomedical applications

Chen *et al* used sulfated chitosan hydrogel prepared by enzymatic crosslinking for tissue engineering application. Sulfated chitosan modified with HPP was crosslinked with HRP and H_2O_2. *In vitro* test showed that the hydrogel had no cytotoxicity towards human umbilical vein endothelial cells (HUVECs). *In vivo* test on animal model showed no thrombus formation and good tissue compatibility showing its potential for tissue application (90). Jin *et al* used an injectable chitosan hydrogel for cartilage application. Chondrocytes cultured in the hydrogel showed cell viability and remained round for up to 2 weeks. The hydrogel also exhibited biodegradability in the presence of lysozyme (88). *In vitro* study of the hydrogel prepared by Gohil *et al* via enzymatic crosslinking of HPP-GC demonstrated excellent viability of encapsulated 7F2 osteoblast cells, demonstrating the hydrogel's cytocompatibility (89). *In vivo* study was performed

in Col3.6 transgenic fluorescent mice by creating bilateral critical size calvarial bone defect to evaluate the efficacy of the gel to locally deliver BMP in a biologically active form. The study showed that the hydrogels maintained bioactivity of recombinant BMP-2, supported cell-mediated mineralization, and led to complete regeneration of critical size defect. (89). Although the study showed the feasibility of developing an HPP-GC-based injectable system for growth factor delivery, it had a few demerits. *In vivo* study showed that at even at 8 weeks (Figure 1.6), there was a considerable residue of hydrogel present in the defect area. Another issue was the lack of spreading of the encapsulated osteoblasts in the hydrogel despite their excellent viability.

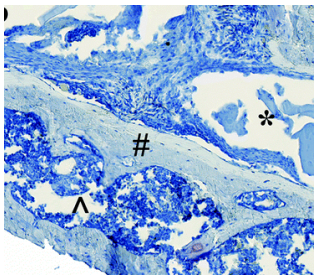

Figure 1.6: Shows the hematoxylin-stained critical size defect after 8 weeks. '*'indicates non-degraded hydrogel (89)

1.6. Conclusion

Chitosan, which is a deacetylated derivative of chitin, is a versatile polymer with inherent properties including biocompatibility, antimicrobial activity, mucoadhesivity, biodegradability and low toxicity. It is extensively used for a wide range of biomedical applications like tissue engineering and drug delivery. Chitosan polymer can be used for developing hydrogels via physical and chemical crosslinking methods. Recent studies show the feasibility of forming injectable hydrogels *in situ*. Injectable hydrogels are easy to handle, are minimally invasive, and easily fill up the defect area. Injectable hydrogels can be of different types such as thermogelling, pH-activated, photocrosslinked and enzymatically crosslinked. Enzyme-based crosslinking is

generally considered mild, nontoxic and biocompatible. A previous study performed in our group demonstrated the feasibility of developing injectable HPP-GC hydrogels that can be enzymatically crosslinked using HRP and H_2O_2. The study showed the ability of the hydrogels to retain the viability of encapsulated cells. Moreover, the hydrogels showed a unique advantage to locally present bioactive molecules such as BMP in a highly active manner to support complete regeneration of critical size calvarial model in a spatially controlled manner. The injectable system however, presented some limitations. One of the limitations was the lack of degradation of the matrix, which can adversely affect tissue regeneration. Another limitation was the lack of cell spreading in the hydrogel, which may adversely affect the functions of adherent cells such as osteoblasts. The studies described in Chapters 2-4 have been designed to address these two limitations of enzymatically crosslinked HPP-GC hydrogels.

CHAPTER 2: DEVELOPMENT OF INJECTABLE HYDROGELS FROM GLYCOL CHITOSAN AND ACETYLATED GLYCOL CHITOSAN

2.1. Introduction

2.1.1. Glycol chitosan

Glycol chitosan (GC) is a water soluble derivative of chitosan that contains a glycol functional group at the site of the C-6 hydroxyl group (Figure 2.1). The glycol moiety is responsible for the water soluble nature of this derivative and for retaining all the desired properties of chitosan at the same time (89). GC can be prepared by reacting chitin with ethylene oxide and then deacetylating the resulting polymer (91). GC maintains its amine group, which helps in further modification of the polymer for different biomedical applications (92). Extensive research has been carried out on GC in the last 10 years or so for various therapeutic applications such as growth factor delivery (89), cell based therapies (92), nanoparticle carrier for anticancer drugs, peptides (93), gene transfection (94), and as nanoprobes for cancer diagnosis (95).

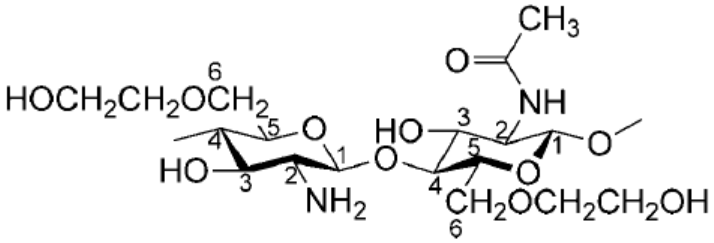

Figure 2.1: Structure of glycol chitosan (91)

2.1.2. Literature review on glycol chitosan

Due to excellent water solubility, GC has been used in various forms such as hydrogels, coatings, nanoparticles, and nanogels for biomedical applications. Various methods have been investigated to crosslink GC to develop hydrogels and nanoparticles. Cao *et al* developed an *in*

situ-crosslinked injectable GC hydrogel using multi-functionalized benzyaldehyde PEG analog derivative for cartilage regeneration. *In vitro* study showed chondrocyte viability as well as proliferation upon encapsulation in GC hydrogel. The hydrogel showed good biocompatibility as demonstrated by an *in vivo* subcutaneous study. The hydrogel was present *in vivo* even after 12 weeks post-implantation. (96). Anna *et al* developed a cell delivery system based on photocrosslinked MeGC for the delivery of pancreatic islets for the treatment of type 1 diabetes. In the study, they first encapsulated the cells in calcium alginate beads and then coated the beads with MeGC followed by photocrosslinking to form capsules. Coating alginate beads with MeGC improved the swelling and biocompatibility properties of the beads. *In vit*ro encapsulation study demonstrated sustained and controlled release of insulin over a period of time as well as viability of islet cells in MeGC-coated alginate beads. *In vivo* results showed the biocompatible nature of the MeGC-coated alginate capsules when compared to alginate/poly-l-ornithine/alginate capsules (92). Yoon *et al* used self-assembled amphiphilic GC-5β-cholanic acid-conjugated nanoparticles as a delivery system for the treatment of cancer. The study demonstrated the feasibility of encapsulating doxorubicin and Bcl-2 siRNA in GC nanoparticles. The *in vivo* study showed a dose-dependent release of the drug from the nanoparticles and desirable biodistribution, factors that are essential for cancer treatment (97). For siRNA delivery, Periera *et al* developed a self-assembled GC-based nanogel system that was synthesized by grafting hydrophobic chains. When incubated with HeLa cells, the GC nanogel was detected on the surface of the cells and was non-toxic to the cells. Thus, the GC nanogel demonstrated the potential to be developed as a targetable siRNA vehicle (98).

Our laboratory developed an enzymatically crosslinked injectable GC hydrogel as a cell and growth factor delivery system for regenerative engineering application as discussed in section

1.5.4.1. *In vivo* study was performed on Col3.6 transgenic fluorescent reporter mouse model. Retention of bioactivity of recombinant human BMP-2 was observed in GC-based hydrogels in bilateral critical size calvarial bone defects. The study demonstrated osteoinductivity of rhBMP-2, as indicated by the presence of fluorescent osteoblast cells migrating to the defect area and by the evidence of wound closure in 8 weeks (89). As discussed in Chapter 1, even though the enzymatically crosslinked GC hydrogel showed good cytocompatibility and the ability to retain the growth factors in the hydrogel in a bioactive form, the *in vivo* study demonstrated a lack of degradation of the hydrogel, which limited the extent of tissue growth. The purpose of the study discussed in this chapter is to further characterize the GC hydrogel and to evaluate the feasibility of chemically modifying GC to increase its enzymatic degradability. This chapter focuses on the sterilization of GC and the development of novel acetylated derivatives of enzymatically crosslinked GC hydrogels for biomedical applications.

2.2. Materials and methods

2.2.1. Materials

The following items and chemicals were used for carrying out the experiments: GC (Sigma Aldrich), morpholinoethanesulfonic acid (MES) powder (Fisher), N-3-dimethylaminopropyl-N-ethyl carbodiimide hydrochloride (EDC) (Sigma Aldrich), N-hydroxysuccinimide (98%) (NHS) (Sigma Aldrich), 3-(4-hydroxyphenyl) propionic acid (98%) (HPP) (Sigma Aldrich), horseradish peroxidase (HRP) (Sigma Aldrich), hydrogen peroxide (Sigma Aldrich), acetic anhydride (Sigma Aldrich), dialysis membrane (Spectra/por7), FITC-albumin (Sigma Aldrich), lysozyme from chicken egg white (Sigma Aldrich), α-MEM media (colorless) (Life Technologies), U100 insulin syringe (Becton Dickinson), LIVE/DEAD® viability/cytotoxicity kit (Life Technologies), deuterium oxide (Cambridge isotope laboratories, Inc) and 7F2 cells (ATCC CRL-12557).

2.2.2. Preparation of HPP-modified glycol chitosan polymers

HPP modification was done on GC using carbodiimide-based coupling reaction. For preparing a batch of HPP-modified GC (HPP-GC) polymers, 500 mg of GC was dissolved in 350 mL of 1 M MES solution (pH 5.5) by stirring at room temperature (RT) for 3 h. For HPP-coupling, EDC (2.608 mmol) and NHS (2.172 mmol) were dissolved in 50 mL of 1 M MES solution for 5 min, followed by the addition of HPP (3.009 mmol) and reaction at RT for 1 h. This solution was then added to the solution containing GC and kept for 24 h at RT. The final solution was then dialyzed against water using dialysis tubings with cut-off size of 10,000 Da. Dialysis was carried out for 3 days during which the water was changed 6 times. After dialysis, the solution was allowed to freeze at -20^{o}C. The frozen solution was then lyophilized for 3 days and stored at -20^{o}C (89).

2.2.3. Sterilization of HPP-modified glycol chitosan polymers

The following different methods were used for sterilizing the HPP-GC solution:

a) *Filtration*: The lyophilized HPP-GC polymer was dissolved in MilliQ water and filtered using membranes with pore sizes of 0.45 µm and 0.22 µm. The filtered solution was frozen at -20 ^{o}C followed by lyophilization for 3 days.

b) *UV:* HPP-GC solution at a concentration of 20 mg/mL was prepared and an aliquot of 500 µL was taken in a microcentifuge tube and exposed to UV-B light for 30 min.

c) *Autoclaving:* Two different methods were used. In the first method, 40 mg of lyophilized HPP-GC polymer was autoclaved directly at 121 ^{o}C and 15 psi for 30 min. In the second method, 40 mg of lyophilized HPP-GC was dissolved in 2 mL of α-MEM at a concentration of 20 mg/mL. The solution was then autoclaved at 121 ^{o}C and 15 psi for 30 min.

2.2.4. Preparation of HPP-modified glycol chitosan hydrogels

HPP-GC polymer was dissolved in α-MEM at a concentration of 20 mg/mL. 20 units of HRP was added to the solution and mixed uniformly. To prepare the hydrogel, enzymatic crosslinking of the polymer solution containing HRP was done using H_2O_2 added at a concentration of 7.34 mM. This procedure was followed for both sterilized as well as unsterilized HPP-GC polymers.

2.2.5. Rheological characterization of HPP-modified glycol chitosan hydrogels

HPP-GC polymer was sterilized as described in section 2.2.3. 100 µL of the polymer solution containing HRP was then enzymatically crosslinked in syringe molds as described in section 2.2.4. Rheological properties of the sterilized, preformed HPP-GC hydrogel was determined using Discovery HR3 hybrid rheometer (TA instruments), with parallel plate geometry (12 mm), gap width of 600 µm, and frequency sweep from 0.1 to 100 rad s^{-1} at a strain of 5%. Three hydrogel samples were tested for each polymer (n=3).

2.2.6. Acetylation of HPP-modified glycol chitosan polymers

The lyophilized HPP-GC polymer (from section 2.2.2) was used for making acetylated HPP-GC polymer. 100 mg of lyophilized HPP-GC polymer was weighed out and first dissolved in 2 mL of distilled water under stirring. To this, 4 mL of methanol was added and mixed well. Acetic anhydride solution was prepared by adding acetic anhydride to 4 mL of methanol and mixing thoroughly under the fume hood. The acetic anhydride solution was added dropwise to the HPP-GC solution and allowed to react for 24 h under stirring. Different sets of acetylated polymers were prepared and labeled as 0GC, 0.1GC, 0.2GC, 0.3GC, 0.5GC and 1GC, where the numbers

represent the molar ratio of acetic anhydride added (Table 2.1) to amine groups present in completely deacetylated GC (Appendix A1). Samples of 0GC, 0.1GC, 0.2GC and 0.3GC were prepared using bench-top stirring. To ensure uniform mixing and to avoid gel formation during mixing, overhead stirring method was used for samples of 0.5GC and 1GC. The sample was purified using dialysis against water for 3 days with 6 changes of water. After dialysis, the solution was frozen overnight at -20 ^{o}C, lyophilized for 3 days and then kept at -20^{o}C for long term storage.

Table 2.1: Shows the amount of acetic anhydride used for different acetylated HPP-GC samples

Acetylated GC	**Acetic anhydride**	
	Volume	**Moles**
0GC	-	-
0.1GC	4.6 µL	48. 7 µmol
0.2GC	9.2 µL	97. 3 µmol
0.3GC	13.8 µL	146.0 µmol
0.5GC	23 µL	243.3 µmol
1GC	46 µL	487.3 µmol

2.2.7. Characterization of acetylated HPP-modified glycol chitosan polymers

2.2.7a. Attenuated total reflectance-Fourier transform infrared spectroscopy (ATR-FTIR)

ATR-FTIR was performed using Nicolet iS10 spectrophotometer (Thermoscientific) with SMART iTR diamond ATR accessory. Spectra for the different acetylated HPP-GC polymers were obtained between wavenumbers of 400 and 4000 cm^{-1} at a resolution of 2 cm^{-1}. 200 scans were collected during each FTIR run.

2.2.7b. NMR

^{1}H-NMR was performed on the acetylated HPP-GC polymer using an 800 MHz Agilent VNMRS spectrophotometer with a triple resonance HCN cold probe. Briefly, 5 mg of the

acetylated HPP-GC polymer was dissolved in 0.5 mL of deuterium oxide. ^{1}H-NMR spectra were obtained using the following parameters: 68 ^{o}C, 8992.8 Hz bandwidth, 128 transients, and 90^{o} flip angle. Mnova software (Mestrelab Research, Spain) was used for analyzing the data. Three different samples were analyzed for each polymer (n=3).

2.2.8. Preparation of acetylated HPP-modified glycol chitosan hydrogels

Acetylated HPP-GC polymer was dissolved in α-MEM at a concentration of 20 mg/mL. 20 units of HRP was added to the solution and mixed uniformly. To prepare the hydrogel, enzymatic crosslinking of the polymer solution containing HRP was done using H_2O_2 added at a concentration of 7.34 mM.

2.2.9. Swelling behavior of acetylated HPP-modified glycol chitosan hydrogels

The different acetylated HPP-GC hydrogels – 0GC, 0.1GC, 0.2GC, 0.3GC, 0.5GC and 1GC – were prepared in syringe molds as described in section 2.2.8. Four hydrogel samples were tested for each polymer (n=4). Hydrogels prepared from 150 µL of the respective polymer solutions were weighed in glass vials (W_{si}) and incubated in PBS in a shaker at 37 ^{o}C. Weights of the hydrogels with the vials were determined after removing excess PBS (W_{sf}) at days 1, 3, 5, 7 and 14. The PBS removed was replaced with fresh PBS after the measurement at each time point. The swelling ratio was determined using the following equation [2]:

$$\%Swelling = \frac{W_{sf} - W_{si}}{W_{si}} \times 100 - - - - - [2]$$

2.2.10. Protein release profile from acetylated HPP-modified glycol chitosan hydrogels

Hydrogels prepared from acetylated HPP-GC polymers – 0GC, 0.1GC, 0.3GC, 0.5GC and 1GC – were used for the protein release study. First, a stock solution with a polymer concentration of 40 mg/mL was prepared in sterile water. For loaded samples, 1.5 mL of the polymer stock solution was mixed with 0.75 mL of FITC-albumin stock solution (20 mg/mL), 0.75 mL of α-MEM, and 60 units of HRP. For unloaded samples, 0.5 mL of the polymer stock solution was mixed with 0.5 mL of α-MEM and 20 units of HRP. Disc-shaped hydrogel was then prepared by mixing 162 µL of loaded or unloaded polymer solution in a syringe mold with H_2O_2. The H_2O_2 concentration in the final solution was 8.17 mM. Four hydrogel samples were tested for each polymer (n=4). The loaded and unloaded hydrogel samples were then placed in 3 mL of i) 10 µg/mL lysozyme in PBS containing 1% Anti-Anti ii) 50 µg/mL lysozyme in PBS containing 1% Anti-Anti and iii) PBS containing 1% Anti-Anti. The samples were then incubated in a shaker at 37 ^{o}C. At each time point, 1.5 mL of PBS with lysozyme or PBS alone were removed from each sample and replaced with a fresh batch of the respective solutions. Time points used for the study were: 1 h, 3 h, 16 h, 24 h, 38 h, 48 h, 72 h, 96 h, 120 h, and 144 h. FITC release was measured in a plate reader at 495 nm. A standard curve was plotted using serial dilution of solution containing 400 µg/mL of FITC-albumin.

2.2.11. Viability and spreading of osteoblast cells encapsulated in acetylated HPP-modified glycol chitosan hydrogels

For cytocompatability study, osteoblastic cell line 7F2 (derived from mouse bone marrow) was used. Cells were grown and maintained in α-MEM (2 mM L-glutamine, 1 mM sodium pyruvate, with no ribonucleosides and deoxyribonucleosides) with 10% horse serum and 1% penicillin-streptomycin (pen-strep). The acetylated HPP-GC polymer was dissolved in α-MEM at

a concentration of 20 mg/mL and sterilized under UV light for 30 min prior to the cell encapsulation step. Cells were trypsinized and suspended in the acetylated HPP-GC polymer solution with 20 units/mL of HRP at a cell density of 0.8 million/mL. 10 µL of polymer solution containing HRP and cells was taken in a syringe mold and mixed with H_2O_2. The H_2O_2 concentration in the final solution was 7.34 mM. The hydrogel with encapsulated cells was incubated in Costar® ultra-low attachment plate with media at 37 ^oC and 5% CO_2. Media was changed every 3 days to keep the cells healthy. At specific time points, the hydrogel with encapsulated cells was transferred to MatTek glass-bottom 35 mm dish and stained using LIVE/DEAD® viability/cytotoxicity kit for mammalian cells. Confocal microscopy imaging was done using a Zeiss LSM 510 Meta microscope.

2.2.12. Statistical analysis

All results presented in the chapter are expressed as mean ± standard deviation. Statistical analysis was done using One-way ANOVA followed by Student's Newman-Keuls (SNK) test in SigmaStat (ver 2.3). Statistical significance was set at $p < 0.05$.

2.3. Results and discussion

2.3.1. Synthesis of HPP-modified glycol chitosan and characterization of sterilization method for regenerative application

HPP-GC was prepared using the method described by Gohil *et al* (89). HPP, which contains the phenol group, was added to GC using standard carbodiimide chemistry. The modification happens in two steps – i) EDC activates the carboxyl group of HPP, which leads to the formation of an active intermediate called O-acylisourea ii) which then reacts with the primary amine groups present in GC and forms HPP-GC. Incorporating the phenolic group in GC helps in

developing an enzymatically crosslinked injectable hydrogel system that can gel in physiological conditions (89). The HRP-catalyzed crosslinking of phenol-rich polymers is extensively investigated due to the ability of the process to form hydrogels with desirable and tunable properties (99). Figure 2.2 explains HPP addition to GC based on standard carbodiimide chemistry.

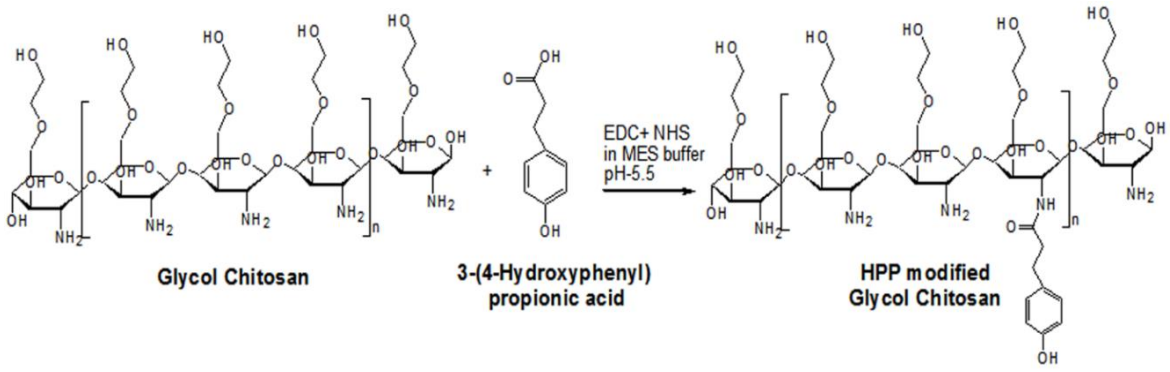

Figure 2.2: Schematic diagram of HPP-GC synthesis (89)

HPP-GC retains the excellent aqueous solubility of GC and can be dissolved in aqueous media at physiological pH. Gohil *et al* used a 1:1 (v/v) solution of water and α-MEM (89). In order to optimize the HPP-GC hydrogels for cell encapsulation, the HPP-GC polymer was dissolved in α-MEM in the present study. To understand the effect of the dissolution media on the pH of the HPP-GC solution, the pH of the solution at a concentration of 20 mg/mL was measured at RT. The pH of HPP-GC dissolved in 1:1 solution of water and α-MEM was found to be 6.97 ± 0.045 and the pH of HPP-GC dissolved in α-MEM was found to be 7.12 ± 0.046. Based on the data, both solutions showed neutral pH and hence may be acceptable for hydrogel preparation. However, for the cell encapsulation study, dissolving HPP-GC in α-MEM may be more beneficial for providing appropriate amount of nutrients.

Any biomaterial to be used for human implantation or any regenerative application must be sterilized in order to avoid bacterial and fungal contamination (100). Since HPP-GC is

developed as an injectable hydrogel, sterilization is very important before using it in biomedical applications. Even though different sterilization methods are available, the mode of sterilization has been shown to affect the physiochemical properties and functionality of polymeric materials (101). Hence, selecting a suitable sterilization procedure that causes minimal variation in the physiochemical and functional properties is essential. For biopolymer solutions, the most commonly used sterilization methods include filter sterilization, UV sterilization (102) and autoclaving. The effect of these different sterilization methods on HPP-GC was studied and the best method was determined by testing gelation after the treatment and by comparing rheological properties to those of unsterilized HPP-GC. The different methods tested for HPP-GC sterilization are i) membrane filtration using 0.45 µm filter ii) membrane filtration using 0.22 µm filters iii) UV-B sterilization of HPP-GC polymer solution iv) autoclaving the lyophilized HPP-GC powder and autoclaving the HPP-GC polymer solution prepared in α-MEM. Figure 2.3 shows the appearance of unsterilized and sterilized HPP-GCs.

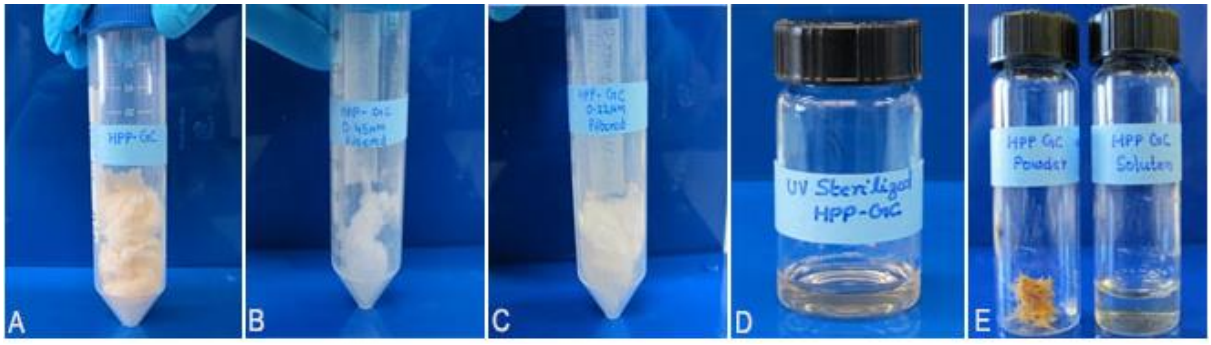

Figure 2.3: (A) Untreated HPP-GC (B) Filtered (0.45 µm) and lyophilized HPP-GC (C) Filtered (0.22 µm) and lyophilized HPP-GC (D) UV-sterilized HPP-GC solution (E) Autoclaved HPP-GC powder (left) and autoclaved HPP-GC solution (right)

Figures 2.3B and C show HPP-GC solution filtered through filters with pores of size 0.45 µm and 0.22 µm. Filtering followed by lyophilization of the polymer solution did not significantly

affect the appearance of the HPP-GC. Similarly, as seen in Figure 2.3D, the UV-sterilized polymer solution did not show any change in its appearance as well.

However, autoclaving the HPP-GC powder and solution showed significant changes in their properties. The autoclaving seemed to char the polymer (Figure 2.3E [left]). Autoclaving the HPP-GC solution on the other hand led to the formation of an insoluble polymer film in the tube (Figure 2.3E [right]). Based on these observations, it was concluded that autoclaving in powder or solution form is not a feasible sterilization method for HPP-GC. The filter-sterilized and UV-sterilized polymer solutions were further tested for gelation and rheological properties to identify the most suitable sterilization process for the *in vitro* studies.

The sterilized samples were dissolved in α-MEM at a concentration of 20 mg/mL. Appropriate volume of HRP was added to the solution to adjust its concentration to 20 units/mL. Enzymatically crosslinked hydrogel was formed by the addition of H_2O_2 to the HPP-GC/HRP solution. The H_2O_2 concentration in the final solution was 7.34 mM. The gelation process is mediated by the reaction of heme group present in HRP with H_2O_2, forming a complex of porphyrin-based cationic radical and oxoferryl center. The complex formed then acts as a reducing agent and gets oxidized by reacting with the phenolic oxidizing agent. Thereafter, the two phenolic radicals react to form a covalently crosslinked network. Crosslinking can be of two types – i) C-C covalent bond between aromatic rings of ortho-carbon groups or ii) C-O bond between phenolic oxygen and ortho-carbon of aromatic ring (89).

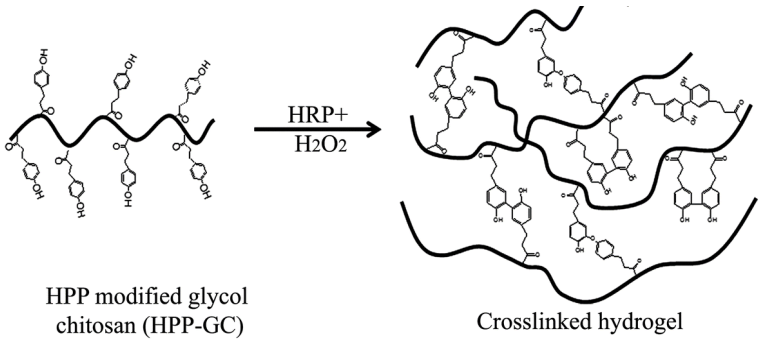

Figure 2.4: Schematic representation of enzymatic crosslinking in HPP-GC hydrogel (89)

For testing gelation, 200 µL of sterilized polymer solution containing HRP was gelled in a glass vial by adding H_2O_2. Hydrogel formation was confirmed by the vial inversion method. Unsterilized HPP-GC was used as the control. MTT [3-(4, 5-dimethylthiazol-2-yl)-2, 5-diphenyltetrazolium bromide] was added to impart color to the solution for better visualization of gel formation. As shown in Figure 2.5, all sterilized samples showed gelation within 1 min similar to the unsterilized sample accompanied by some water loss (synersis). The data demonstrate the potential of all the sterilized samples to undergo gelation under the standard conditions.

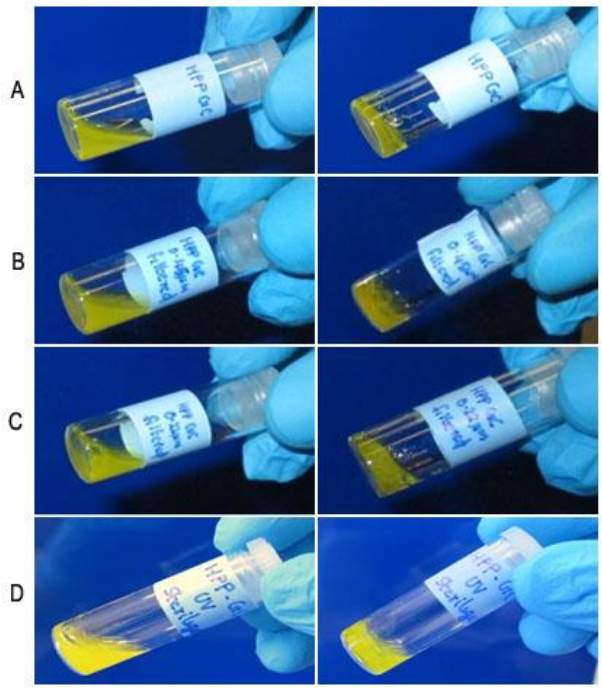

Figure 2.5: Left side shows free-flowing polymer solution and right side shows corresponding hydrogel formation on addition of HRP and H_2O_2 (A) HPP-GC (B) Filter-sterilized HPP-GC (0.45 µm) (C) Filter-sterilized HPP-GC (0.22 µm) (D) UV-sterilized HPP-GC

Further characterization of the sterilized samples was performed by following the rheological behavior of the gels. Frequency sweep was performed on the preformed hydrogels with 5% strain. Figure 2.6 shows the storage modulus of the preformed gels prepared from solutions sterilized by different methods. Storage modulus of unsterilized HPP-GC hydrogel was found to be 890.89 ± 78.69 Pa, whereas hydrogel formed from HPP-GC solution filtered using 0.45 µm filter showed a modulus of 195.33 ± 10.41 Pa and that formed from HPP-GC solution filtered using 0.22 µm filter showed a modulus of 183.69 ± 19.82 Pa. This shows the significant decrease in modulus of hydrogels formed from filtered HPP-GC solution compared to that formed from the unfiltered solution. One potential reason for the lower moduli of the filtered hydrogels is due to the loss of high-molecular weight polymer during the filtration process. The hydrogel prepared

from the UV-sterilized polymer solution on the other hand showed a modulus of 656.71 ± 46.84 Pa, which is significantly higher than that observed with the filter-sterilized solutions. However, as shown in the Figure 2.6, the UV-sterilized solution also showed a decrease in gel modulus compared to the unsterilized solution, indicating the possibility of some polymer degradation during the process. Based on these data, it was concluded that among the tested methods, UV sterilization is the best method to sterilize HPP-GC without significantly affecting its physical, mechanical and gelation properties.

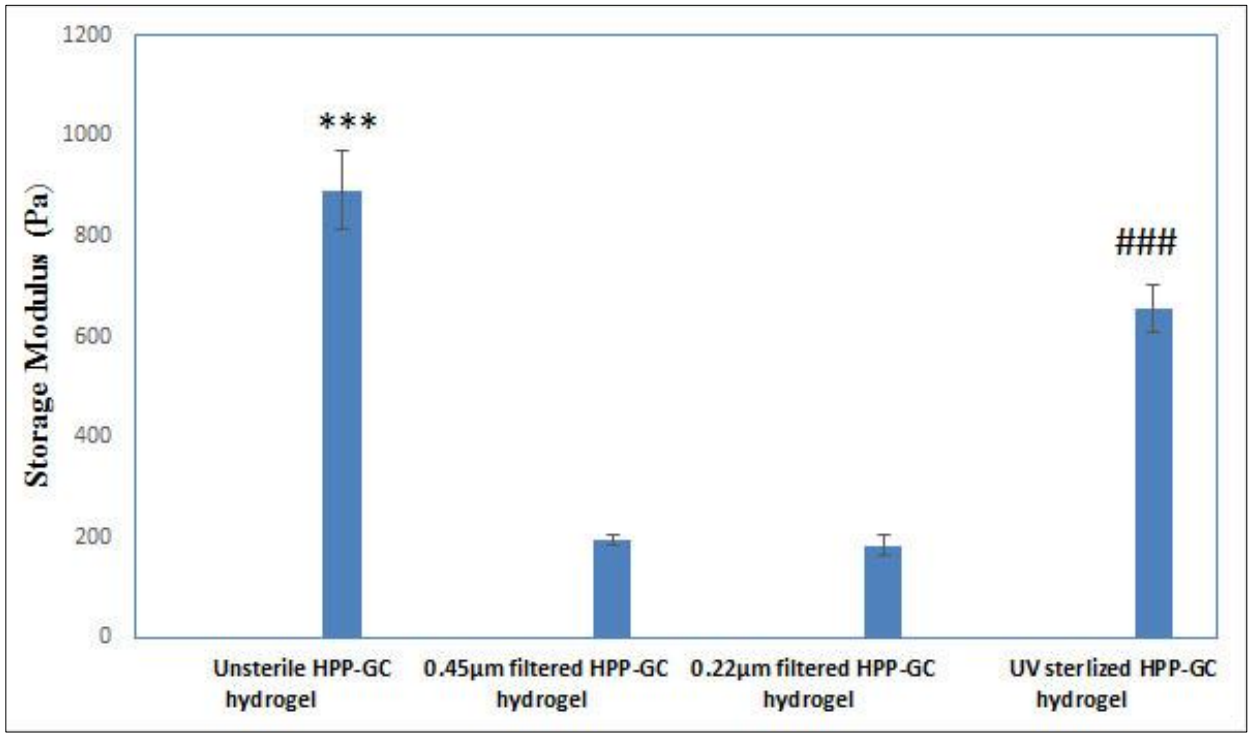

Figure 2.6: Rheological characterization of unsterilized and sterilized HPP-GC. Graph shows the storage modulus obtained by frequency sweep of corresponding hydrogel. Data are expressed as mean ± standard deviation with n=3. One way ANOVA followed by SNK test; $p^{***} < 0.001$ vs. all other groups, $p^{\#\#\#} < 0.001$ vs. all other groups

2.3.2. Synthesis and characterization of acetylated HPP-modified glycol chitosan

Acetylated HPP-GC polymer was prepared by reacting HPP-GC with acetic anhydride as discussed in section 2.2.6. Figure 2.7 shows the schematic indicating the preparation, acetylation and enzymatic crosslinking of HPP-GC.

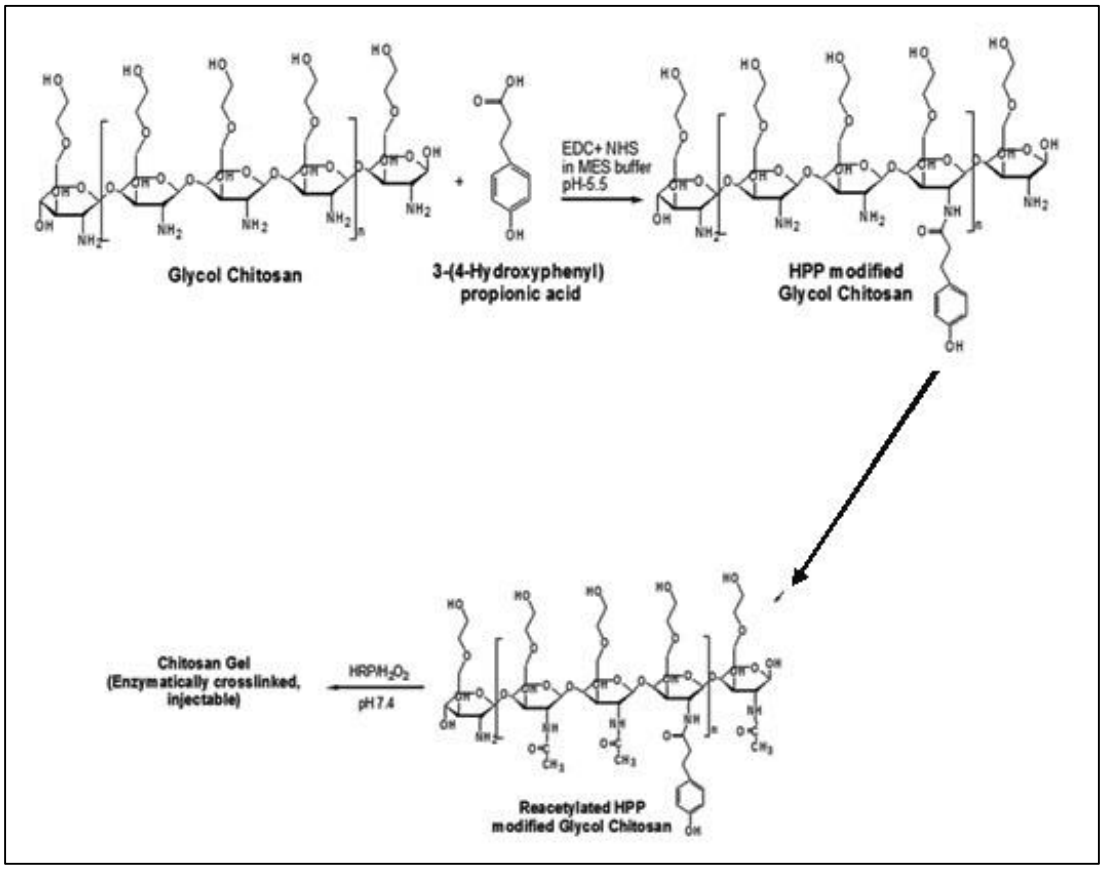

Figure 2.7: Schematic showing HPP modification of GC using carbodiimide-mediated coupling and followed by acetylation of HPP-GC

The addition of acetic anhydride causes selective N-acetylation in chitosan and is the most commonly used method for increasing the degree of acetylation (DA). The acetic anhydride-based method produces no toxic by-products and, being a mild reaction, helps in retaining and preserving

the inherent biological properties of the polymer. By varying the DA in chitosan, many properties such as biocompatibility, mechanical strength and biodegradability can be tuned (103). Different techniques are used for determining degree of deacetylation (DDA) of chitosan, including titration, FTIR, UV/Vis spectroscopy and ^{1}H-NMR (104).

ATR-FTIR spectra for the different acetylated HPP-GC polymers are given Figure 2.8. The spectra show all the characteristic peaks corresponding to GC as reported in the literature (89). In addition, the spectra of all acetylated HPP-GC polymers show a carbonyl peak at 1653 cm^{-1}, which is in agreement with spectra reported for acetylated chitosan (89, 105) The peak can be attributed to the C=O group of the amide formed upon acetylation. Increasing intensity of the peak with increase in acetic anhydride content demonstrates the increasing degree of acetylation going from 0GC to 1GC.

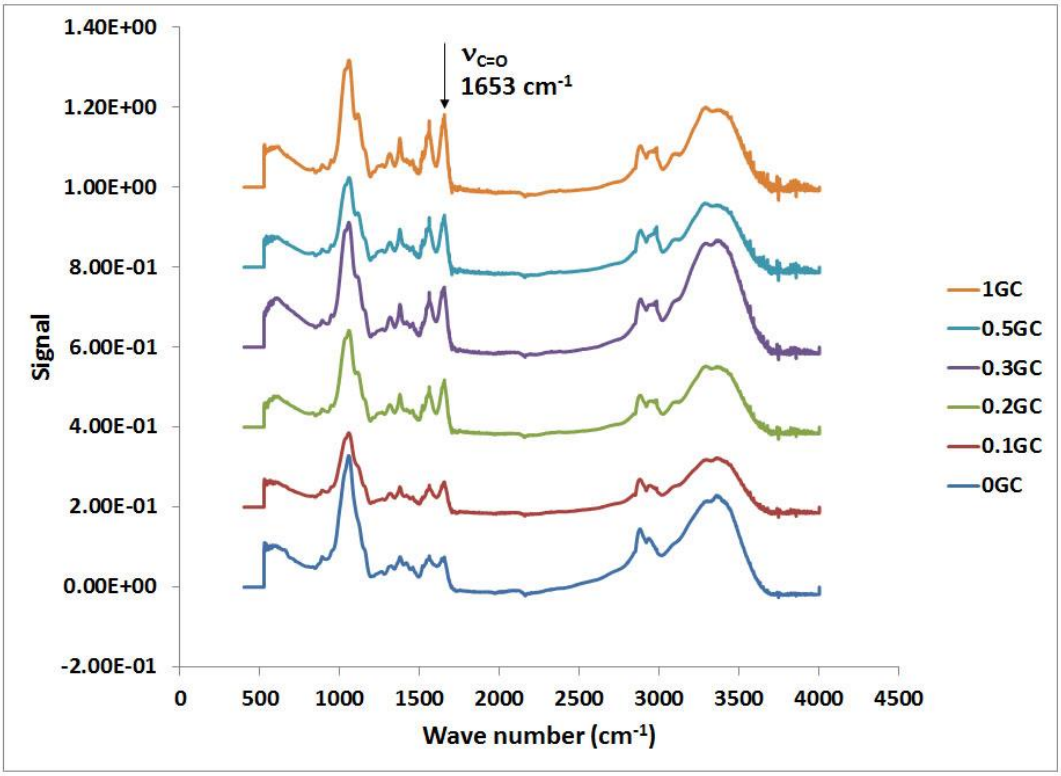

Figure 2.8: ATR-FTIR spectra of different acetylated HPP-GC polymers

Unlike FTIR, ^{1}H-NMR can be used to quantitatively determine the extent of acetylation by integrating the different proton peaks. Moreover, ^{1}H-NMR gives the most accurate and precise measurements for higher DDA as compared to the other methods. The acetylated HPP-GC polymers were characterized using ^{1}H-NMR and Figure 2.9 shows a representative ^{1}H-NMR spectrum of acetylated HPP-GC.

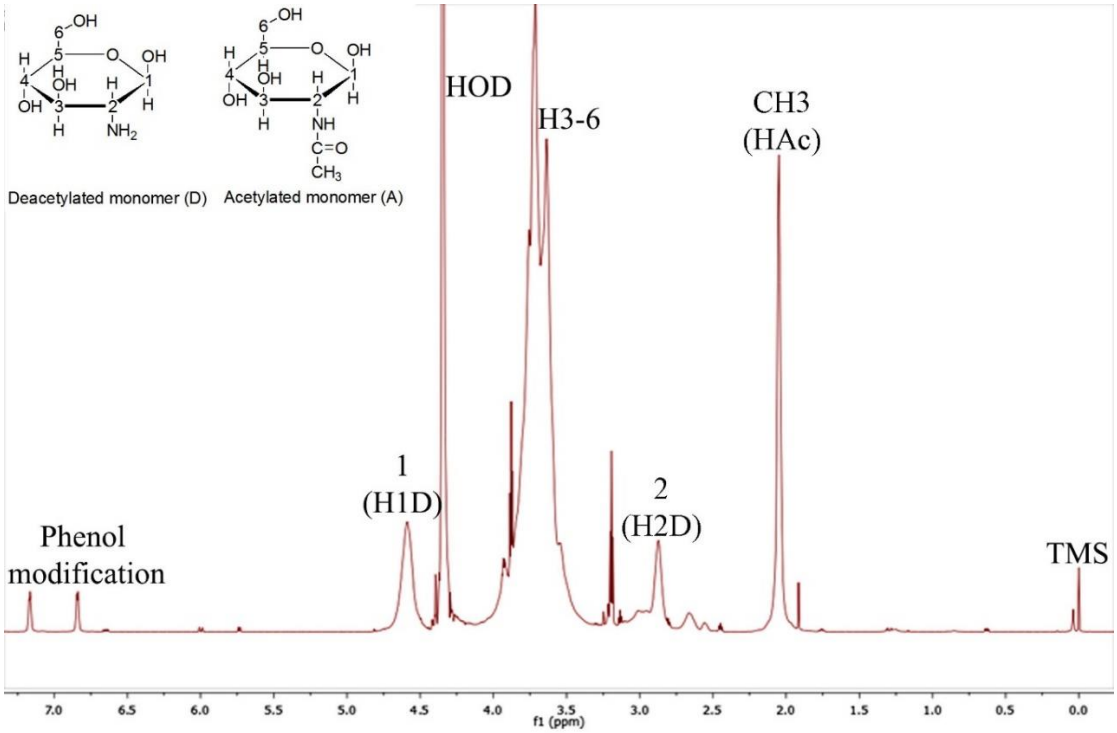

Figure 2.9: Representative ^{1}H-NMR spectrum for acetylated HPP-GC

Percentage DDA value was calculated by finding the integrals of the different proton peaks. The reference peak used was trimethyl silane (TMS), which is indicated in the spectrum. Baseline correction for all the samples was done using the Bernstein correction method. The incorporation of HPP in the polymer is indicated by the two corner peaks near 7 ppm. HOD indicates the solvent proton corresponding to deuterium oxide, which was used for dissolving HPP-GC for the NMR analysis. H1D and H2D correspond to the deacetylated monomer, HAc corresponds to the acetyl

group, and H3 to H6 correspond to the proton peaks. The equations [3] and [4] used for finding the percentage DDA value were as described by Hirai *et al* (106).

$$DDA\% = [1 - \frac{(\frac{1}{3} HAc)}{(\frac{1}{6} H2-6)}] \times 100 - - - - - [3]$$

$$DA\% = 100 - DDA\% - - - - - [4]$$

(Where H2–6 denotes the sum of integrals of the peaks H2, H3, H4, H5, H6 and H6′)

Table 2.2 shows the percentage DA values obtained for the different acetylated HPP-GC polymers. It can be seen that DA increases with increasing acetic anhydride concentration (going from 0GC to 1GC), demonstrating the dose-dependent increase in acetylation of the polymer.

Table 2.2: Percentage DDA and DA of HPP-GC as determined by NMR

Sample	**DDA%**	**DA%**
0GC	92.51 ± 0.54	7.48 ± 0.54
0.1GC	83.65 ± 1.99	16.35 ± 1.99
0.2GC	75.35 ± 3.86	24.65 ± 3.86
0.3GC	71.97 ± 0.63	28.03 ± 0.63
0.5GC	68.30 ± 1.08	31.70 ± 1.08
1GC	64.63 ± 0.69	35.36 ± 0.69

2.3.3. Gelation of acetylated HPP-modified glycol chitosan

Similar to HPP-GC polymers, acetylated HPP-GC polymers also showed gelation in less than 1 min accompanied by synersis (Figure 2.10). The data demonstrate that acetylation does not

significantly affect the HRP-mediated gelation process of HPP-GC in the presence of H_2O_2. The mechanism of gelation of acetylated HPP-GC is similar to that for HPP-GC (section 2.3.1).

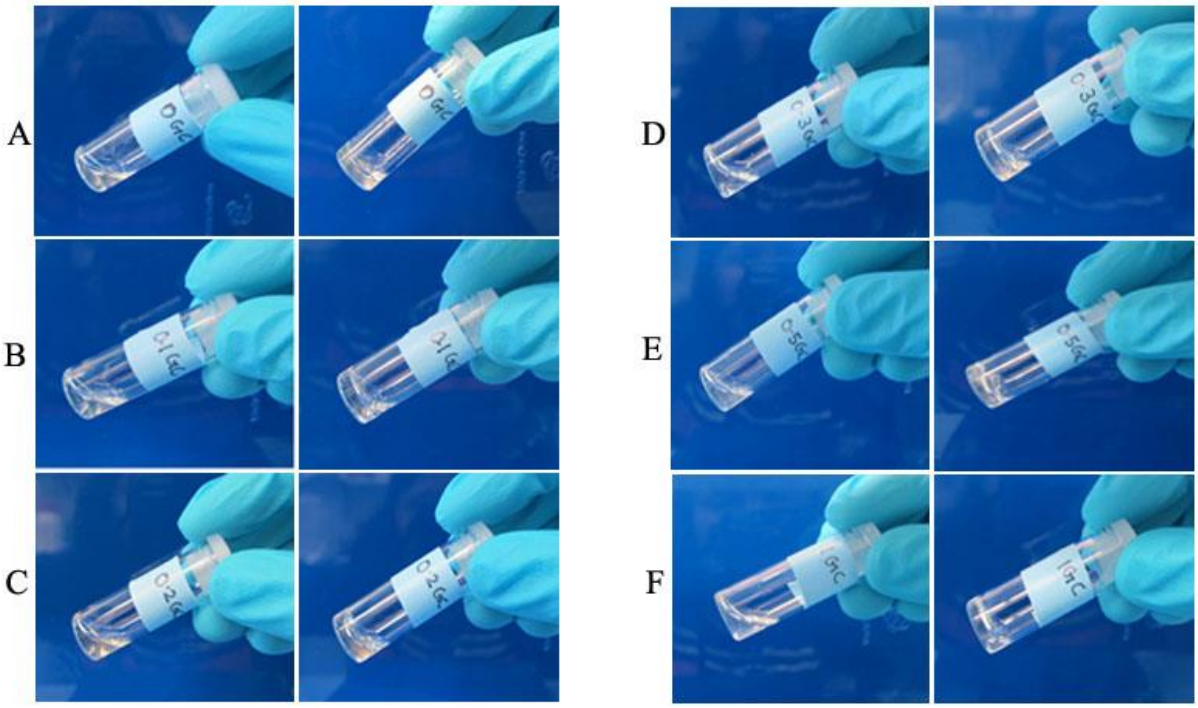

Figure 2.10: Left side shows free-flowing polymer solution and right side shows corresponding hydrogel formation on addition of HRP and H_2O_2 (A) 0GC before and after gelation (B) 0.1GC before and after gelation (C) 0.2GC before and after gelation (D) 0.3GC before and after gelation (E) 0.5GC before and after gelation (F) 1GC before and after gelation

2.3.4. Swelling behavior of acetylated HPP-modified glycol chitosan

Figure 2.11 shows the swelling behavior of the different acetylated HPP-GC hydrogels in PBS with respect to time. Table 2.3 presents the associated statistical analysis and Figure 2.12 shows a photograph of the different hydrogels at the end of the swelling test, with freshly prepared 1GC hydrogel for comparison.

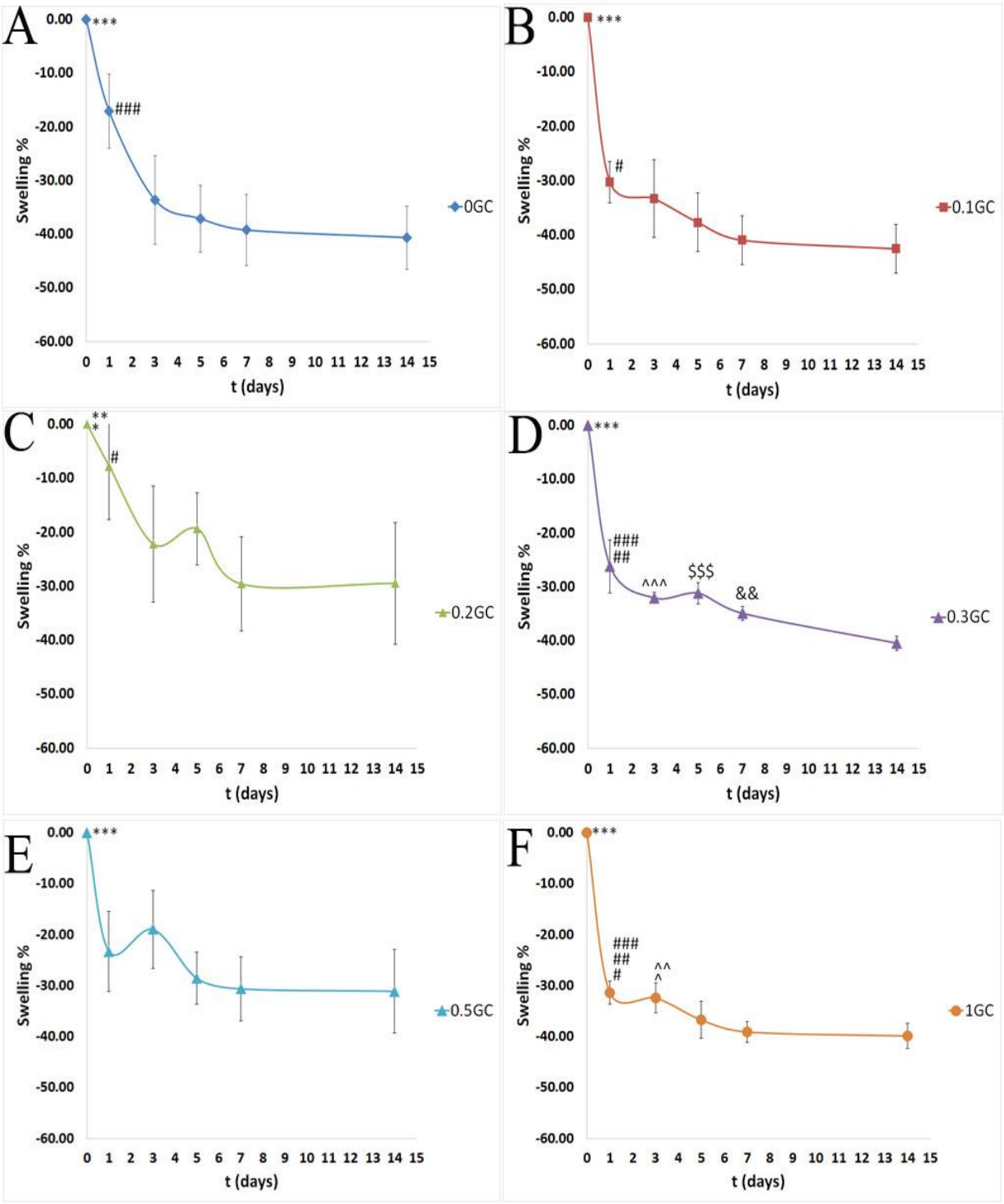

Figure 2.11: Swelling behavior of the acetylated HPP-GC hydrogels**.** Data are expressed as mean ± standard deviation with n = 4. One way Anova followed by SNK test comparing different time points within the same group. Table 2.3 shows details of the statistical analysis

Table 2.3: Statistical analysis for the acetylated HPP-GC hydrogels (Figure 2.11)

A	0GC	*p**** < 0.001 vs. days 1, 3, 5, 7, 14, *p*### < 0.001 vs. days 3, 5, 7, 14
B	0.1GC	*p**** < 0.001 vs. days 1, 3, 5, 7, 14, *p*# < 0.05 vs. days 7, 14
C	0.2GC	*p*** < 0.01 vs. days 3, 7, 14, *p** < 0.05 vs. day 5, *p*# < 0.05 vs. days 7, 14
D	0.3GC	*p**** < 0.001 vs. days 1, 3, 5, 7, 14, *p*### < 0.001 vs. days 7, 14, *p*## < 0.01 vs. days 3, 5, *p*^^^ < 0.01 vs. day 14, *p*$$$ < 0.001 vs. day 14, *p*&& < 0.01 vs. day 14
E	0.5GC	*p****<0.001 vs. days 1, 3, 5, 7, 14
F	1GC	*p**** < 0.001 vs. days 1, 3, 5, 7, 14, *p*### <0.001 vs day 14, *p*## < 0,01 vs day 7, *p*# < 0.05 vs day 5, *p*^^ < 0.01 vs. days 7, 14 , *p*^ < 0.05 vs. day 5

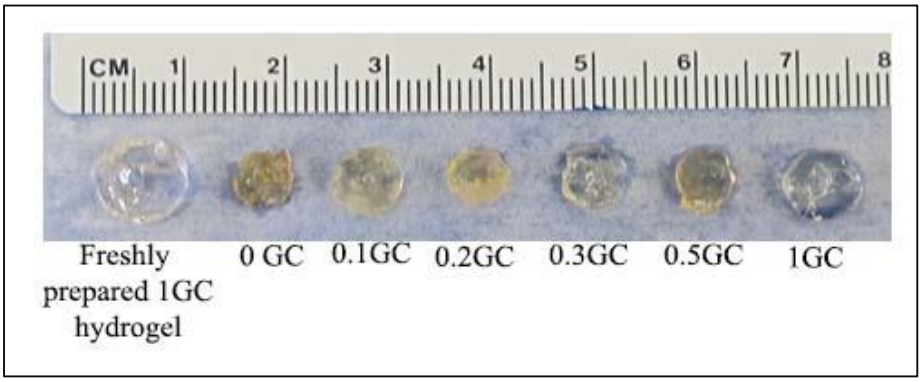

Figure 2.12: Acetylated HPP-GC hydrogels after 14 days of swelling

Swelling of the hydrogel is indicative of its ability to take up water under given conditions. Swelling properties of hydrogels depend on different factors including crosslinking density, solvent nature, temperature and pH of the solvent. However, previous studies using HPP-GC showed a decrease in weight of the hydrogels upon incubation in PBS at 37 ^{o}C (107). So, a study was undertaken to understand the swelling behavior of acetylated HPP-GC hydrogels upon incubation in PBS at 37 ^{o}C. As mentioned earlier, HPP-GC and acetylated HPP-GC hydrogels were prepared from 20 mg/mL polymer solutions containing 20 units of HRP/mL and 7.34 mM H_2O_2. As indicated by Figures 2.11 and 2.12, all acetylated HPP-GC hydrogels showed decrease

in gel weight upon incubation in PBS at 37 ^{o}C. As shown in Figure 2.11, a significant decrease in weight was observed in all the hydrogels by day 3. One potential reason is the increase in crosslinking density of the hydrogel with time at the concentration of HRP and H_2O_2 used in the present study. This is evident from the visual shrinking of the gel, indicating potential synersis with time. A previous study demonstrated that an increase in crosslinking density resulted in decrease in swelling ratio of the hydrogels. Using poly(L-glutamic acid) grafted with tyramine and PEG, the study demonstrated a decrease in the equilibrium swelling ratio of the hydrogels with increasing HRP and H_2O_2 concentrations (108). Our data demonstrate that acetylation did not significantly affect the swelling behavior of the HPP-GC hydrogels. Further studies based on our results can be focused on varying HRP and H_2O_2 concentrations in order to optimize the extent of crosslinking to modulate hydrogel behavior.

2.3.5. Protein release profile from acetylated HPP-modified glycol chitosan hydrogels

Biodegradable injectable hydrogels are investigated as drug reservoir systems that can provide controlled release of bioactive agents and proteins in a sustained manner. The efficacy of acetylated HPP-GC hydrogels to serve as protein delivery vehicle was evaluated using bovine serum albumin (BSA) as a model protein. In the present study, FITC-labeled BSA was used for ease of quantification. As discussed in section 1.4, chitosan is susceptible to degradation in the presence of lysozyme.

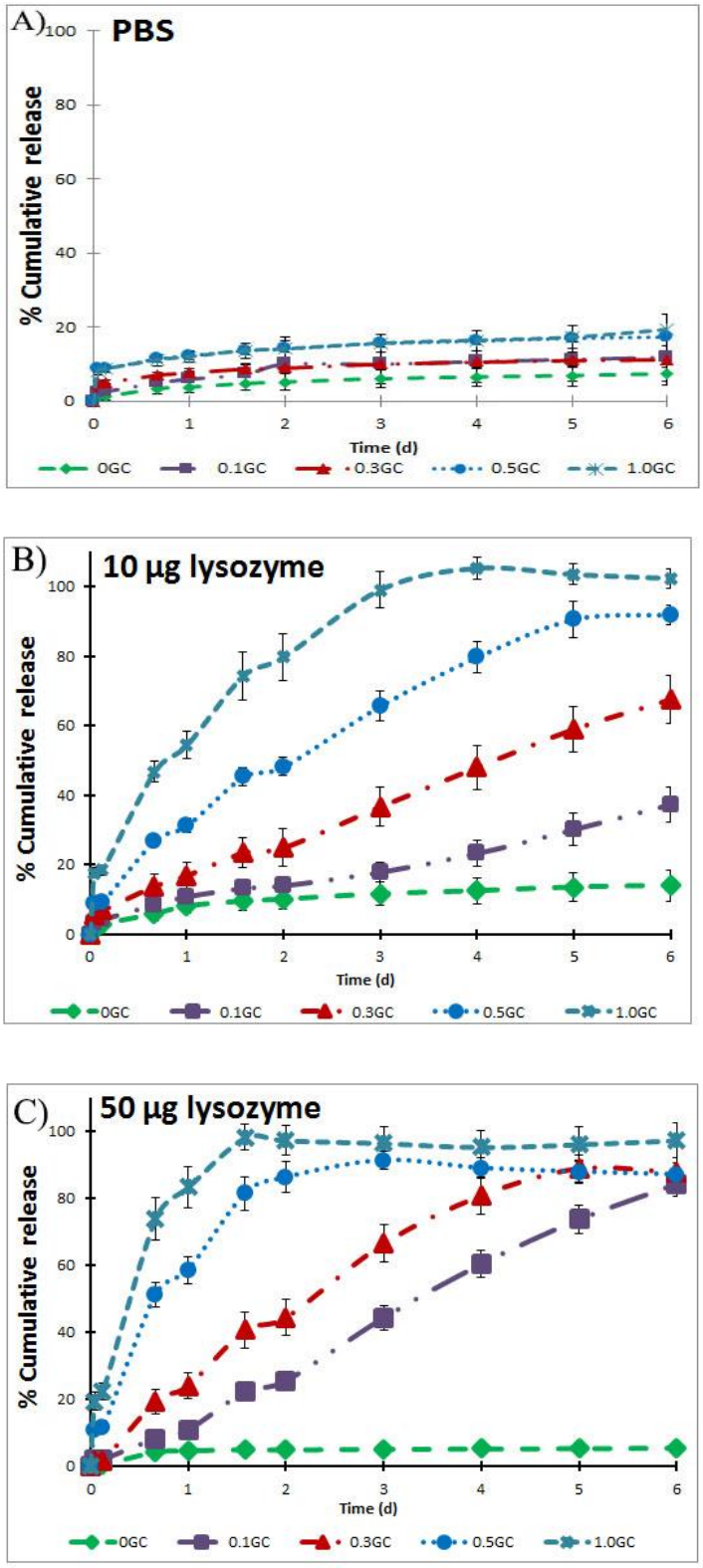

Figure 2.13: *In vitro* studies showing the release of FITC-albumin under different conditions A) PBS alone B) 10µg lysozyme in PBS and C) 50µg lysozyme in PBS (n=4)

Figure 2.13A shows the extent of release of BSA from various acetylated HPP-GC hydrogels incubated in PBS alone. All the hydrogels showed similar release profile irrespective of the extent of acetylation, with the final percentage release being between 7 and 20%. More importantly, the hydrogels showed very low release of the protein even after 6 days of incubation in PBS at 37 ^{o}C. The data indicate significant binding of the protein to the HPP-GC hydrogel irrespective of the degree of acetylation. Our previous study using alginic acid and hyaluronic acid (109) showed similar retention of BSA in these enzymatically crosslinked hydrogels. Albumin is a globular protein with several tyrosine residues and the FITC molecule also contains a phenol functional group. So, in the present study, there is a possibility that the phenol groups present in albumin are reacting with the phenol groups of HPP-GC and the protein is chemically conjugated to the gel matrix, resulting in the very low release of the protein.

Hence, another study was performed to understand whether degradation of the hydrogel could lead to the release of the bound protein in the gel. Since acetylated HPP-GC retains the bonds that are sensitive to the enzyme, it is possible that acetylated HPP-GC hydrogels will undergo degradation in the presence of lysozyme. So, the release study was performed by incubating the FITC-albumin-loaded acetylated HPP-GC hydrogels in 10 and 50 µg/mL of lysozyme-containing PBS at 37 ^{o}C. Figures 2.13B and C show the cumulative release of FITC-albumin from the hydrogels into lysozyme-containing media as a function of time. As can be seen, the presence of lysozyme made a significant difference to the release profile of the protein from the hydrogels. In the presence of 10 µg lysozyme, the 0GC hydrogel did not show significant release of FITC-albumin and showed similar release profile to that in PBS alone. However, 0.1GC showed a maximum release of FITC-albumin of ~37.27% at day 6. The 0.3GC hydrogel showed a maximum release of ~67.45% at day 6, while 0.5GC hydrogel exhibited a maximum release of ~91.93% at

day 6. The 1GC hydrogel showed complete release (~100%) at day 3. In the presence of 50 µg lysozyme, the 0GC hydrogel showed a release profile similar to that in PBS alone and PBS containing 10µg lysozyme. The 0.1GC hydrogel showed a maximum release of ~84.28% at day 6, while 0.3GC showed a higher release of ~87.70% at day 6. The 0.5GC hydrogel showed a maximum release of ~88.86% at day 4. The 1GC hydrogel showed fast release with a maximum release value of about ~97.97% in 38 h. Thus, an increase in protein release was observed with an increase in the concentration of lysozyme in the case of acetylated HPP-GC hydrogels but not in the case of the 0GC hydrogel.

The data demonstrate that in the presence of lysozyme, the release of protein from the hydrogel is highly dependent on degradation. Moreover, the concentration of lysozyme also plays a key role in the extent of release, presumably by modulating the rate of hydrogel degradation. This supports the possibility that the protein was bound to the gel and that gel degradation led to protein release. Since lysozyme is present in human body, these hydrogels can serve as a platform to develop delivery systems with tunable release profile based on the degree of acetylation of the polymer

2.3.6. Viability and spreading of osteoblast cells in encapsulated acetylated HPP-modified glycol chitosan hydrogels

Biopolymers are highly biocompatible and the mild enzymatic process makes them attractive candidates as protein and cell delivery vehicles. One of the disadvantages in using polysaccharide-based hydrogels for cell delivery is the lack of cell-adhesive groups in the polymer that can support adhesion and spreading of encapsulated cells. Our previous studies using enzymatically crosslinked alginic acid, hyaluronic acid (109) as well as HPP-GC hydrogels (89) showed the feasibility of encapsulating the cells and retaining their viability. However, the

encapsulated cells did not show spreading within the hydrogel matrix. So, a study was performed to understand the effect of acetylation on the cellular compatibility of HPP-GC hydrogels.

One of the challenges observed in terms of culturing cells in acetylated GC was the fast degradation of the hydrogels when incubated in cell culture media containing fetal bovine serum (FBS). Table 2.4 shows the behavior of acetylated HPP-GC hydrogels upon incubation in media containing FBS. The data clearly show that all the acetylated HPP-GC hydrogels underwent fast degradation in the presence of FBS. In addition to lysozyme, chitosan is known to be degradable in the presence of an enzyme called "chitinase". Like lysozyme chitinase also acts on the acetyl groups for initiating degradation. It has been reported that high level of chitinase enzyme is present in the serum of cow, hen, sheep and goat. However, chitinase enzyme activity is not present in the serum of horse, human, rabbit, hamster, guinea pig and cat (110). Horse serum has therefore been used previously for studies involving acetylated chitosan (103). Another study was therefore performed by incubating the most degradable acetylated HPP-GC (1GC) in media containing horse serum. As shown in table 2.5, the hydrogel remained intact after 8 days, thereby showing the stability of acetylated HPP-GC in horse serum.

Table 2.4: Hydrogel integrity optimization in FBS containing media at day 8

Acetylated Hydrogels	**FBS alone**	**Media alone**	**Media + 10% FBS**	**Media + 5 % FBS**	**Media + 2 % FBS**
0GC	Intact	Intact	Intact	Intact	Intact
0.1GC	Degraded	Intact	Degraded	Degraded	Intact
0.3GC	Degraded	Intact	Degraded	Degraded	Degraded
0.5GC	Degraded	Intact	Degraded	Degraded	Degraded
1GC	Degraded	Intact	Degraded	Degraded	Degraded

Table 2.5: Hydrogel integrity optimization in media containing horse serum at day 8

Acetylated Hydrogel	**Horse serum alone**	**α-MEM Media alone**	**10% horse serum in media**	**5% horse serum in media**	**2% horse serum in media**
1GC	Intact	Intact	Intact	Intact	Intact

7F2 osteoblast cells were used for the study. The acetylated HPP-GC hydrogel with encapsulated cells was incubated in low cell-attachment plate to prevent cell adhesion on the tissue culture plate. Prior to confocal imaging, the hydrogel was transferred to glass bottom dish for imaging. Cell spreading and viability was assessed using LIVE DEAD® staining. Figure 2.14 shows the confocal images of cells in the hydrogels at days 7 and 14 post-encapsulation. As can be seen from the presence of green fluorescence and absence of red fluorescence, the encapsulated cells in all the hydrogels maintained their viability at both days 7 and 14, demonstrating the excellent cytocompatibility of the hydrogels. However, none of the hydrogels investigated supported cellular spreading upon encapsulation, demonstrating the need to further modify the gel to support greater attachment and spreading of osteoblast cells.

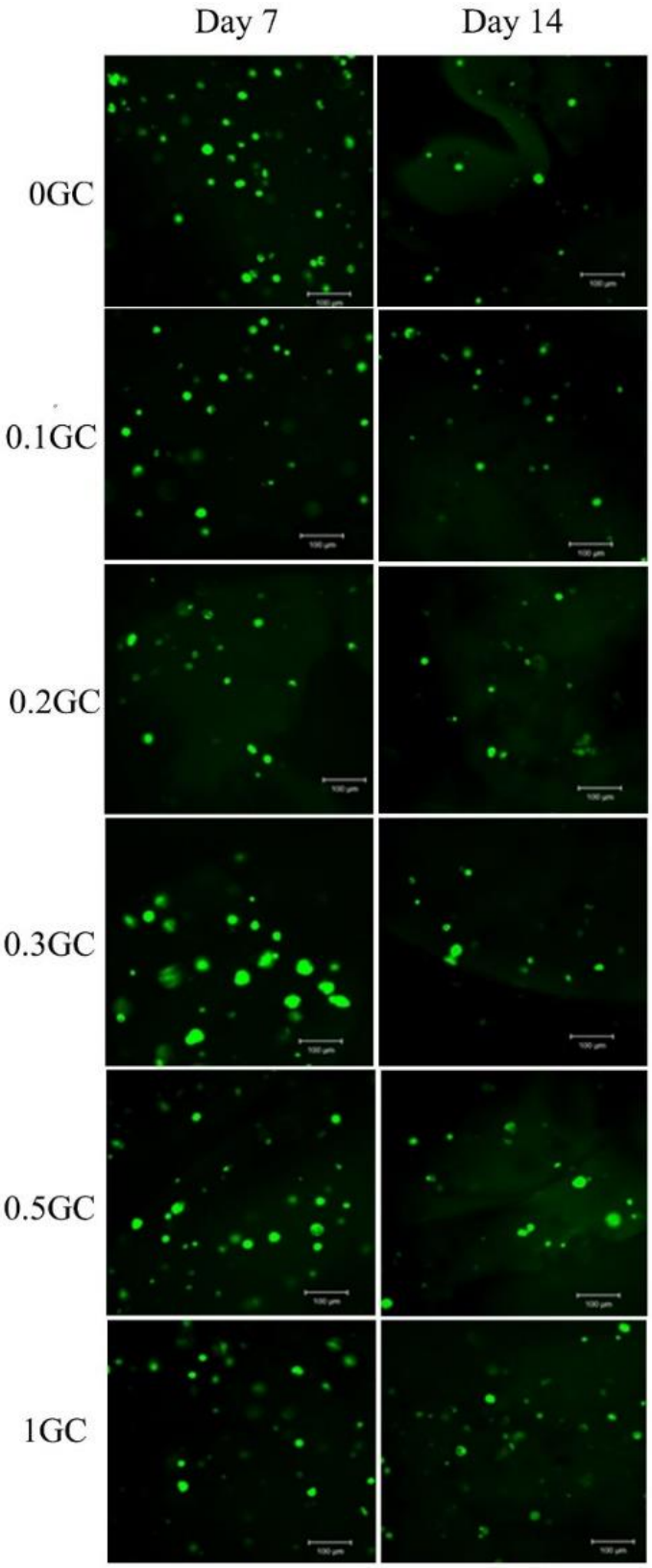

Figure 2.14: Confocal image showing viability of 7F2 osteoblast cells encapsulated in acetylated HPP-GC hydrogels (20x)

2.4. Conclusion

The study demonstrated the feasibility of developing injectable enzymatically crosslinked hydrogels from acetylated HPP-GC similar to HPP-GC. Among the different sterilization methods tested for sterilizing the HPP-GC solution, UV sterilization showed least the effect on the polymer and the corresponding hydrogel properties. The extent of acetylation of HPP-GC polymer prepared by reacting it with acetic anhydride was determined by FTIR and ^{1}H NMR. Irrespective of the extent of acetylation, all the hydrogels showed fast gelation (< 1 min). The swelling behavior of acetylated HPP-GC hydrogels in PBS was similar to that of HPP-GC hydrogels. Significant decrease in weight was observed by day 3, presumably due to an increase in the crosslinking density of the hydrogel with time. The release study in PBS alone demonstrated the ability of the hydrogels, irrespective of the degree of acetylation, to retain the encapsulated protein within the gel. However, in the presence of lysozyme, sustained release of protein from the hydrogel was observed depending on the extent of acetylation. The higher protein release observed in HPP-GC hydrogels with higher acetyl content is attributed to higher degradation of the hydrogels in the presence of lysozyme. Finally, the cell encapsulation study demonstrated excellent *in vitro* cytocompatibility of the hydrogels irrespective of the acetyl content. However, the encapsulated cells remain round without any spreading even after 14 days in culture.

CHAPTER 3: EVALUATION OF THE *IN VIVO* DEGRADATION OF ACETYLATED HPP-GC HYDROGELS USING MOUSE SUBCUTANEOUS MODEL

3.1. Introduction

3.1.1. Subcutaneous implantation

Degradable biomaterials are in increasing demand for developing therapeutic vehicles for regenerative applications. Ideally, the degradable biomaterial should be non-toxic, should possess a long shelf life, and should not trigger a strong immune response. The degradation should also be parallel to the regenerative process. *In vivo* degradation of the biomaterial happens in the presence of enzymes or by hydrolytic cleavage of the polymers. Mostly, natural polymers undergo enzymatic degradation, the rate of which depends on various factors such as implant site of the polymer, presence of the enzymes at the implant site, enzyme concentration, and chemical modification of the polymer (111). As mentioned in chapters 1 and 2, chitosan degradation is mediated by the action of the enzymes, lysozyme and chitinase (112). The degradation of chitosan increases with the degree of acetylation of the polymer because lysozyme identifies and targets acetyl residues. Lysozyme is present in the human body particularly in body fluids such as tears, serum and saliva. Moreover, injury or surgical procedure can lead to acute inflammation resulting in the production of lysozyme secreted mostly by neutrophils and macrophages. This can significantly affect the degradation of the implanted natural polymer scaffolds (113, 114). In addition to lysozymes, chitinase has been reported to show enzymatic activity on both chitosan and chitin. Chitinase activity also depends on the acetylation of chitosan as it requires β-(1, 4)-linked *N*-acetylglucosamine at the subsite for the catalytic cleavage (112). However, the presence of chitinase in human beings is associated only with disorders like infection, asthama and allergy

(115) (116). Therefore, lysozyme will be the main enzyme for the degradation of acetylated polymers in the human body.

3.1.2. Literature review

Azab *et al* has conducted a study on rat to evaluate the biocompatibility and biodegradability of chitosan hydrogels crosslinked with glutaraldehyde for the application of brachytherapy. For the study, they implanted slow-degrading and fast-degrading hydrogels subcutaneously and intraperitoneally. The study showed that the hydrogels were degraded by a process mediated by lysozyme. Neutrophils released oxidants at the implant site. The oxidants influenced lysozyme activity, which was responsible for the degradation of the hydrogels. The degraded products were then cleared from the implant site through ingestion by macrophages. Histological evaluation showed a milder response than typical foreign body response when compared to 'Vicril®' (absorbable sutures) used for the surgery. The study also showed that the hydrogel was not detected in any body organ and did not cause any tissue damage. It was reported as a safe and biocompatible device for the delivery of radioisotopes for brachytherapy (117). Pinto *et al* performed an *in vivo* evaluation of chitosan-poly (butylene succinate) fiber mesh by subcutaneous implantation. The tissue response to the scaffold was evaluated using histological and immunohistochemistry methods. The implants elicited normal immune response with a cascade of events; at first, the neutrophils appeared on the implant site, which was followed by macrophages and lymphocytes in the later phases. By week 12, the *in vivo* degradation became profound, which was evident by the presence of host cells and the separation of the strands of the fiber mesh (118). Vandevord *et al* studied the biocompatibility of porous chitosan scaffold in mouse model via subcutaneous implantation. The study revealed that there was less inflammatory response in the implant area. Histological analysis suggested neutrophil accumulation in the

implant area that disappeared over time. Collagen was deposited in the pore spaces of chitosan. Overall, the study suggested that chitosan had biocompatibility and could be used for regenerative applications (119). Tomihata *et al* evaluated the degradation of deacetylated chitin-derived films *in vivo* via subcutaneous implantation. The study showed higher biodegradation rate for chitin and 68.8 mol% deacetylated chitin and slower degradation rate for 73.3 mol% deacetylated chitin. Despite the presence of cationic primary amine group in chitin and deacetylated chitin, the materials showed milder tissue reaction (120).

The studies discussed above suggest that acetylation of chitosan can significantly increase the *in vivo* degradation of the polymer. However, the effect of acetylation on the degradation of HPP-GC hydrogels has not been investigated. The focus of this chapter is to evaluate the *in vivo* biodegradability of acetylated HPP-GC hydrogels as a function of time.

3.2. Materials and methods

3.2.1. Materials

The following items and chemicals were used for carrying out the experiments: filter-sterilized HRP (Sigma Aldrich), filter-sterilized hydrogen peroxide (Sigma Aldrich), α-MEM (colorless) (Life Technologies), dialysis membrane (Spectra/por7), isoflurane (Phoenix), buprenorphine, U100 insulin syringe (Becton Dickinson), and xylene (Fisher).

3.2.2. Enzymatically crosslinked acetylated HPP-modified glycol chitosan hydrogels

Acetylated HPP-GCs (0GC, 0.1 GC, 0.2GC, 0.3GC, 0.5GC and 1GC) were prepared as described in section 2.2.8. The polymers were dissolved in α-MEM at a concentration of 20 mg/mL. 20 units of HRP (filter-sterilized) was added to the solution and mixed uniformly. The hydrogels were prepared in syringe molds. 30 µL of polymer solution containing HRP was mixed

with H_2O_2 (filter-sterilized) at a final concentration of 7.34 mM, which resulted in the formation disc-shaped hydrogels.

3.2.3. Subcutaneous implantation of hydrogels in mouse model

Subcutaneous implantation was performed on BALB/C mice. Briefly, the mouse was anesthetized using 1.75% isoflurane. Dorsal surface of the animal was shaved using automated shaving razor (Peanut WAHL®). Then, the skin was dabbed with 75% ethanol wipes. Four incisions were made on the dorsal region of the mouse to make a pouch. 30 µL of hydrogel was prepared as described in section 3.2.2 in a 1 mL syringe mold and inserted into each pouch. The skin was then closed using 5-0 VICRYL® sutures. Post-surgery, buprenorphine was injected into the mouse based on its bodyweight. Based on a pilot study, different end points were selected for hydrogels with varying degree of acetylation. Table 3.1 shows the predetermined time points at which the animals were sacrificed by CO_2 asphyxiation. The subcutaneous skin tissue with the hydrogel samples were then collected for histology. Hydrogel alone was collected for SEM.

Table 3.1: Time points used for the subcutaneous implantation study

Acetylated polymer	**1 week**	**2 weeks**	**4 weeks**	**6 weeks**
0GC *	+	+	+	+
0.1GC*	+	+	+	+
0.2GC*	+	+	+	+
0.3GC*	+	+	+	-
0.5GC*	+	+	+	-
1.0GC*	+	+	-	-
Sham#	+	+	+	+

(*2 mice at each time point, #1 mouse at each time point, + time point, - no time point)

(n = 2 samples for SEM and n = 6 samples for histology)

3.3.4. Hematoxylin and eosin (H&E) staining of subcutaneous hydrogel implants

The subcutaneous skin tissue with the hydrogel was fixed in 10% formalin for 1 day. The fixed tissue was then transferred to 30% sucrose solution prepared in PBS (pH 7.4) for 2 h. The tissue sample was placed in a plastic mold (Fisherband® disposable base molds) and embedded using Shandon Cryomatrix™ (Thermoscientific) by placing it in dry ice. The sample was then stored in plastic bags at -80°C until it was used for cryosectioning. 7 µm cryosections were obtained by sectioning using a disposable steel blade (MX35 Premier+ Thermoscientific) on a cryostat (Leica CM 3050S). The cryosections were obtained using tape (Cryofilm type IIC [10] section – Lab Co.) transfer method and placed on glass slides (Superfrost®Plus microscopic slides [Fisherband®]). The cryosections were then transferred to clean slides smeared with adhesive (Norland optical adhesive 61) and kept at 4 °C overnight followed by UV curing for 7 min. The samples were stored at 4 °C until H&E staining.

H&E staining: Slides containing the cryosections were incubated in 70% ethanol for 10 min. The slides were then kept in PBS for 10 min and then in water for 2 min. The slides were then dipped in Mayer's modified hematoxyline (Polyscientific R&D Corp.) for 2 min followed by washes in double distilled water and then in Shandon™ bluing reagent (Thermoscientific™) and then again in double distilled water. Following this, the slides were dipped in Shandon™ Eosin-Y (Thermoscientific) for 1 min and then again washed in double distilled water for 10 s. The slides were then serially dipped in 70%, 90% and thrice in 100% ethanol. Finally, the slides were dipped thrice for a minute each time in 100% xylene. This was followed by smearing of Shandon™ mount toluene on the slide with a cover slip. The slides were then imaged using Axion Scan Z1 (ZEISS).

3.3.5. SEM imaging

The hydrogel samples separated from skin tissue were collected in PBS (pH 7.4). PBS was then removed and the sample was stored at -20^{o}C followed by lyophilization. The lyophilized hydrogels were cut using thin disposable scalpel blades and placed on die-cut carbon-conductive double-sided adhesive disc (SPI supplies) attached on an aluminum stub. Before imaging, the samples were platinum-coated for improved electrical conductivity. Imaging was done using a JEOL 6335 Field Emission SEM. Operating parameters used for the imaging were 10 kV accelerating voltage and 12 µA beam current.

3.3. Results and discussion

3.3.1. Surgery

In order to study the biodegradability of acetylated HPP-GC hydrogels, subcutaneous implantation was performed in male BALB/c mice 10-11 weeks old. Figure 3.1 shows a detailed representation of the subcutaneous implantation surgery. After the surgery, the hydrogels appeared as small round protrusions outside the skin, which indicated that the preformed hydrogels that were inserted remained intact.

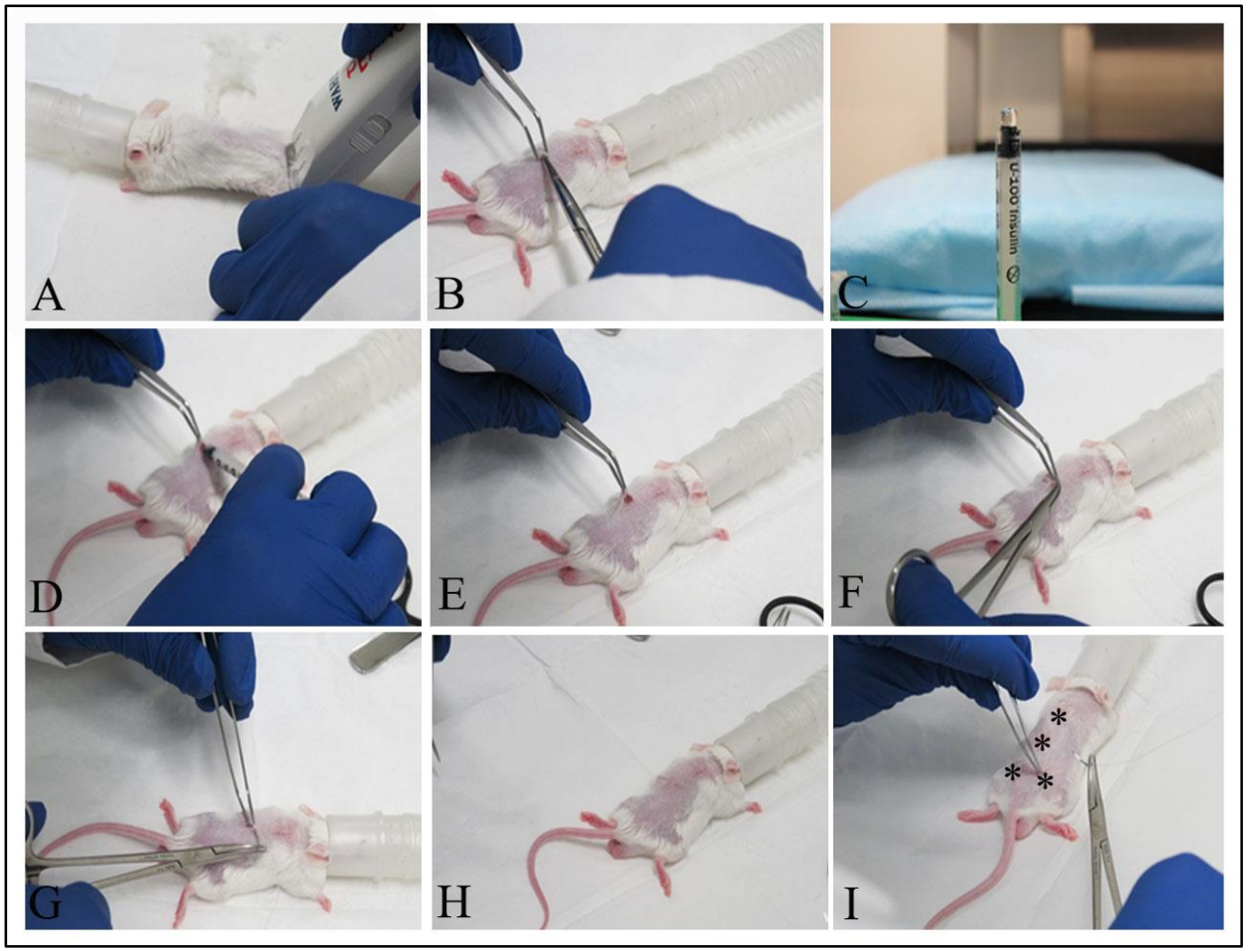

Figure 3.1: Shows the different steps involved in the surgery for subcutaneous implantation of acetylated HPP-GC hydrogels (A) BALB/c mouse anesthetized using 1.75% isoflurane and dorsal side shaved (B) Incisions made on dorsal region of mouse for making a pouch (C) 30 µL hydrogels prepared in syringe mold (D) Insertion of hydrogel into the dorsal pouch (E), (G), (F) and (H) Closing of the skin pouch using 5-0 VICRYL® sutures (I) Subcutaneous implantation of four hydrogels in the mouse; areas are indicated by '*'

3.3.2. Subcutaneously degraded hydrogel implants

The mice remained in good health for the duration of the study. The skin incision that was made to insert the hydrogels healed normally. Figure 3.2 shows the skin tissue with the hydrogel collected at the predetermined time points. Macroscopic examination of the implants indicated that the hydrogel degraded over a period of time depending on the degree of acetylation of the polymer.

The higher the degree of acetylation, the faster the hydrogel degraded and disappeared *in vivo*. The samples were analyzed further using H&E staining and SEM imaging.

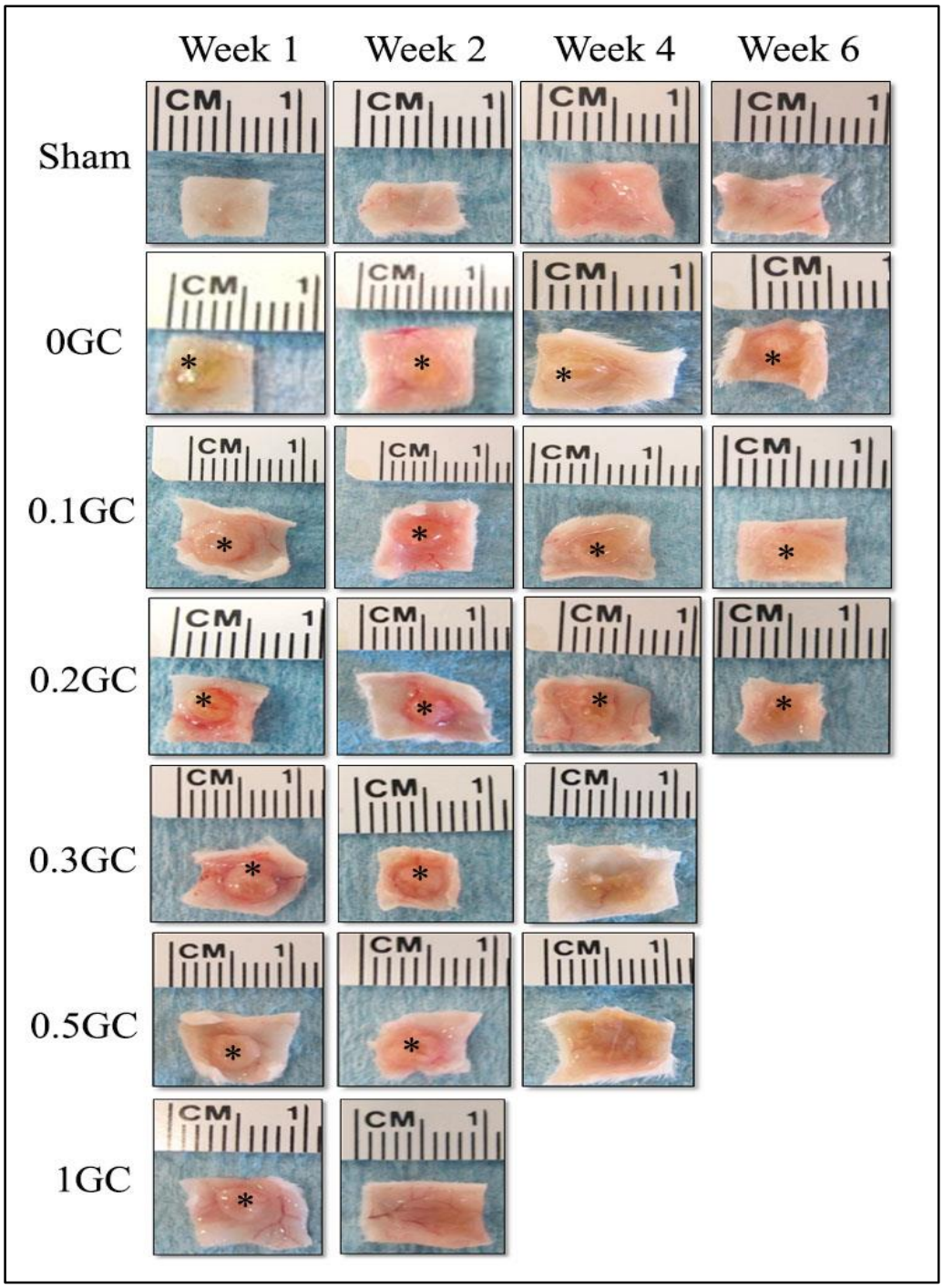

Figure 3.2: Photographs of acetylated HPP-GC hydrogel implants obtained from BALB/C mice at different time points – week 1, week 2, week 4 and week 6. '*' indicates the location of the hydrogel in the skin tissue

3.3.3. SEM imaging and histological evaluation of subcutaneously degrading hydrogel implants

To obtain the gross morphology of the implants at predetermined times after subcutaneous implantation, SEM imaging was performed on the isolated samples. Figures 3.3a and b show the SEM images of the explanted hydrogels along with the surrounding fibrous tissue at various time points post-implantation. At week 1, all the polymers (0GC, 0.1GC, 0.2GC, 0.3GC and 0.5GC) except 1GC showed intact hydrogel at the implanted site surrounded by a fibrous sheath as shown in the figure. The explanted and lyophilized hydrogels showed a porous structure similar to that reported previously for lyophilized HPP-GC hydrogel (89). Even at week 6 post-implantation, 0GC and 0.1GC samples showed the presence of intact hydrogel, even though the hydrogel showed some signs of disintegration at that time. At week 6 post implantation, the 0.2GC hydrogel showed significant decrease in size, showing the degradability of the hydrogel *in vivo*. Compared to the 0.2GC hydrogel, the 0.3GC and 0.5 GC hydrogels showed significantly higher degradation. Even at week 2, only very small amounts of hydrogel residues were present. By week 4, complete degradation of the hydrogels was observed at the implantation site. The data show significant increase in degradation of the hydrogels with increase in degree of acetylation of HPP-GC. This is supported by the extremely fast degradation of the 1GC hydrogel. Only very small residue of the 1GC hydrogel was observed at week 1 post-implantation and by week 2, no hydrogel residue was observed, demonstrating the complete degradation of the hydrogel. The study demonstrated the excellent *in vivo* degradation of acetylated HPP-GC hydrogels and the effect of degree of acetylation on the rate of degradation of the hydrogels.

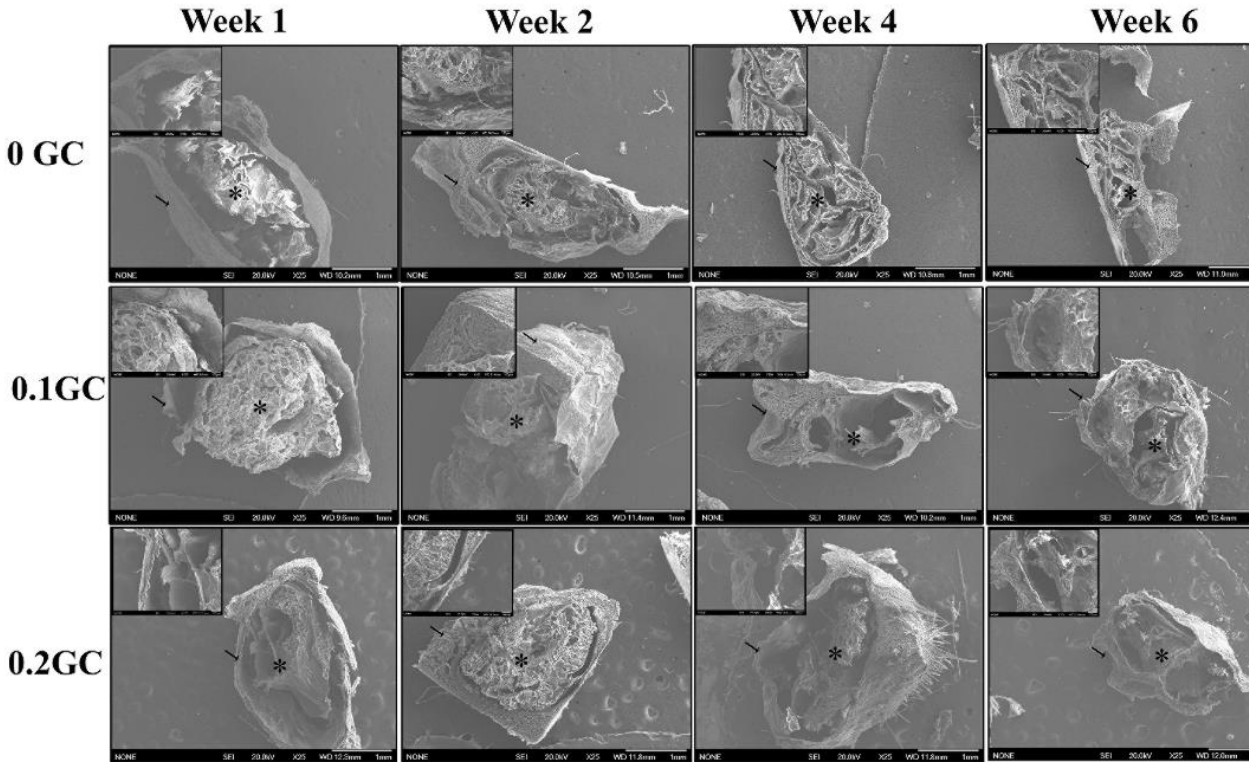

Figure 3.3a: *In vivo* degradation studies by subcutaneous implantation – representative gross morphology of explanted hydrogels by SEM (25x, inset 100x).'*' sign indicates the GC hydrogel, '↟' sign indicates the fibrous layer surrounding the hydrogel

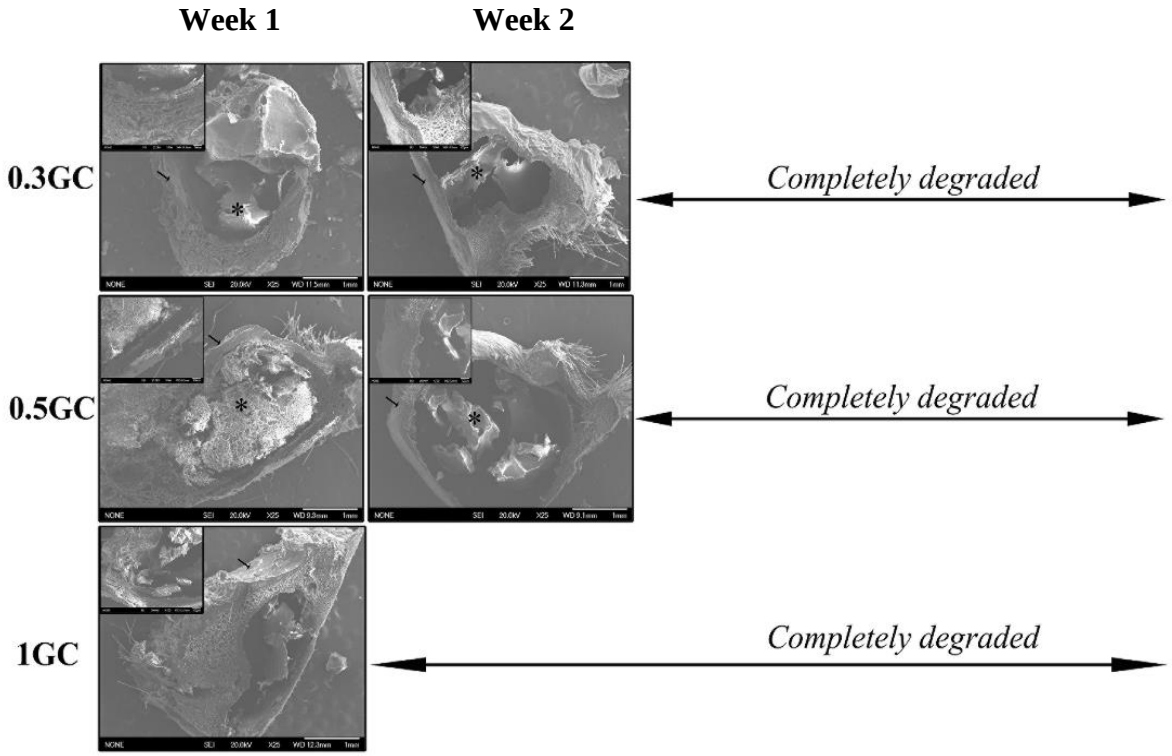

Figure 3.3b: *In vivo* degradation studies by subcutaneous implantation – representative gross morphology of explanted hydrogels by SEM (25x, inset 100x).'*' sign indicates the GC hydrogel, '↑' sign indicates the fibrous layer surrounding the hydrogel

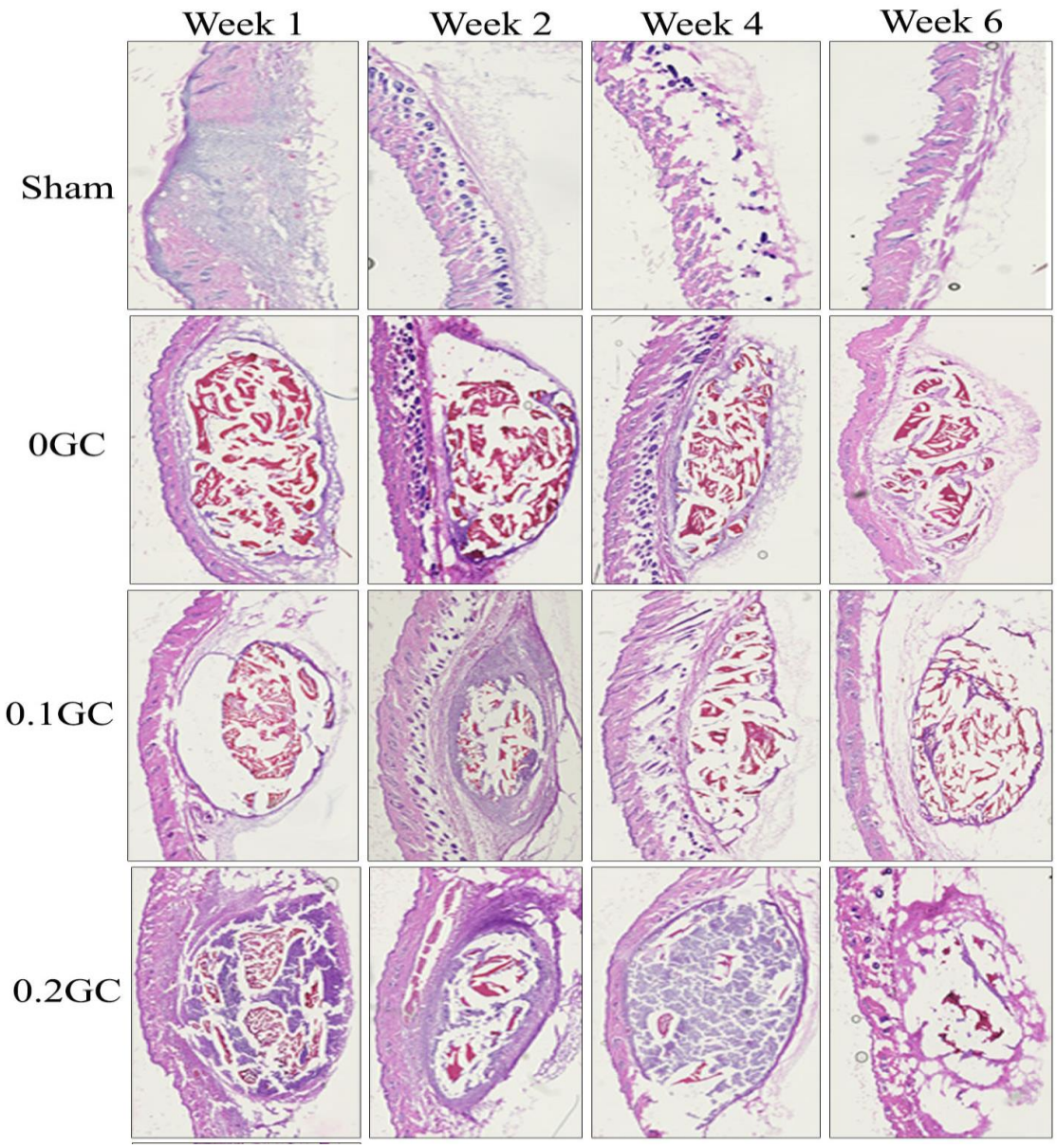

Figure 3.4a: *In vivo* degradation studies by subcutaneous implantation – representative image of H&E sections of explanted hydrogels at different time points (10x)

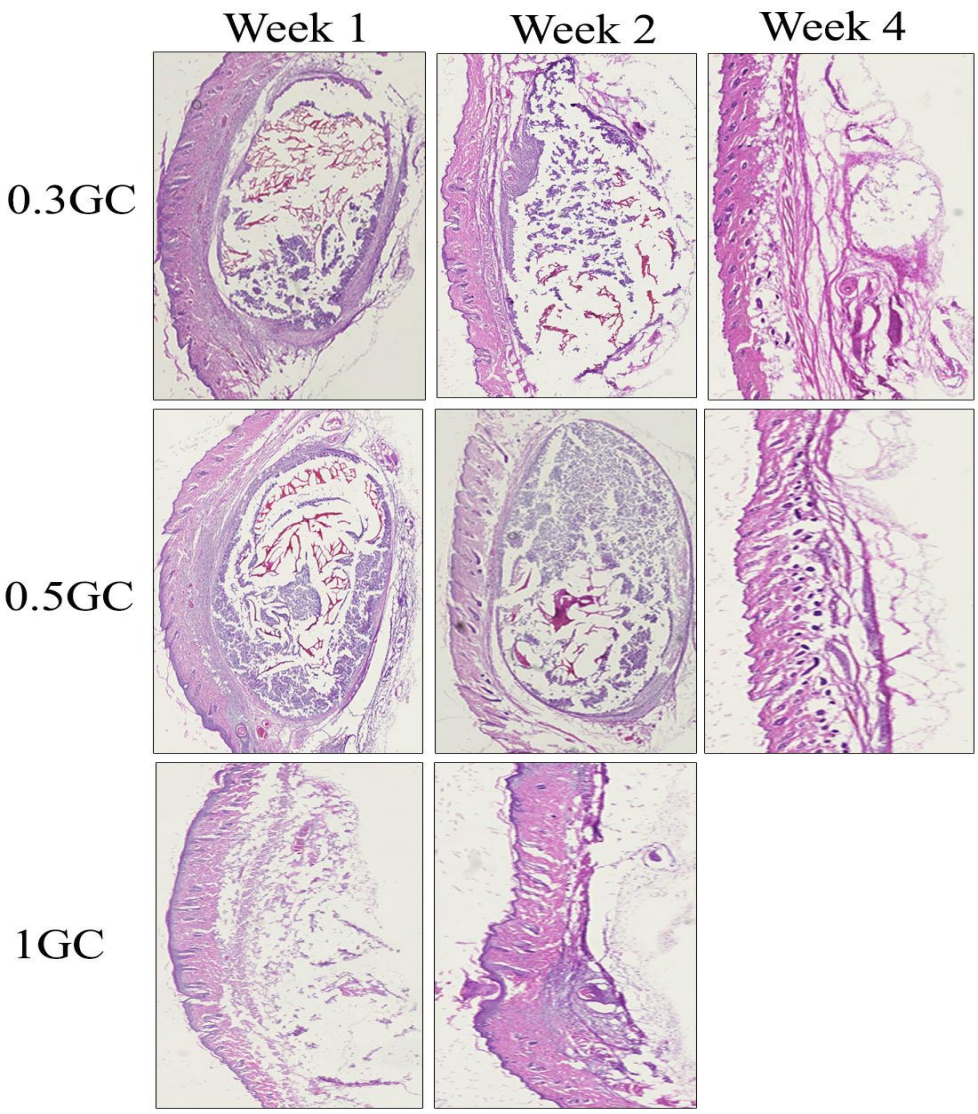

Figure 3.4b: *In vivo* degradation studies by subcutaneous implantation – representative image of H&E sections of explanted hydrogels at different time points (10x)

The results were further corroborated by the histological evaluation of the explanted samples as a function of time. Figures 3.4a and b show H&E staining, showing *in vivo* degradation of the acetylated HPP-GC hydrogels at different time points upon subcutaneous implantation. Sham group at week 1 showed significant cellular infiltration, presumably due to the acute inflammatory phase following the surgical incision. However, at week 2, the inflammatory cell infiltrate disappeared and normal skin tissue morphology was observed. At weeks 4 and 6, the sham sample showed a response similar to that at week 2, demonstrating that the acute inflammatory phase had subsided by week 1 and healing was complete by week 2. In the case of the 0GC hydrogel, week 1 showed the presence of intact hydrogel under the skin with minimal cell infiltrate. The hydrogel was surrounded by a thin fibrous capsule, which showed the presence of some inflammatory cells. At weeks 2 and 4, the response was found to be similar to that at week 1, with more or less intact hydrogel present under the skin with minimal cell infiltration along with the presence of a fibrous sheath that showed inflammatory cell activity. Even at week 6, the histological image showed the presence of an intact hydrogel with minimal cell infiltration, along with the presence of a thin fibrous layer and no degradation. In the case of 0.1GC, the image at week 1 showed an intact hydrogel with a thin fibrous layer and minimal cell infiltration. At week 2, the hydrogel was intact with a fibrous layer. The presence of inflammatory cells was found to be more profound compared to 0GC. At week 4, the gel was still intact with minimal cell infiltration. However, at week 6, the gel showed some disintegration compared to 0GC gel at that time point. The image at week 1 for 0.2GC on the other hand showed a fibrous layer and significant inflammatory cell infiltration along with hydrogel degradation. A previous report has shown that non-degraded chitosan gets stained with eosin, imparting a reddish pink color to the hydrogel. In contrast, degraded chitosan gets stained with hematoxylin (a basophilic stain), which is indicated

by blue color. This can be explained as follows. When chitosan is present in physiological condition, it has a positive charge and gets stained with eosin, which is a negatively charged stain. However, when chitosan degrades, a shift in charge occurs and it becomes negatively charged, causing a change in the staining mechanism (117). Images at weeks 2 and 4 showed profound degradation of the 0.2GC hydrogel as indicated by the degraded gel (blue color) along with inflammatory cell infiltration. At week 6, it showed maximum degradation with very few residual gel fragments and minimal inflammatory cell presence. The 0.3GC and 0.5GC hydrogels showed significant cell infiltration along with hydrogel degradation at weeks 1 and 2. At week 4, complete degradation of the hydrogel occurred and the gel was completely cleared from the implant site. Significant infiltration of inflammatory cells at earlier time point can significantly facilitate hydrogel degradation. Degradation of the hydrogels in the study happened due to the secretion of lysozyme by inflammatory cells such as neutrophils and macrophages that infiltrate the gels (118). Oxidants are reported to be essential to mediate lysozyme activity and neutrophils are shown to release oxidants at the implantation sites. The degraded hydrogels are then ingested by the macrophages, which helps in eliminating them from the implantation site. Among all the gels tested, the 1GC hydrogel showed maximum degradation at week 1. Inflammatory cell infiltration had also subsided by week 1. By week 2 complete clearance of the fibrous layer and gel from the implant site was observed. These observations indicate that acetylation of HPP-GC hydrogels can result in a family of polymers that can show a range of degradation and thereby allow the development of tailored hydrogels for a variety of regenerative applications.

3.4. Conclusion

This chapter focused on demonstrating the *in vivo* biodegradability of acetylated HPP-GC hydrogels. The hydrogels were subcutaneously implanted on the dorsal surface of BALB/c mice. H&E staining and SEM imaging showed the presence of a fibrous layer surrounding the hydrogel. Results indicate that 0GC was the slowest-degrading hydrogel and remained intact till week 6. The fastest-degrading hydrogel was 1GC, which degraded within 1 week. The results of this study demonstrate the feasibility of designing and preparing enzymatically crosslinked acetylated HPP-GC hydrogels with a wide range of degradation properties for different regenerative applications.

CHAPTER 4: EVALUATION OF CELLULAR VIABILITY AND SPREADING IN HPP-GC/TYR-GELATIN COMPOSITE HYDROGELS

4.1. Introduction

4.1.1. Glycol chitosan-gelatin composite

As shown in Chapters 1 and 2 and in the work of Gohil *et al* (89), GC showed cellular viability but did not display cell spreading. In order to improve the biological properties of GC, mixing with other polymers that have cell adhesion properties can increase adhesion and spreading of cells encapsulated in HPP-GC hydrogels. Gelatin is basically derived from collagen by partial denaturation. Its structure is $NH_2COOH–CH–R$ (R stands for glycin, proline or hydroxyproline). Collagen is known to have antigenicity because it is obtained from animal tissues, whereas gelatin has less antigenicity and contains the signaling molecules that are present in collagen. Gelatin contains sequences similar to Arg–Gly–Asp (RGD), which can promote cell adhesion, differentiation, proliferation and migration (121). Besides, gelatin is also reported to have biocompatibility, biodegradability, plasticity and cell-adhesive nature (122). Several groups have studied the potential of incorporating gelatin in chitosan-based materials for different applications such as cardiac (123), cartilage (124), bone (121, 125), hepatic (126) and skin (127) regeneration. Chitosan-gelatin composite can be prepared by a simple mixing of the two solutions or by using different crosslinkers such as glutaraldehyde (128), genipin (129) or by using various enzymes (130).

4.1.2. Literature review

Arakawa *et al* prepared an *in situ*-photocrosslinkable hydrogel using methacrylated GC (MeGC) and semi-interpenetrating collagen (Col) for application in bone regenerative engineering.

Photocrosslinking was performed in the presence of a riboflavin photinitiator using light of wavelength 400-500 nm. Collagen was incorporated to improve the mechanical strength and cell-adhesive nature of the MeGC hydrogel. The study showed that the MeGC-Col composite showed better attachment, spreading and proliferation of bone marrow stromal cells in comparison to MeGC alone (76). Pok *et al* prepared multilayered three dimensional scaffolds for cardiac tissue engineering using polycaprolactone (PCL) as the core containing chitosan-gelatin hydrogel in it. The PCL core provided tensile strength and surgical handling. The porous chitosan-gelatin hydrogel was included for providing cellular attachment and mechanical support, which is very essential for cardiomyocyte functioning and migration. Electron microscopy revealed that the pore size of the hydrogel was ~80 μm and also showed the viability and migration of neonatal rat ventricular myocytes. The scaffold presented a biomimetic environment and could be used as a cardiac patch for repairing congenital cardiac defects (123). Kathurai *et al* prepared a hybrid cryogel made of chitosan and gelatin for cartilage tissue engineering application. *In vitro* study showed that the cryogels showed better cellular proliferation of cos-7 cell line (122). Cheng *et al* used a thermosensitive hydrogel made of chitosan-gelatin-β-GP salt for intervertebral disc nucleus pulposus (NP) regeneration. Addition of gelatin to the hydrogel significantly improved gel strength, gelation time and gene expression. The hydrogel also showed cell viability and proliferation of NP cells (131). Nagahama *et al* used chitosan hydrogel to prepare chitosan/gelatin membrane for biomedical application. They carried out a cell adhesion study using MG-63 osteoblast-like cells on the membranes. The study revealed that the membranes were able to attach cells within 1 day (132). Han *et al* designed chitosan-gelatin sponge for skin regenerative application. *In vitro* study with the sponge showed cell attachment and proliferation for up to 21 days. *In vivo* study also indicated the ability of the sponge to enhance cell attachment for wound

healing (127). Miranda *et al* used a porous chitosan-gelatin scaffold for bone regenerative engineering. Rat bone marrow mesenchymal stem cells cultured in the three dimensional scaffold showed cell viability, adhesion and spreading. *In vivo* study also showed cell adhesion and differentiation of the stem cells in the direction of osteogenic lineage (125). Amini *et al* demonstrated the feasibility of developing an injectable hydrogel system using gelatin modified with tyramine in the presence of HRP and H_2O_2 as a delivery vehicle for osteoblast cells. The gelatin hydrogels showed MCT3T3-E1 osteoblast cell adhesion and spreading in the three dimensional environment (133). In the present chapter, the feasibility of developing a composite injectable hydrogel by crosslinking HPP-GC and tyramine gelatin (Tyr-Gelatin) in the presence of HRP and H_2O_2 will be discussed. The swelling properties of the composite hydrogel as well as cell adhesion and spreading in the composite hydrogels will also be presented.

4.2. Materials and methods

4.2.1. Materials

The following items and chemicals were used for carrying out the experiments: GC (Sigma Aldrich), MES powder (Fisher), EDC (Sigma Aldrich), NHS (98%) (Sigma Aldrich), HPP (98%) (Sigma Aldrich), HRP (Sigma Aldrich), hydrogen peroxide (Sigma Aldrich), gelatin (Type A) (MP), tyramine-HCl (Sigma Aldrich), LIVE/DEAD® viability/cytotoxicity kit (Life Technologies), and 7F2 cells (ATCC® CRL-12557™).

4.2.2. Preparation of HPP-modified glycol chitosan

HPP modification was done on GC using carbodiimide-based coupling reaction. For preparing a batch of HPP-GC, 500 mg of GC was dissolved in 350 mL of 1 M MES solution (pH 5.5). The solution containing GC was dissolved by stirring at room temperature (RT) for 3 h. For

HPP-coupling, EDC (2.608 mmol) and NHS (2.172 mmol) were dissolved in 50 mL of 1 M MES solution for 5 min, followed by the addition of HPP (3.009 mmol) and reaction for 1 h at RT. This solution was then added to the solution containing GC and kept for 24 h at RT. The solution mixture was then dialyzed against water using dialysis tubings with cut-off size of 10,000 Da. Dialysis was carried out for 3 days during which the water was changed 6 times. After dialysis, the solution was frozen at -20^{o}C. The frozen solution was then lyophilized for 3 days and stored at -20^{o}C.

4.2.3. Preparation of tyramine-modified gelatin

Tyramine modification was performed on gelatin using carbodiimide-based coupling reaction. For preparing a batch of Tyr-Gelatin, 875 mg of gelatin (Type A) was dissolved in 20 mL of water under stirring at 37 ^{o}C for 2 h. After dissolving the gelatin, 55 mL of MES buffer was added to the solution. Tyramine-HCl (2.937 mmol) was added to the solution followed by EDC (2.660 mmol) and NHS (1.303 mmol). The solution was allowed to react at RT for 24 h. The solution was then dialyzed against water using dialysis tubings with cut-off size of 10,000 Da. Dialysis was carried out for 3 days during which the water was changed 6 times. After dialysis, the solution was frozen at -20^{o}C. The frozen solution was then lyophilized for 3 days and stored at -20^{o}C.

4.2.4. Characterization of HPP-modified glycol chitosan and tyramine-modified gelatin

The extent of phenolic group substitution in GC and gelatin was characterized using a UV spectrophotometer (Evolution 60, Thermoscientifc). For determining the extent of HPP modification in GC, unmodified and HPP-modified GC were dissolved in ultra-pure water at a concentration of 1 mg/mL and the absorbance was measured at 275 nm. Phenolic group

substitution was calculated by plotting a calibration curve obtained using known concentrations of HPP dissolved in ultra-pure water. Similarly, for determining the extent of tyramine modification in gelatin, unmodified and tyramine-modified gelatin were dissolved in ultra-pure water at a concentration of 1 mg/mL and the absorbance was measured at 275 nm. Phenolic group substitution was calculated by plotting a standard calibration curve obtained using known concentrations of tryamine-HCl dissolved in ultra-pure water.

4.2.5. Preparation of composite hydrogels using HPP-modified glycol chitosan and tyramine-modified gelatin

HPP-GC solution was prepared in α-MEM at a concentration of 20 mg/mL. Tyr-Gelatin solution was also prepared in α-MEM at a concentration of 20 mg/mL. (Note: α-MEM was always thawed at 37 ^{o}C prior to dissolving gelatin because gelatin is less soluble at lower temperatures). The two solutions were mixed in the following different ratios (v/v) – GC:Gelatin (10:90), GC:Gelatin (30:70), GCGelatin (50:50), GC:Gelatin (70:30) and GC:Gelatin (90:10) – and kept for vortexing at 1500 rpm for 24 h at RT to ensure uniform mixing. HPP-GC alone and Tyr-Gelatin alone were used as controls. Either 20 units or 5 units of HRP was added to the solution and mixed uniformly. Enzymatic crosslinking was done by adding H_2O_2. The H_2O_2 concentration in the final solution was 7.34 mM.

4.2.6. Swelling behavior of HPP-modified glycol chitosan/tyramine-modified gelatin composite hydrogels

Hydrogels of HPP-GC alone, gelatin alone, GC:Gelatin (10:90), GC:Gelatin (30:70), GC: Gelatin (50:50), GC:Gelatin (70:30) and GC:Gelatin (90:10) were prepared in syringe molds as described in section 4.2.5. Four hydrogel samples were tested for each polymer (n=4). Hydrogels

prepared from 150 µL of the respective polymer solutions were placed in glass vials and the initial weights were determined (W_{si}). To each of the vials, 1mL PBS was added and incubated in a shaker at 37 ^{o}C. Weights of the hydrogels with the vials were determined after removing excess PBS (W_{sf}) at day 1, day 3, day 5, day 7 and day 14. The PBS removed was replaced with fresh PBS after the measurement at each time point. The swelling ratio was determined using the following equation [5].

$$\%Swelling = \frac{W_{sf} - W_{si}}{W_{si}} \times 100 - - - - - [5]$$

4.2.7. Viability and morphological study of HPP-modified glycol chitosan and semi-interpenetrating gelatin hydrogels with encapsulated osteoblast cells

Osteoblastic cell line 7F2 (derived from mouse bone marrow) was used for the study. Cells were grown and maintained in α-MEM (2 mM L-glutamine, 1 mM sodium pyruvate, with no ribonucleosides and deoxyribonucleosides) with 10% FBS and 1% pen-strep. HPP-GC solution was prepared in α-MEM at a concentration of 20 mg/mL. Gelatin A solution was prepared in α-MEM at a concentration of 20 mg/mL by vortexing at 37 ^{o}C. Both solutions were sterilized under UV light for 30 min prior to the cell encapsulation step. HRP was added to these solutions at a concentration of 20 units/mL. Cells were trypsinized and suspended in GC:Gelatin (70:30), GC:Gelatin (90:10) and HPP-GC alone at a cell density of 0.8 million per mL. To prepare the hydrogel, 10 µL of the polymer solution with cells and HRP was mixed with H_2O_2 in a syringe mold. H_2O_2 concentration in the final solution was 7.34 mM. The hydrogel with the encapsulated cells was incubated in Costar® ultra-low attachment plate with media at 37 ^{o}C and 5% CO_2. Media was changed every 3 days to keep the cells healthy. At specific time points, the hydrogel with the encapsulated cells was transferred to MatTek glass bottom 35 mm dish and stained using

LIVE/DEAD® viability/cytotoxicity kit for mammalian cells. Confocal microscopy imaging was done using a Zeiss LSM 510 Meta microscope.

4.2.8. Viability and spreading of osteoblast cells encapsulated in HPP-modified glycol chitosan/tyramine-modified gelatin composite hydrogels

Osteoblastic cell line 7F2 (derived from mouse bone marrow) was used for the study. Cells were grown and maintained in α-MEM (2 mM L-glutamine, 1 mM sodium pyruvate, with no ribonucleosides and deoxyribonucleosides) with 10% FBS and 1% pen-strep. Separate solutions of HPP-GC and Tyr-Gelatin dissolved in α-MEM at concentrations of 20 mg/mL were mixed at different ratios (v/v) – GC:Gelatin (10:90), GC:Gelatin (30:70), GC:Gelatin (50:50), GC:Gelatin (70:30) and GC:Gelatin (90:10) – and kept for vortexing at 1500 rpm for 24 h to ensure uniform mixing of the polymer solutions. Solutions of HPP-GC alone and gelatin alone were used as controls. The polymer solutions were sterilized under UV light for 30 min prior to the cell encapsulation step. HRP was added to these solutions at a final concentration of 20 units/mL. Cells were trypsinized and suspended in HPP-GC/Tyr-Gelatin composite solutions at a cell density of 0.8 million per mL. To prepare the hydrogel, 10 μL of the polymer solution with cells and HRP was mixed with H_2O_2 in a syringe mold. H_2O_2 concentration in the final solution was 7.34 mM. The hydrogel with the encapsulated cells was incubated in Costar® ultra-low attachment plate with media at 37 ^oC and 5% CO_2. Media was changed every 3 days to keep the cells healthy. At specific time points, the hydrogel with encapsulated cells was transferred to MatTek glass bottom 35 mm dish and stained using LIVE/DEAD® viability/cytotoxicity kit for mammalian cells. Confocal microscopy imaging was done using a Zeiss LSM 510 Meta microscope.

4.2.9. Statistical analysis

All results presented in the chapter are expressed as mean ± standard deviation. Statistical analysis was done using One-way ANOVA followed by SNK test in SigmaStat (ver 2.3). Statistical significance was set at $p < 0.05$.

4.3. Results and discussion

4.3.1. Synthesis of HPP-modified glycol chitosan and tyramine-modified gelatin

HPP-GC polymer was prepared as mentioned in section 2.2.2. Tyramine is also a phenol-containing molecule similar to HPP. Therefore, Tyr-Gelatin was prepared using carbodiimide chemistry using EDC and NHS by a method similar to that described in section 2.3.1. Conjugation occurs through the formation of an amide bond between the amine group of tyramine and carboxylic group of gelatin after it has been activated by EDC and NHS (133, 134).

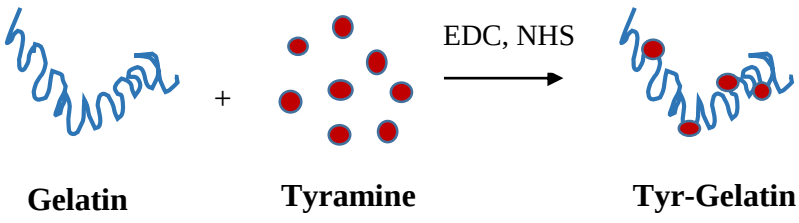

Figure 4.1: Schematic showing Tyr-Gelatin synthesis (133)

4.3.2. Characterization of HPP-modified glycol chitosan and tyramine-modified gelatin

Phenol content in HPP-GC and Try-Gelatin was quantified using UV spectroscopy. Figure 4.2 shows the standard curves obtained using different concentrations of HPP and tyramine-HCl separately, indicating linearity in the concentration range tested. Absorbance values for HPP-GC and Tyr-Gelatin were also recorded at 275 nm followed by the subtraction of background absorbance values corresponding to GC and gelatin alone, respectively. Concentration of phenol

group per mg of HPP-GC polymer and Tyr-Gelatin was obtained as 0.377 ± 0.061 µmol and 0.228 ± 0.001 µmol, respectively. Results suggest the successful incorporation of phenolic groups in GC and gelatin.

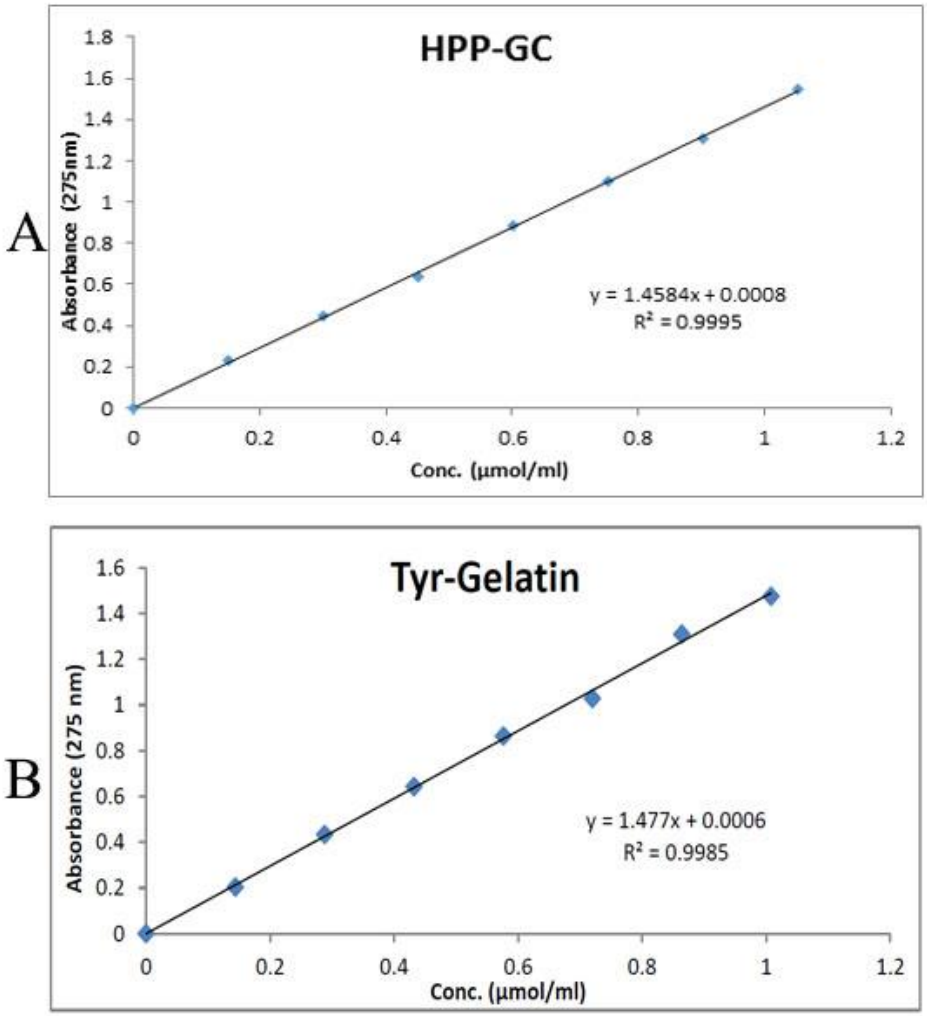

Figure 4.2: (A) Standard curve used to determine HPP concentration in GC (B) Standard curve used to determine Tyr concentration in gelatin

4.3.3. Gelation time of HPP-modified glycol chitosan/tyramine-modified gelatin composite hydrogels

HPP-GC and Tyr-Gelatin solutions in α-MEM were mixed in different ratios and enzymatically crosslinked using 20 units of HRP/mL. H_2O_2 was added at a concentration of 7.34 mM. The mechanism of gelation is the same as described in section 2.3.1. The ratios used for the studies were GC: Gelatin (10:90), GC: Gelatin (30:70), GC: Gelatin (50:50), GC: Gelatin (70:30) and GC: Gelatin (90:10). HPP-GC alone and Tyr-gelatin alone were used as controls. Gelation times recorded using vial inversion test are shown in Figure 4.3. Results indicate a significant difference between the gelation times of HPP-GC alone compared to the other groups tested. Gelation time for HPP-GC alone (4s) was the lowest and that for gelatin alone (16 s) was the highest. Gelation times for HPP-GC/Tyr-Gelatin composites were in between gelation times for HPP-GC and Tyr-Gelatin. As can be seen, increasing GC concentration led to a decrease in the gelation time. No significant differences in gelation times were observed between the HPP-GC alone hydrogel and GC-gelatin (90:10) hydrogel.

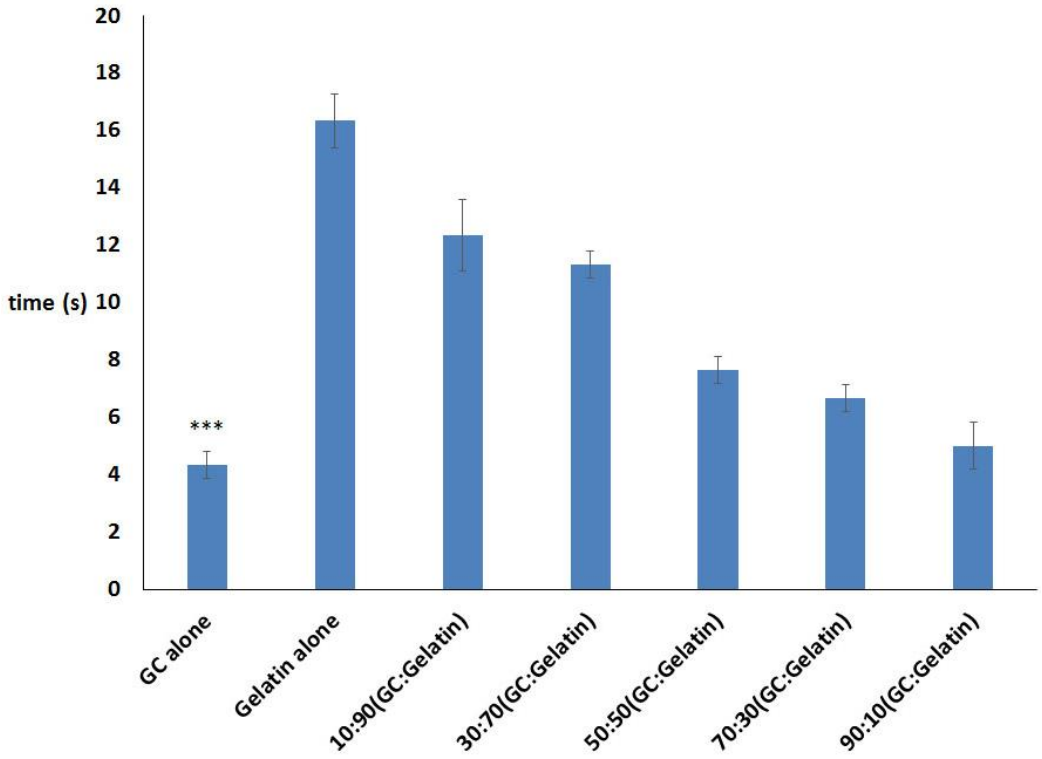

Figure 4.3: Gelation times of HPP-GC/Tyr-Gelatin composites. Data are expressed as mean ± standard deviation with n = 3. One way Anova followed by SNK comparing different groups against HPP-GC alone. *p**** < 0.001 vs. Gelatin alone, GC:Gelatin (10:90), GC:Gelatin (30:70), GC:Gelatin (50:50), GC:Gelatin (70:30)

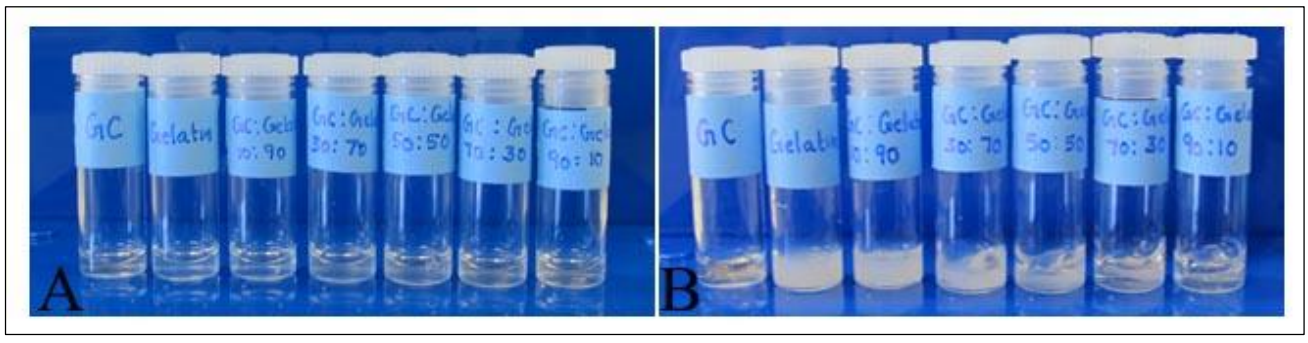

Figure 4.4: (A) Shows free-flowing polymer solution (B) Shows hydrogel formation in all ratios of HPP-GC/Tyr-Gelatin

Figure 4.4 shows the ability of the composites to form robust hydrogels at all the concentrations studied. As can be seen, HPP-GC alone results in a transparent gel whereas gelatin alone results in a translucent gel. The composite gels showed higher transparency with an increase in GC content.

4.3.4. Swelling behavior of HPP-modified glycol chitosan/tyramine-modified gelatin composite hydrogels

Swelling behavior of different enzymatically crosslinked HPP-GC/Tyr-Gelatin composite hydrogels was studied by incubating them in PBS at 37 ^{o}C. At predetermined time points, PBS was removed and wet weight was measured to obtain percentage swelling as a function of time. Figure 4.5 depicts the swelling percentage on different days – day 1, day 3, day 5, day 7 and day 14 – for all the hydrogels. Swelling percentage was found to decrease over time for all HPP-GC/Tyr-Gelatin composites as well as for the Tyr-Gelatin alone and HPP-GC alone hydrogels. Figure 4.6 shows the statistical comparison with respect to time within the same hydrogel. Table 4.1 and Figure 4.7 show the statistical comparison of the behavior of HPP-GC alone against the other hydrogels.

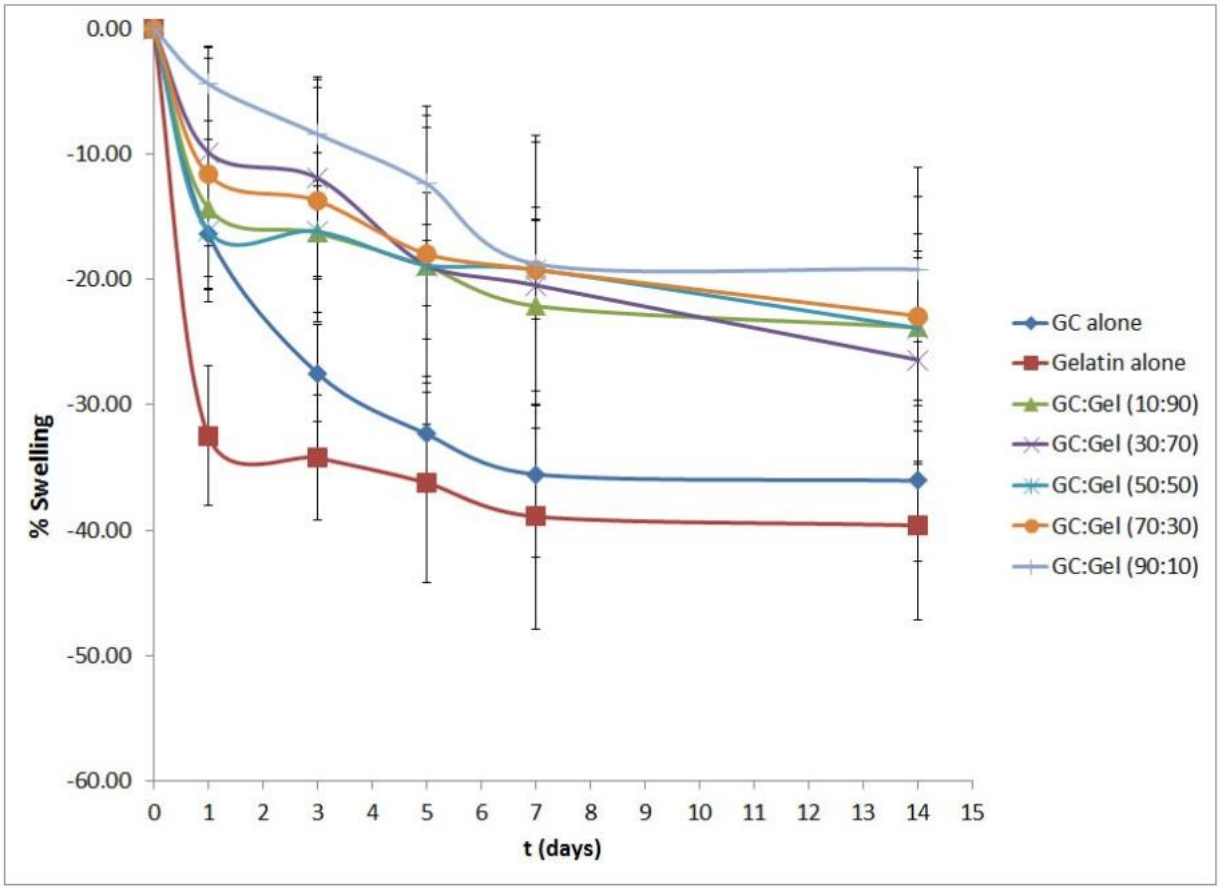

Figure 4.5: Swelling behavior of HPP-GC/Tyr-Gelatin composites

Table 4.1: Statistical analysis corresponding to Figure 4.6 below, comparing different time points within the same group. Data are expressed as mean ± standard deviation (n=4)

A	HPP-GC alone	*P**** < 0.001 vs. days 1, 3, 5, 7, 14), *p*### < 0.001 vs. days 5, 7, 14, *p*## < 0.01 vs.day 3
B	Gelatin alone	*p**** < 0.001 vs. days 1, 3, 5, 7, 14
C	10:90	*P**** < 0.001 vs. days 7, 14
D	30:70	*p*** < 0.01 vs. day 14, *p** < 0.05 vs. days 5, 7
E	50:50	*p**** < 0.001 vs. days 1, 3, 5, 7, 14
G	90:10	*p**** < 0.001 vs. days 7,14, *p*** < 0.01 vs. day 5, *p** < 0.05 vs. day 3, *p*### < 0.001 vs. days 7, 14, *p*# < 0.05 vs. day 5, *p*^^ < 0.01 vs. days 7, 14

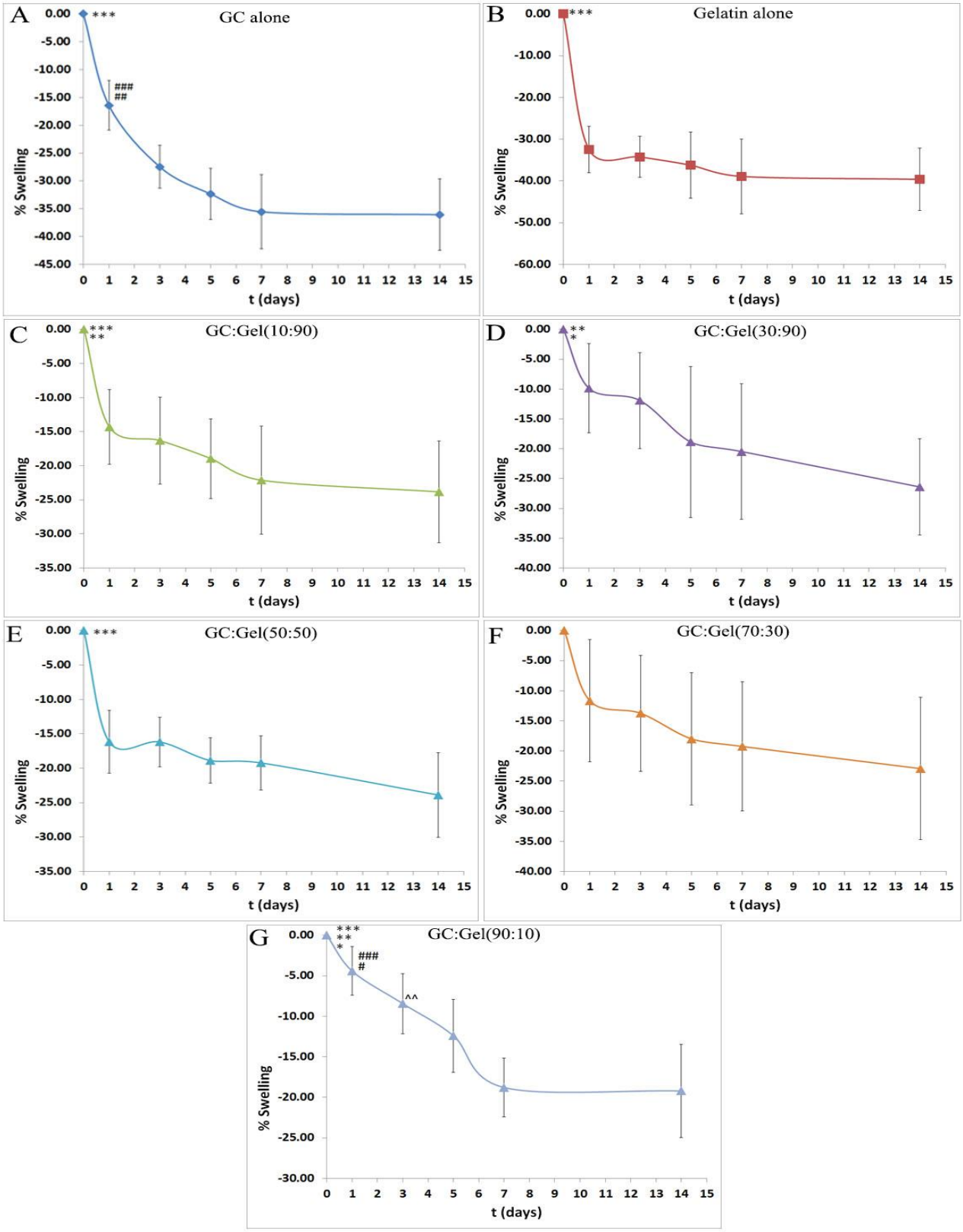

Figure 4.6: Swelling behavior of HPP-GC/Tyr-Gelatin composite hydrogels. Statistics comparing different time points within the same group are shown in Table 4.1 above

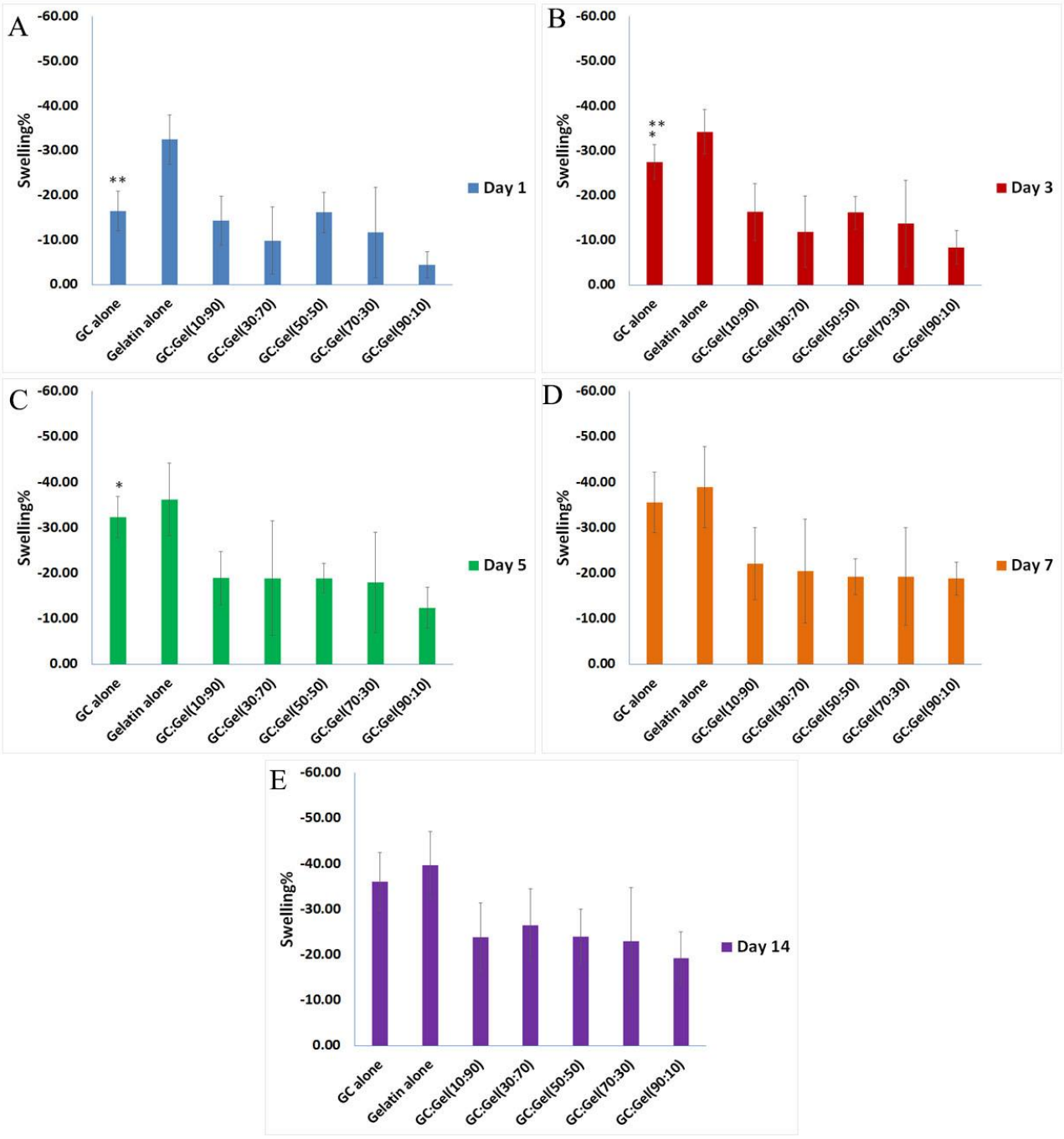

Figure 4.7: Swelling behavior of HPP-GC/Tyr-Gelatin composite hydrogels. Data are expressed as mean ± standard deviation with n = 4. One way Anova followed by SNK test, comparing the behavior of HPP-GC alone against that of all other hydrogels with respect to different time points. (A) Day 1 HPP-GC alone: $p^{**} < 0.10$ vs gelatin alone, (B) Day 3 HPP-GC alone: $p^{**} < 0.10$ vs GC:Gelatin (90:10), $p^{*} < 0.05$ vs GC:Gelatin (10:90), GC: Gelatin (30:70), GC:Gelatin (50:50), GC:Gelatin (70:30), (C) Day 5 HPP-GC alone: $p^{*} < 0.10$ vs GC:Gelatin (90:10)

Shrinkage of the hydrogel was much greater for HPP-GC alone and gelatin alone as compared to all the different composite hydrogels studied. As seen in Figure 4.7, decrease in swelling for HPP-GC alone at day 3 was statistically significant compared to all other hydrogels except gelatin alone. However, at day 5, decrease in swelling for HPP-GC alone was different only to GC:Gelatin (90:10). At days 7 and 14, no statistically significant difference in swelling was observed between the HPP-GC alone hydrogel and gelatin alone hydrogel as well as between the different composite hydrogels tested. Similar to the observations detailed in section 2.3.4, the HPP-GC alone hydrogel showed a continuous decrease in weight upon incubation in PBS till 3 days and after that no further decrease was observed. The Tyr-Gelatin hydrogel on the other hand showed a faster decrease in weight at day 1 itself and no further weight decrease was observed after that. The composite hydrogels [GC-gelatin (10:90); GC-gelatin (30:70); GC-gelatin (50:50); GC-gelatin (70:30)] show behavior similar to Tyr-Gelatin hydrogel, with a faster decrease in weight at day 1 and no further weight decrease after that. However, the extent of weight decrease in these composite hydrogels was significantly lower than that of Tyr-gelatin gel. The composite hydrogel GC-gelatin (90:10) on the other hand showed behavior similar to that of HPP-GC hydrogel with a continuous decrease in weight till day 7. The data demonstrate the feasibility of modulating the swelling behavior of HPP-GC and Tyr-gelatin hydrogels by developing composite hydrogels. The decrease in swelling with respect to time may be attributed to the increase in crosslinking density of these hydrogels over time. Similar behavior was observed in the case of acetylated HPP-GC hydrogels as discussed in section 2.3.4. Further studies are required to clearly understand the factors contributing to the significant decrease in weight for these hydrogels upon incubation in PBS.

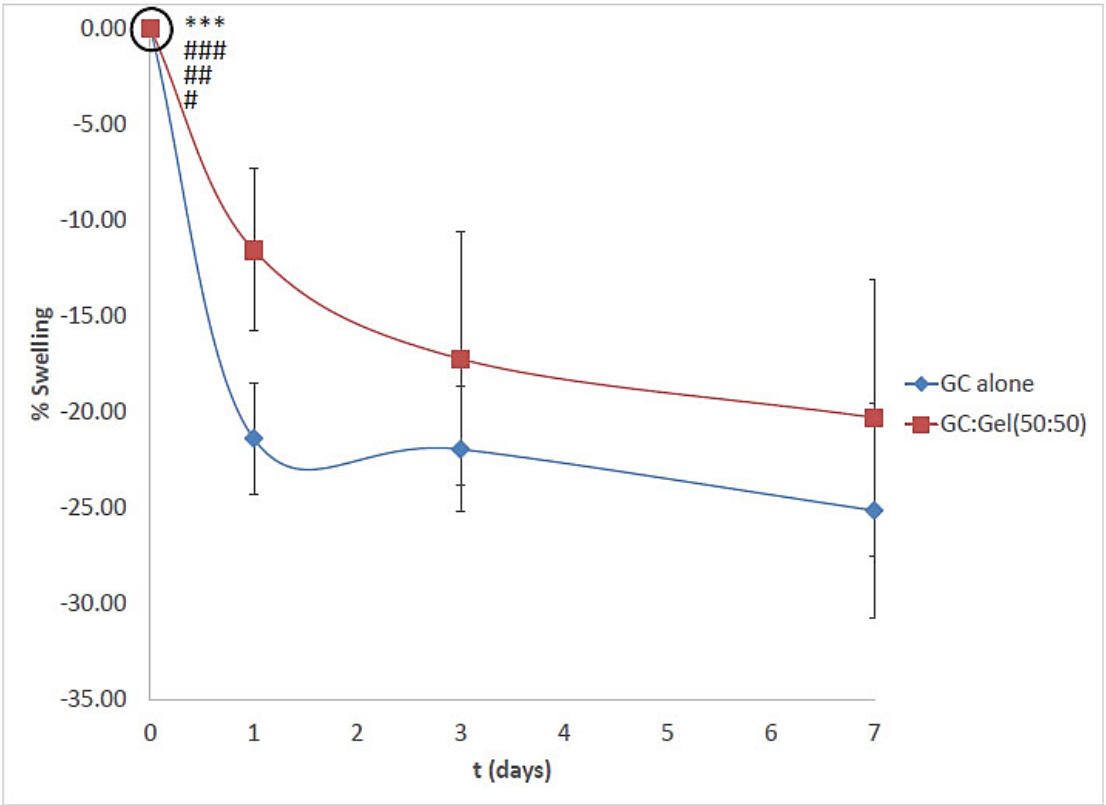

Figure 4.8: Swelling behavior of hydrogels prepared using 5 units of HRP/mL. Data are expressed as mean ± standard deviation with n = 4.One way Anova followed by SNK test. HPP-GC alone: $p^{***} < 0.001$ vs. days 1, 3, 7, GC: Gelatin (50:50): $p^{\#\#\#} < 0.001$ vs. day 7, $p^{\#\#} < 0.01$ vs. day 3, $p^{\#} < 0.05$ vs. day 1

A preliminary study was conducted by varying the concentration of HRP to understand the effect of reagent concentrations on the swelling behavior of HPP-GC and composite hydrogels. The study tested the HPP-GC hydrogel and GC:Gelatin (50:50) composite hydrogel prepared using 5 units of HRP instead of 20 units used in the previous study (Figures 4.5 to 4.7). Figure 4.8 shows the results of the swelling study. As in the case of 20 units of HRP, the hydrogels showed a decrease in weight upon incubation in PBS. No difference in swelling behavior was observed and the trends in Figure 4.8 were similar to those observed with hydrogels prepared using 20 units of HRP (Figures 4.5 to 4.7). It has been reported that by changing the HRP and H_2O_2 concentrations, the

crosslinking density can be varied (108). Further studies are required using a wide range of HRP, H_2O_2 and HPP concentrations to understand their effect on the gelation and swelling properties of the enzymatically crosslinked hydrogels.

4.3.5. Viability and morphological study of HPP-modified glycol chitosan and semi-interpenetrating gelatin hydrogel with encapsulated osteoblast cells

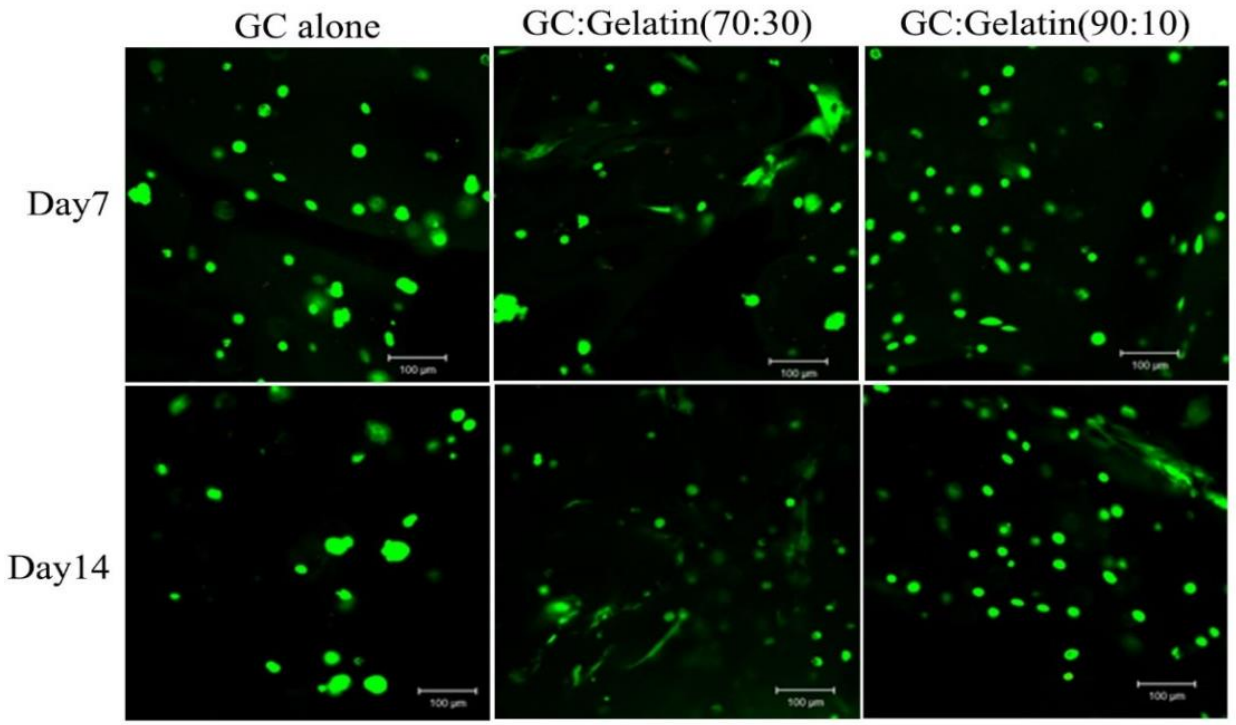

Figure 4.9: Confocal image showing viability and morphology of 7F2 osteoblast encapsulated in HPP-GC/semi-interpenetrating gelatin hydrogel (20x)

A previous study has shown that addition of collagen to photocrosslinked GC hydrogels can increase cell adhesion and spreading (76). So, a study was performed to develop a semi-interpenetrating network by mixing HPP-GC and unmodified gelatin followed by crosslinking in the presence of HRP and H_2O_2. Cell suspension was added to the polymer solution before gelling

as explained in section 4.2.7. LIVE/DEAD® staining was performed at days 7 and 14 to evaluate the viability and spreading of the encapsulated cells in the hydrogel (Figure 4.9). As shown in the figure, the encapsulated cells showed 100% viability at days 7 and 14 in culture irrespective of HPP-GC concentration. As reported before (section 2.3.6), the cells encapsulated in HPP-GC alone hydrogel did not show any cell spreading at both the time points. The addition of gelatin to the hydrogel slightly improved cell spreading in the hydrogel. The GC:Gelatin (90:10) group showed cell behavior similar to that of the HPP-GC alone hydrogel, with most of the encapsulated cells showing a round morphology at day 7. At day 14, a few spread cells were observed along with predominantly round cell morphology and, more importantly, the spread cells were localized at certain areas presumably rich in gelatin. The GC:Gelatin (70:30) group on the other hand showed improved cell spreading at both days 7 and 14. However, even at this gelatin concentration, the spread cells were found in localized areas along with cells having round morphology. The results are in contrast with the data reported elsewhere using collagen-MeGC hydrogels, where a small concentration of collagen was able to impart significant cell spreading (76). The presence of localized cell spreading in the present study implies the potential separation of HPP-GC and gelatin phases in the hydrogel and the process not leading to a homogeneous hydrogel formation.

4.3.6. Viability and cell spreading study of HPP-modified glycol chitosan/tyramine-modified gelatin composite hydrogels with encapsulated 7F2 osteoblast cells

The study was carried out to investigate the uniformity of cell spreading in the composite hydrogels by using Tyr-Gelatin to form interpenetrating polymer networks. HPP-GC and Tyr-Gelatin composites were prepared and 7F2 cells were encapsulated to obtain three dimensional hydrogels (section 4.2.8). Huang *et al* reported that when chitosan and gelatin solutions were kept at room temperature for longer times, they showed phase separation with gelatin at the bottom and

chitosan on top. (135). Hence, the hydrogel was prepared after incubating the composite solution in a shaker for 24 h followed by vortexing before cell encapsulation in order to avoid the reported phase separation between the different solutions. To prevent cell adhesion on the culture plate, the hydrogel with encapsulated cells was cultured on low attachment dish and transferred to glass bottom dish prior to confocal imaging. Viability test was performed at days 7 and 14.

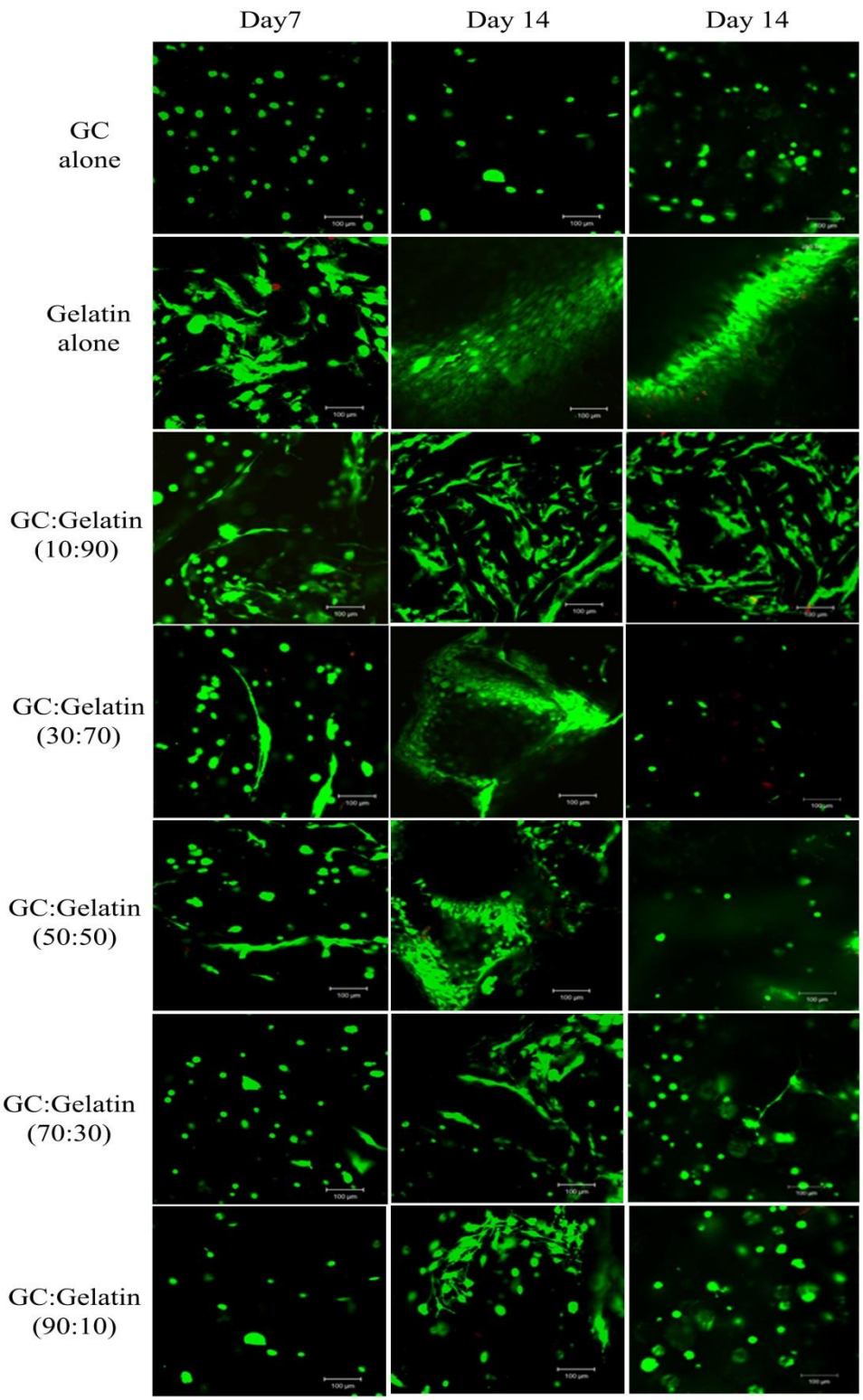

Figure 4.10: Confocal image showing viability and morphology of 7F2 osteoblast cells encapsulated in HPP-GC/Tyr-Gelatin composite hydrogel (20x)

LIVE/DEAD® staining was performed at days 7 and 14 to evaluate the viability and spreading of the encapsulated cells in the hydrogel (Figure 4.10). As indicated by the green fluorescence in Figure 4.10, majority of the cells showed viability in HPP-GC alone (control), Tyr-Gelatin alone (control) and all composite hydrogels irrespective of the HPP-GC concentration. However, HPP-GC alone showed no cell spreading at days 7 and 14. Tyr-Gelatin, known for its cell adhesion and spreading property (133), showed uniform cell spreading at day 7, which increased significantly at day 14. Addition of Tyr-Gelatin improved spreading in the composites. GC:Gelatin (10:90) hydrogel showed cell spreading at day 7 along with few cells with round morphology. Cell spreading increased significantly at day 14 and was uniform throughout the gel. GC: Gelatin (30:70) showed little cell spreading along with cells with round morphology at day 7. However, at day 14, the cells showed uniform spreading in majority of the areas. However, few areas can be observed with very few cells, showing both round cell and spread cell morphology as indicated in the image (in the 3rd column). The GC: Gelatin (50:50) hydrogel showed behavior similar to that of GC: Gelatin (30:70) with some cell spreading at day 7 followed by uniform cell spreading except in certain areas by day 14 (image in the 2nd column). Unlike these groups, GC: Gelatin (70:30) and GC: Gelatin (90:10) showed minimal cell spreading at day 7. However, by day 14, significant increase in cell spreading was observed in certain areas of the gel (2nd column). At the same time, many areas in the gels showed cells with round morphology in both these gels (3rd column). The reason for localized cell spreading can be due to non-uniform gelation of gelatin in the composite, causing cells to spread in the areas rich in gelatin. The study showed that in order to achieve uniform cell spreading within the hydrogel, high concentrations of gelatin are required, presumably due to the non-uniform distribution of gelatin within the gel.

4.4. Conclusion

The study showed the development of composite injectable hydrogels based on HPP-GC and gelatin, and investigated the maintenance of cell viability and cell spreading in the hydrogels. HPP-GC and Tyr-Gelatin polymers were synthesized and then characterized using UV spectroscopy. HPP-GC/Tyr-Gelatin composite hydrogels were prepared using enzymatic crosslinking. Swelling behavior of the composite hydrogels in PBS showed a decrease in percentage swelling, thereby implying an increase in crosslinking density over time. Cell viability was observed in the controls and all the composite hydrogels irrespective of the composition. Uniform cell spreading was observed in the GC: Gelatin (10:90) hydrogel at days 7 and 14. As the gelatin concentration decreased, areas with cells showing round morphology increased, indicating the non-uniform distribution of gelatin within the crosslinked hydrogel matrix. This implies the need to develop a more robust method such as the conjugation of cell-adhesive peptide directly on HPP-GC to support uniform cell spreading.

FUTURE DIRECTIONS

The goal of the study discussed in Chapters 2-4 was to address the two limitations of enzymatically crosslinked HPP-GC hydrogels, namely the lack of hydrogel degradation and lack of cell spreading in the hydrogels. Chapter 2 demonstrated the feasibility of making injectable, degradable acetylated HPP-GC hydrogels and their potential for developing systems for controlled protein delivery. Results from an *in vitro* study showed that the release of encapsulated FITC-albumin was dependent on the degradation of the hydrogels. Increasing the degree of acetylation of the hydrogels resulted in faster degradation, leading to an increase in protein release. As the next step, these results need to be corroborated by *in vivo* studies to develop translational technologies. Subcutaneous implantation of the acetylated HPP-GC hydrogels containing protein tagged with a fluorescent dye can be used in conjunction with an *in vivo* imaging system to non-invasively monitor the protein release.

Chapter 3 demonstrated the *in vivo* biodegradability of injectable acetylated HPP-GC hydrogels. Results confirmed that the degree of acetylation could be used to tailor the *in vivo* degradation of the hydrogels. In addition to biodegradation, biocompatibility of the hydrogels is a very important property required for biomedical applications. Histomorphometric analysis needs to be performed to assess cellular response to the hydrogels. Cell response can be determined by quantifying the presence of inflammatory cells such as lymphocytes, macrophages, foreign body giant cells and polymorphonuclears using H&E stained images. Quantification of inflammatory marker cells need to be scored from absence (-) to significant presence (+++) to assess the severity of the cell response to the hydrogels.

Chapter 4 investigated composite injectable hydrogels prepared by combining HPP-GC and Tyr-gelatin, and assessed the cell spreading properties of these hydrogels. Uniform cell spreading was observed only in the composite with the highest concentration of gelatin; cell spreading property decreased with a decrease in the gelatin content in the hydrogel. As the next step, a more robust system is required to obtain uniform cell spreading in HPP-GC hydrogels. One direction that can be pursued is to use RGD (Arginine-Glycine-Aspartic acid), which is a tripeptide sequence that is ubiquitous in different extracellular matrix proteins such as fibronectin, laminin and collagen and that has been reported to promote cellular adhesion and spreading. Chemically conjugating RGD to HPP-GC polymer using standard carbodiimide chemistry could lead to uniform cell spreading in the system.

REFERENCES

1. Lin C-C, Metters AT. Hydrogels in controlled release formulations: Network design and mathematical modeling. Advanced Drug Delivery Reviews. 2006;58(12–13):1379-1408.

2. Alpesh P, Kibret M. Hydrogel Biomaterials2011 2011-08-01.

3. Lee KY, Mooney DJ. Hydrogels for Tissue Engineering. Chemical Reviews. 2001;101(7):1869-1880.

4. Hunt JA, Chen R, van Veen T, Bryan N. Hydrogels for tissue engineering and regenerative medicine. Journal of Materials Chemistry B. 2014;2(33):5319-5338.

5. Jin R, Dijkstra P. Hydrogels for Tissue Engineering Applications. In: Ottenbrite RM, Park K, Okano T, editors. Biomedical Applications of Hydrogels Handbook: Springer New York; 2010. p. 203-225.

6. Tan H, Marra KG. Injectable, Biodegradable Hydrogels for Tissue Engineering Applications. Materials. 2010;3(3):1746.

7. Zhu J, Marchant RE. Design properties of hydrogel tissue-engineering scaffolds. Expert review of medical devices. 2011;8(5):607-626.

8. Gibas I, Janik H. Review: synthetic polymer hydrogels for biomedical applications. 2010.

9. Miguel SP, Ribeiro MP, Brancal H, Coutinho P, Correia IJ. Thermoresponsive chitosan–agarose hydrogel for skin regeneration. Carbohydrate Polymers. 2014;111(0):366-373.

10. Sivashanmugam A, Arunkumar R, Priya MV, Nair SV, Jayakumar R. An overview of injectable polymeric hydrogels for tissue engineering. European Polymer Journal. 2015.

11. Ravi Kumar MNV. A review of chitin and chitosan applications. Reactive and Functional Polymers. 2000;46(1):1-27.

12. Rinaudo M. Chitin and chitosan: Properties and applications. Progress in Polymer Science. 2006;31(7):603-632.

13. Narayanan D, Jayakumar R, Chennazhi KP. Versatile carboxymethyl chitin and chitosan nanomaterials: a review. Wiley Interdisciplinary Reviews: Nanomedicine and Nanobiotechnology. 2014;6(6):574-598.

14. Tokura S, Itoyama K, Nishi N, Nishimura S-I, Saiki I, Nishimura IA. Selective Sulfation of Chitin Derivatives for Biomedical Functions. Journal of Macromolecular Science, Part A. 1994;31(11):1701-1718.

15. Pillai CKS, Paul W, Sharma CP. Chitin and chitosan polymers: Chemistry, solubility and fiber formation. Progress in Polymer Science. 2009;34(7):641-678.

16. Dash M, Chiellini F, Ottenbrite RM, Chiellini E. Chitosan—A versatile semi-synthetic polymer in biomedical applications. Progress in Polymer Science. 2011;36(8):981-1014.

17. Croisier F, Jérôme C. Chitosan-based biomaterials for tissue engineering. European Polymer Journal. 2013;49(4):780-792.

18. Yuan Y, Chesnutt BM, Haggard WO, Bumgardner JD. Deacetylation of Chitosan: Material Characterization and in vitro Evaluation via Albumin Adsorption and Pre-Osteoblastic Cell Cultures. Materials. 2011;4(8):1399.

19. Cartier N, Domard A, Chanzy H. Single crystals of chitosan. International Journal of Biological Macromolecules. 1990;12(5):289-294.

20. Rinaudo M, Milas M, Dung PL. Characterization of chitosan. Influence of ionic strength and degree of acetylation on chain expansion. International Journal of Biological Macromolecules. 1993;15(5):281-285.

21. Roberts GAF, Domszy JG. Determination of the viscometric constants for chitosan. International Journal of Biological Macromolecules. 1982;4(6):374-377.

22. Mourya VK, Inamdar NN. Chitosan-modifications and applications: Opportunities galore. Reactive and Functional Polymers. 2008;68(6):1013-1051.

23. Mourya VK, Inamdar NN, Tiwari A. Carboxymethyl chitosan and its applications. Advanced Materials Letters. 2010;1(1):11-33.

24. Upadhyaya L, Singh J, Agarwal V, Tewari RP. Biomedical applications of carboxymethyl chitosans. Carbohydrate Polymers. 2013;91(1):452-466.

25. Pereira P, Pedrosa SS, Correia A, Lima CF, Olmedo MP, González-Fernández Á, et al. Biocompatibility of a self-assembled glycol chitosan nanogel. Toxicology in Vitro. 2015;29(3):638-646.

26. Trapani A, Di Gioia S, Ditaranto N, Cioffi N, Goycoolea FM, Carbone A, et al. Systemic heparin delivery by the pulmonary route using chitosan and glycol chitosan nanoparticles. International Journal of Pharmaceutics. 2013;447(1–2):115-123.

27. Jiang G, Sun J, Ding F. PEG-g-chitosan thermosensitive hydrogel for implant drug delivery: Cytotoxicity, in vivo degradation and drug release. Journal of Biomaterials Science, Polymer Edition. 2014;25(3):241-256.

28. Ding K, Wang Y, Wang H, Yuan L, Tan M, Shi X, et al. 6-O-sulfated chitosan promoting the neural differentiation of mouse embryonic stem cells. ACS Applied Materials and Interfaces. 2014;6(22):20043-20050.

29. Vikhoreva G, Bannikova G, Stolbushkina P, Panov A, Drozd N, Makarov V, et al. Preparation and anticoagulant activity of a low-molecular-weight sulfated chitosan. Carbohydrate Polymers. 2005;62(4):327-332.

30. Heras A, Rodríguez NM, Ramos VM, Agulló E. N-methylene phosphonic chitosan: a novel soluble derivative. Carbohydrate Polymers. 2001;44(1):1-8.

31. Zhu D, Yao K, Bo J, Zhang H, Liu L, Dong X, et al. Hydrophilic/lipophilic N-methylene phosphonic chitosan as a promising non-viral vector for gene delivery. J Mater Sci: Mater Med. 2010;21(1):223-229.

32. Sajomsang W, Nuchuchua O, Saesoo S, Gonil P, Chaleawlert-umpon S, Pimpha N, et al. A comparison of spacer on water-soluble cyclodextrin grafted chitosan inclusion complex as carrier of eugenol to mucosae. Carbohydrate Polymers. 2013;92(1):321-327.

33. Berger J, Reist M, Mayer JM, Felt O, Gurny R. Structure and interactions in chitosan hydrogels formed by complexation or aggregation for biomedical applications. European Journal of Pharmaceutics and Biopharmaceutics. 2004;57(1):35-52.

34. Aziz MA, Cabral JD, Brooks HJL, Moratti SC, Hanton LR. Antimicrobial properties of a chitosan dextran-based hydrogel for surgical use. Antimicrobial Agents and Chemotherapy. 2012;56(1):280-287.

35. He P, Davis SS, Illum L. In vitro evaluation of the mucoadhesive properties of chitosan microspheres. International Journal of Pharmaceutics. 1998;166(1):75-88.

36. Lee Y-H, Chang J-J, Yang M-C, Chien C-T, Lai W-F. Acceleration of wound healing in diabetic rats by layered hydrogel dressing. Carbohydrate Polymers. 2012;88(3):809-819.

37. Han T, Nwe N, Furuike T, Tokura S, Tamura H. Methods of N-acetylated chitosan scaffolds and its In-vitro biodegradation by lysozyme. 2012.

38. Verheul RJ, Amidi M, van Steenbergen MJ, van Riet E, Jiskoot W, Hennink WE. Influence of the degree of acetylation on the enzymatic degradation and in vitro biological properties of trimethylated chitosans. Biomaterials. 2009;30(18):3129-3135.

39. Chung Y-C, Chen C-Y. Antibacterial characteristics and activity of acid-soluble chitosan. Bioresource Technology. 2008;99(8):2806-2814.

40. Kim S-K. Chitin and chitosan derivatives: Advances in drug discovery and developments: CRC Press; 2013.

41. Bhattarai N, Gunn J, Zhang M. Chitosan-based hydrogels for controlled, localized drug delivery. Advanced drug delivery reviews. 2010;62(1):83-99.

42. Schuetz YB, Gurny R, Jordan O. A novel thermoresponsive hydrogel based on chitosan. European Journal of Pharmaceutics and Biopharmaceutics. 2008;68(1):19-25.

43. Sheridan WS, Grant OB, Duffy GP, Murphy BP. The application of a thermoresponsive chitosan/β-GP gel to enhance cell repopulation of decellularized vascular scaffolds. Journal of Biomedical Materials Research Part B: Applied Biomaterials. 2014;102(8):1700-1710.

44. Lu W-N, Lü S-H, Wang H-B, Li D-X, Duan C-M, Liu Z-Q, et al. Functional improvement of infarcted heart by co-injection of embryonic stem cells with temperature-responsive chitosan hydrogel. Tissue Engineering Part A. 2008;15(6):1437-1447.

45. Niranjan R, Koushik C, Saravanan S, Moorthi A, Vairamani M, Selvamurugan N. A novel injectable temperature-sensitive zinc doped chitosan/β-glycerophosphate hydrogel for bone tissue engineering. International journal of biological macromolecules. 2013;54:24-29.

46. Liu X, Chen Y, Huang Q, He W, Feng Q, Yu B. A novel thermo-sensitive hydrogel based on thiolated chitosan/hydroxyapatite/beta-glycerophosphate. Carbohydrate polymers. 2014;110:62-69.

47. Chenite A, Buschmann M, Wang D, Chaput C, Kandani N. Rheological characterisation of thermogelling chitosan/glycerol-phosphate solutions. Carbohydrate Polymers. 2001;46(1):39-47.

48. Han HD, Seo DH, Kim TW, Shin BC, Choi HS. Preparation and biodegradation of thermosensitive chitosan hydrogel as a function of pH and temperature. Macromolecular Research. 2004;12(5):507-511.

49. Kafedjiiski K, Krauland AH, Hoffer MH, Bernkop-Schnürch A. Synthesis and in vitro evaluation of a novel thiolated chitosan. Biomaterials. 2005;26(7):819-826.

50. Khodaverdi E, Tafaghodi M, Ganji F, Abnoos K, Naghizadeh H. In vitro insulin release from thermosensitive chitosan hydrogel. AAPS PharmSciTech. 2012;13(2):460-466.

51. Nair LS, Starnes T, Ko J-WK, Laurencin CT. Development of injectable thermogelling chitosan–inorganic phosphate solutions for biomedical applications. Biomacromolecules. 2007;8(12):3779-3785.

52. Kim JH, Lee SB, Kim SJ, Lee YM. Rapid temperature/pH response of porous alginate-g-poly (N-isopropylacrylamide) hydrogels. Polymer. 2002;43(26):7549-7558.

53. Qiu Y, Park K. Environment-sensitive hydrogels for drug delivery. Advanced drug delivery reviews. 2012;64:49-60.

54. Chen JP, Cheng TH. Thermo-Responsive Chitosan-graft-poly (N-isopropylacrylamide) Injectable Hydrogel for Cultivation of Chondrocytes and Meniscus Cells. Macromolecular bioscience. 2006;6(12):1026-1039.

55. Dessì M, Borzacchiello A, Mohamed TH, Abdel-Fattah WI, Ambrosio L. Novel biomimetic thermosensitive β-tricalcium phosphate/chitosan-based hydrogels for bone tissue engineering. Journal of Biomedical Materials Research Part A. 2013;101(10):2984-2993.

56. McMahon SS, Nikolskaya N, Choileáin SN, Hennessy N, O'Brien T, Strappe PM, et al. Thermosensitive hydrogel for prolonged delivery of lentiviral vector expressing neurotrophin-3 in vitro. The journal of gene medicine. 2011;13(11):591-601.

57. Hosny KM. Preparation and evaluation of thermosensitive liposomal hydrogel for enhanced transcorneal permeation of ofloxacin. AAPS PharmSciTech. 2009;10(4):1336-1342.

58. Zhang D, Xie D, Wei X, Zhang D, Chen M, Yu X, et al. Microwave ablation of the liver abutting the stomach: Insulating effect of a chitosan-based thermosensitive hydrogel. International Journal of Hyperthermia. 2014;30(2):126-133.

59. Cheng Y-H, Yang S-H, Lin F-H. Thermosensitive chitosan-gelatin-glycerol phosphate hydrogel as a controlled release system of ferulic acid for nucleus pulposus regeneration. Biomaterials. 2011;32(29):6953-6961.

60. Park KM, Lee SY, Joung YK, Na JS, Lee MC, Park KD. Thermosensitive chitosan–Pluronic hydrogel as an injectable cell delivery carrier for cartilage regeneration. Acta biomaterialia. 2009;5(6):1956-1965.

61. Crompton K, Goud J, Bellamkonda R, Gengenbach T, Finkelstein D, Horne M, et al. Polylysine-functionalised thermoresponsive chitosan hydrogel for neural tissue engineering. Biomaterials. 2007;28(3):441-449.

62. Jiang H-L, Kim Y-K, Lee S-M, Park M-R, Kim E-M, Jin Y-M, et al. Galactosylated chitosan-g-PEI/DNA complexes-loaded poly (organophosphazene) hydrogel as a hepatocyte targeting gene delivery system. Archives of pharmacal research. 2010;33(4):551-556.

63. Chien Y, Liao Y-W, Liu D-M, Lin H-L, Chen S-J, Chen H-L, et al. Corneal repair by human corneal keratocyte-reprogrammed iPSCs and amphiphatic carboxymethyl-hexanoyl chitosan hydrogel. Biomaterials. 2012;33(32):8003-8016.

64. Mao J, Kondu S, Ji HF, McShane MJ. Study of the near-neutral pH-sensitivity of chitosan/gelatin hydrogels by turbidimetry and microcantilever deflection. Biotechnology and bioengineering. 2006;95(3):333-341.

65. Bostan MS, Senol M, Cig T, Peker I, Goren AC, Ozturk T, et al. Controlled release of 5-aminosalicylicacid from chitosan based pH and temperature sensitive hydrogels. International journal of biological macromolecules. 2013;52:177-183.

66. Chiu Y-L, Chen S-C, Su C-J, Hsiao C-W, Chen Y-M, Chen H-L, et al. pH-triggered injectable hydrogels prepared from aqueous N-palmitoyl chitosan: in vitro characteristics and in vivo biocompatibility. Biomaterials. 2009;30(28):4877-4888.

67. Li J, Hu W, Zhang Y, Tan H, Yan X, Zhao L, et al. pH and glucose dually responsive injectable hydrogel prepared by in situ crosslinking of phenylboronic modified chitosan and oxidized dextran. Journal of Polymer Science Part A: Polymer Chemistry. 2015;53(10):1235-1244.

68. Ding C, Zhao L, Liu F, Cheng J, Gu J, Dan S-, et al. Dually responsive injectable hydrogel prepared by in situ cross-linking of glycol chitosan and benzaldehyde-capped PEO-PPO-PEO. Biomacromolecules. 2010;11(4):1043-1051.

69. Obara K, Ishihara M, Ishizuka T, Fujita M, Ozeki Y, Maehara T, et al. Photocrosslinkable chitosan hydrogel containing fibroblast growth factor-2 stimulates wound healing in healing-impaired db/db mice. Biomaterials. 2003;24(20):3437-3444.

70. Ishihara M, Obara K, Ishizuka T, Fujita M, Sato M, Masuoka K, et al. Controlled release of fibroblast growth factors and heparin from photocrosslinked chitosan hydrogels and subsequent effect on in vivo vascularization. Journal of Biomedical Materials Research Part A. 2003;64(3):551-559.

71. Ono K, Ishihara M, Ozeki Y, Deguchi H, Sato M, Saito Y, et al. Experimental evaluation of photocrosslinkable chitosan as a biologic adhesive with surgical applications. Surgery. 2001;130(5):844-850.

72. Hayashi T, Matsuyama T, Hanada K, Nakanishi K, Uenoyama M, Fujita M, et al. Usefulness of photocrosslinkable chitosan for endoscopic cancer treatment in alimentary tract. Journal of Biomedical Materials Research Part B: Applied Biomaterials. 2004;71(2):367-372.

73. Zhou Y, Ma G, Shi S, Yang D, Nie J. Photopolymerized water-soluble chitosan-based hydrogel as potential use in tissue engineering. International journal of biological macromolecules. 2011;48(3):408-413.

74. Tsuda Y, Hattori H, Tanaka Y, Ishihara M, Kishimoto S, Amako M, et al. Ultraviolet light-irradiated photocrosslinkable chitosan hydrogel to prevent bone formation in both rat skull and fibula bone defects. Journal of tissue engineering and regenerative medicine. 2013;7(9):720-728.

75. Ono K, Saito Y, Yura H, Ishikawa K, Kurita A, Akaike T, et al. Photocrosslinkable chitosan as a biological adhesive. Journal of biomedical materials research. 2000;49(2):289-295.

76. Arakawa C, Ng R, Tan S, Kim S, Wu B, Lee M. Photopolymerizable chitosan–collagen hydrogels for bone tissue engineering. Journal of tissue engineering and regenerative medicine. 2014.

77. Fujita M, Ishihara M, Morimoto Y, Simizu M, Saito Y, Yura H, et al. Efficacy of photocrosslinkable chitosan hydrogel containing fibroblast growth factor-2 in a rabbit model of chronic myocardial infarction. Journal of Surgical Research. 2005;126(1):27-33.

78. Horio T, Ishihara M, Fujita M, Kishimoto S, Kanatani Y, Ishizuka T, et al. Effect of photocrosslinkable chitosan hydrogel and its sponges to stop bleeding in a rat liver injury model. Artificial organs. 2010;34(4):342-347.

79. Kim S, Bedigrew K, Guda T, Maloney WJ, Park S, Wenke JC, et al. Novel osteoinductive photo-cross-linkable chitosan-lactide-fibrinogen hydrogels enhance bone regeneration in critical size segmental bone defects. Acta biomaterialia. 2014;10(12):5021-5033.

80. Kim S, Kang Y, Mercado-Pagán ÁE, Maloney WJ, Yang Y. In vitro evaluation of photo-crosslinkable chitosan-lactide hydrogels for bone tissue engineering. Journal of Biomedical Materials Research Part B: Applied Biomaterials. 2014;102(7):1393-1406.

81. Choi B, Kim S, Lin B, Wu BM, Lee M. Cartilaginous extracellular matrix-modified chitosan hydrogels for cartilage tissue engineering. ACS applied materials & interfaces. 2014;6(22):20110-20121.

82. Rickett TA, Amoozgar Z, Tuchek CA, Park J, Yeo Y, Shi R. Rapidly photo-cross-linkable chitosan hydrogel for peripheral neurosurgeries. Biomacromolecules. 2010;12(1):57-65.

83. Chiu L, Janic K, Radisic M. Engineering of oriented myocardium on three-dimensional micropatterned collagen-chitosan hydrogel. Int J Artif Organs. 2012;35(4):237-250.

84. Teixeira LSM, Feijen J, van Blitterswijk CA, Dijkstra PJ, Karperien M. Enzyme-catalyzed crosslinkable hydrogels: emerging strategies for tissue engineering. Biomaterials. 2012;33(5):1281-1290.

85. Sakai S, Yamada Y, Zenke T, Kawakami K. Novel chitosan derivative soluble at neutral pH and in-situ gellable via peroxidase-catalyzed enzymatic reaction. Journal of Materials Chemistry. 2009;19(2):230-235.

86. da Silva MA, Bode F, Drake AF, Goldoni S, Stevens MM, Dreiss CA. Enzymatically Cross-Linked Gelatin/Chitosan Hydrogels: Tuning Gel Properties and Cellular Response. Macromolecular bioscience. 2014;14(6):817-830.

87. Kang GD, Lee KH, Ki CS, Nahm JH, Park YH. Silk fibroin/chitosan conjugate crosslinked by tyrosinase. Macromolecular Research. 2004;12(5):534-539.

88. Jin R, Teixeira LM, Dijkstra PJ, Karperien M, Van Blitterswijk C, Zhong Z, et al. Injectable chitosan-based hydrogels for cartilage tissue engineering. Biomaterials. 2009;30(13):2544-2551.

89. Gohil SV, Brittain SB, Kan H-M, Drissi H, Rowe DW, Nair LS. Evaluation of enzymatically crosslinked injectable glycol chitosan hydrogel. Journal of Materials Chemistry B. 2015.

90. Chen Z, Wang W, Guo L, Yu Y, Yuan Z. Preparation of enzymatically cross-linked sulfated chitosan hydrogel and its potential application in thick tissue engineering. Sci China Chem. 2013;56(12):1701-1709.

91. Knight DK, Shapka SN, Amsden BG. Structure, depolymerization, and cytocompatibility evaluation of glycol chitosan. Journal of Biomedical Materials Research Part A. 2007;83A(3):787-798.

92. Hillberg AL, Oudshoorn M, Lam JBB, Kathirgamanathan K. Encapsulation of porcine pancreatic islets within an immunoprotective capsule comprising methacrylated glycol chitosan and alginate. Journal of Biomedical Materials Research Part B: Applied Biomaterials. 2015;103(3):503-518.

93. Rhee J-K, Park OK, Lee A, Yang DH, Park K. Glycol Chitosan-Based Fluorescent Theranostic Nanoagents for Cancer Therapy. Marine Drugs. 2014;12(12):6038-6057.

94. Ferreira T, Hollanda L, Lancellotti M, de Sousa E. Boron nitride nanotubes chemically functionalized with glycol chitosan for gene transfection in eukaryotic cell lines. Journal of Biomedical Materials Research Part A. 2014.

95. Lee S, Kang S-W, Ryu JH, Na JH, Lee D-E, Han SJ, et al. Tumor-Homing Glycol Chitosan-Based Optical/PET Dual Imaging Nanoprobe for Cancer Diagnosis. Bioconjugate Chemistry. 2014;25(3):601-610.

96. Cao L, Cao B, Lu C, Wang G, Yu L, Ding J. An injectable hydrogel formed by in situ cross-linking of glycol chitosan and multi-benzaldehyde functionalized PEG analogues for cartilage tissue engineering. Journal of Materials Chemistry B. 2015;3(7):1268-1280.

97. Yoon HY, Son S, Lee SJ, You DG, Yhee JY, Park JH, et al. Glycol chitosan nanoparticles as specialized cancer therapeutic vehicles: Sequential delivery of doxorubicin and Bcl-2 siRNA. Sci Rep. 2014;4.

98. Pereira P, Morgado D, Crepet A, David L, Gama FM. Glycol Chitosan-Based Nanogel as a Potential Targetable Carrier for siRNA. Macromolecular Bioscience. 2013;13(10):1369-1378.

99. Bae JW, Choi JH, Lee Y, Park KD. Horseradish peroxidase-catalysed in situ-forming hydrogels for tissue-engineering applications. Journal of Tissue Engineering and Regenerative Medicine. 2014

100. San Juan A, Montembault A, Gillet D, Say J, Rouif S, Bouet T, et al., editors. Degradation of chitosan-based materials after different sterilization treatments. IOP Conference Series: Materials Science and Engineering; 2012: IOP Publishing.

101. Jarry C, Chaput C, Chenite A, Renaud MA, Buschmann M, Leroux JC. Effects of steam sterilization on thermogelling chitosan-based gels. Journal of biomedical materials research. 2001;58(1):127-135.

102. Huang H, Ding Y, Sun XS, Nguyen TA. Peptide Hydrogelation and Cell Encapsulation for 3D Culture of MCF-7 Breast Cancer Cells. PLoS ONE. 2013;8(3):e59482.

103. Freier T, Koh HS, Kazazian K, Shoichet MS. Controlling cell adhesion and degradation of chitosan films by N-acetylation. Biomaterials. 2005;26(29):5872-5878.

104. Czechowska-Biskup R, Jarosińska D, Rokita B, Ulański P, Rosiak JM. Determination of degree of deacetylation of chitosan-comparision of methods. Prog Chem Appl Chitin Its Deriv. 2012;17:5-20.

105. Taghizadeh SM, Davari G. Preparation, characterization, and swelling behavior of N-acetylated and deacetylated chitosans. Carbohydrate Polymers. 2006;64(1):9-15.

106. Hirai A, Odani H, Nakajima A. Determination of degree of deacetylation of chitosan by 1H NMR spectroscopy. Polymer Bulletin. 1991;26(1):87-94.

107. Brittain SB. Development and Characterization of a Bioactive Injectable Chitosan Hydrogel for Bone Repair. 2013.

108. Ren K, He C, Cheng Y, Li G, Chen X. Injectable enzymatically crosslinked hydrogels based on a poly (l-glutamic acid) graft copolymer. Polymer Chemistry. 2014;5(17):5069-5076.

109. Ganesh N, Hanna C, Nair SV, Nair LS. Enzymatically Cross-linked Alginic-Hyaluronic acid Composite Hydrogels As Cell Delivery Vehicles. International journal of biological macromolecules. 2013;55:289-294.

110. Lundblad G, Hederstedt B, Lind J, Steby M. Chitinase in goat serum. Preliminary purification and characterization. European Journal of Biochemistry. 1974;46(2):367-376.

111. Nair LS, Laurencin CT. Biodegradable polymers as biomaterials. Progress in Polymer Science. 2007;32(8–9):762-798.

112. Hartl L, Zach S, Seidl-Seiboth V. Fungal chitinases: diversity, mechanistic properties and biotechnological potential. Applied Microbiology and Biotechnology. 2012;93(2):533-543.

113. Vårum KM, Myhr MM, Hjerde RJ, Smidsrød O. In vitro degradation rates of partially N-acetylated chitosans in human serum. Carbohydrate Research. 1997;299(1):99-101.

114. Hirano S, Tsuchida H, Nagao N. N-acetylation in chitosan and the rate of its enzymic hydrolysis. Biomaterials. 1989;10(8):574-576.

115. Paoletti MG, Norberto L, Damini R, Musumeci S. Human Gastric Juice Contains Chitinase That Can Degrade Chitin. Annals of Nutrition and Metabolism. 2007;51(3):244-251.

116. Kzhyshkowska J, Gratchev A, Goerdt S. Human Chitinases and Chitinase-Like Proteins as Indicators for Inflammation and Cancer. Biomarker Insights. 2007;2:128-146.

117. Azab AK, Doviner V, Orkin B, Kleinstern J, Srebnik M, Nissan A, et al. Biocompatibility evaluation of crosslinked chitosan hydrogels after subcutaneous and intraperitoneal implantation in the rat. Journal of Biomedical Materials Research Part A. 2007;83(2):414-422.

118. Costa-Pinto AR, Martins AM, Castelhano-Carlos MJ, Correlo VM, Sol PC, Longatto-Filho A, et al. In vitro degradation and in vivo biocompatibility of chitosan–poly (butylene succinate) fiber mesh scaffolds. Journal of Bioactive and Compatible Polymers: Biomedical Applications. 2014;29(2):137-151.

119. VandeVord PJ, Matthew HW, DeSilva SP, Mayton L, Wu B, Wooley PH. Evaluation of the biocompatibility of a chitosan scaffold in mice. Journal of Biomedical Materials Research. 2002;59(3):585-590.

120. Tomihata K, Ikada Y. In vitro and in vivo degradation of films of chitin and its deacetylated derivatives. Biomaterials. 1997;18(7):567-575.

121. Olad A, Farshi Azhar F. The synergetic effect of bioactive ceramic and nanoclay on the properties of chitosan–gelatin/nanohydroxyapatite–montmorillonite scaffold for bone tissue engineering. Ceramics International. 2014;40(7, Part A):10061-10072.

122. Kathuria N, Tripathi A, Kar KK, Kumar A. Synthesis and characterization of elastic and macroporous chitosan–gelatin cryogels for tissue engineering. Acta Biomaterialia. 2009;5(1):406-418.

123. Pok S, Myers JD, Madihally SV, Jacot JG. A multilayered scaffold of a chitosan and gelatin hydrogel supported by a PCL core for cardiac tissue engineering. Acta biomaterialia. 2013;9(3):5630-5642.

124. Whu SW, Hung K-C, Hsieh K-H, Chen C-H, Tsai C-L, Hsu S-h. In vitro and in vivo evaluation of chitosan–gelatin scaffolds for cartilage tissue engineering. Materials Science and Engineering: C. 2013;33(5):2855-2863.

125. Miranda SCCC, Silva GAB, Hell RCR, Martins MD, Alves JB, Goes AM. Three-dimensional culture of rat BMMSCs in a porous chitosan-gelatin scaffold: A promising association for bone tissue engineering in oral reconstruction. Archives of Oral Biology. 2011;56(1):1-15.

126. Jiankang H, Dichen L, Yaxiong L, Bo Y, Hanxiang Z, Qin L, et al. Preparation of chitosan–gelatin hybrid scaffolds with well-organized microstructures for hepatic tissue engineering. Acta Biomaterialia. 2009;5(1):453-461.

127. Han F, Dong Y, Su Z, Yin R, Song A, Li S. Preparation, characteristics and assessment of a novel gelatin–chitosan sponge scaffold as skin tissue engineering material. International Journal of Pharmaceutics. 2014;476(1–2):124-133.

128. Mao JS, Zhao LG, Yin YJ, Yao KD. Structure and properties of bilayer chitosan–gelatin scaffolds. Biomaterials. 2003;24(6):1067-1074.

129. Cui L, Jia J, Guo Y, Liu Y, Zhu P. Preparation and characterization of IPN hydrogels composed of chitosan and gelatin cross-linked by genipin. Carbohydrate Polymers. 2014;99(0):31-38.

130. Chen T, Embree HD, Brown EM, Taylor MM, Payne GF. Enzyme-catalyzed gel formation of gelatin and chitosan: potential for in situ applications. Biomaterials. 2003;24(17):2831-2841.

131. Cheng Y-H, Yang S-H, Su W-Y, Chen Y-C, Yang K-C, Cheng WT-K, et al. Thermosensitive chitosan–gelatin–glycerol phosphate hydrogels as a cell carrier for nucleus pulposus regeneration: an in vitro study. Tissue Engineering Part A. 2009;16(2):695-703.

132. Nagahama H, Maeda H, Kashiki T, Jayakumar R, Furuike T, Tamura H. Preparation and characterization of novel chitosan/gelatin membranes using chitosan hydrogel. Carbohydrate Polymers. 2009;76(2):255-260.

133. Amini AA, Nair LS. Enzymatically cross-linked injectable gelatin gel as osteoblast delivery vehicle. Journal of Bioactive and Compatible Polymers. 2012;27(4):342-355.

134. Kim KS, Park SJ, Yang JA, Jeon JH, Bhang SH, Kim BS, et al. Injectable hyaluronic acid–tyramine hydrogels for the treatment of rheumatoid arthritis. Acta Biomaterialia. 2011;7(2):666-674.

135. Huang Y, Onyeri S, Siewe M, Moshfeghian A, Madihally SV. In vitro characterization of chitosan–gelatin scaffolds for tissue engineering. Biomaterials. 2005;26(36):7616-7627.

APPENDIX

A1. Sample calculation for labeling acetylated glycol chitosan with 0.1GC as the example

Acetic Anhydride (AA)

Density = 1.08 g/mL

Molecular weight = 102.09 g/mol

Volume of AA taken = 4.6 µL

Moles of AA = $(4.6 \times 10^{-3} \times 1.08)/102.09$ **= 4.866×10^{-5} mol**

Glycol chitosan [Completely deacetylated polymer with degree of polymerization equal to 400]

Molecular weight = 205 x 400 = 82000 g/mol

Weight of GC taken = 0.1 g

Moles of GC = $0.1/82000 = 1.219 \times 10^{-6}$ mol

1 mol of GC polymer contains 400 mols of NH_2. Therefore,

Moles of $NH_2 = 1.219 \times 10^{-6} \times 400$ **= 4.878×10^{-4} mol**

Molar ratio of AA to $NH_2 = (4.866 \times 10^{-5})/(4.878 \times 10^{-4})$ = **0.0997 (Rounded off to 0.1)**

Hence, the polymer was labeled 0.1GC